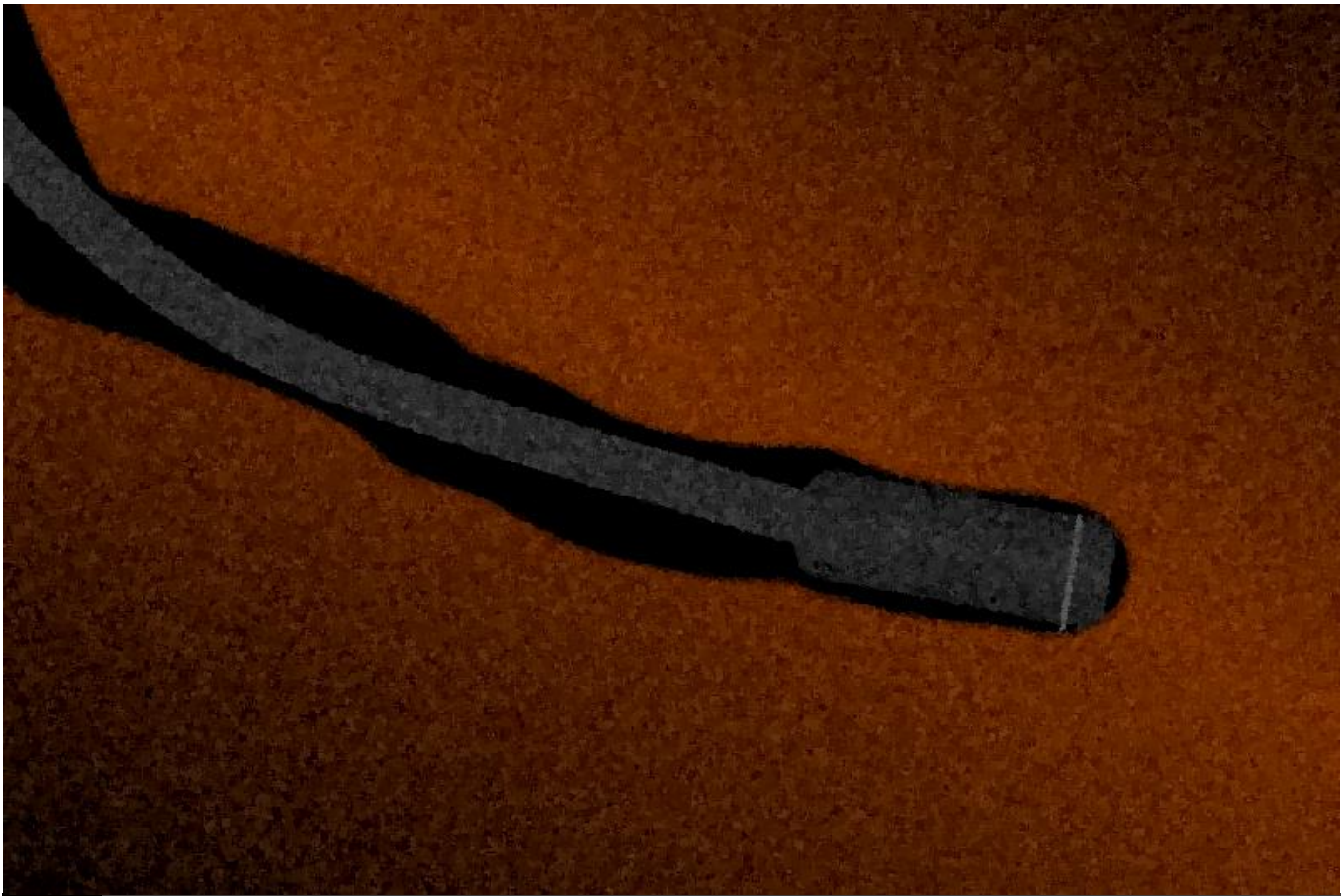

Uncertainty analysis in determining the position of a drill bit

Huy Van (4358554)

BSc Applied Mathematics - Bachelor thesis

31-Aug-18

Technische Universiteit Delft
Faculteit Elektrotechniek, Wiskunde en Informatica
Delft Institute of Applied Mathematics

Het bepalen van de onzekerheden bij het bepalen van de positie van een boorkop

(Engelse titel: Uncertainty analysis in determining the position of a drill bit)

Verslag ten behoeve van het
Delft Institute of Applied Mathematics
als onderdeel ter verkrijging

van de graad van

BACHELOR OF SCIENCE
in
TECHNISCHE WISKUNDE

door

HUY VAN

Delft, Nederland
Augustus 2018

BSc verslag TECHNISCHE WISKUNDE

"Het bepalen van de onzekerheden bij het bepalen van de positie van een boorkop"

(Engelse titel: "Uncertainty analysis in determining the position of a drill bit")

HUY VAN

Technische Universiteit Delft

Begeleiders

Prof.dr.ir. K. Vuik

ir. K.A. Noy
(Shell Global Solutions International)

Overige commissieleden

Dr.ir. L.E. Meester

Dr. B. van den Dries

Augustus, 2018

Delft

Uncertainty analysis in determining the position of a drill bit

Het bepalen van de onzekerheden bij het bepalen van de positie van een boorkop

Huy Van, Delft University of Technology (4358554)

Abstract

In well-bore engineering, oil-well boreholes are made using specialized drilling rigs. The position of the drill bit needs to be indirectly determined through accelero- and magnetometer measurements. To this end, the measurement data is first converted into a survey of direction vectors by applying a series of coordinate transformations. Then, a method called Minimum Curvature Method (MCM) is applied, which outputs a close idealized approximation of the actual drill bit trajectory. However, systematic and random errors in the magnetometer measurements result in error in position vectors.

A novel solution called Multi-Station Analysis (MSA) determines the systematic (Scale and Bias) errors in the magnetometer measurement data. Using reference measurements, a non-linear least squares error function is minimized, which is equivalent to solving a non-linear system of equations. This is done numerically by the Newton-Raphson algorithm. Subsequently, the measurement data is corrected. Reapplying survey conversion and MCM results in an improved estimate for the actual position vectors.

The main objective of this thesis is to derive a method that describes the uncertainty of the MSA solution. This is primarily done through the method of Monte Carlo simulation. As part of validation, the effect of MSA on final drill bit position is studied and compared with results from an uncertainty model used by the well-bore industry. Secondary, a pessimistic quantification of the uncertainty of MSA solution is given through condition numbers of Jacobian matrices from the Newton-Raphson algorithm applied to MSA, which measure the sensitivity of the non-linear least-squares error. The question whether these condition numbers are a representative measure of MSA solution quality is answered. Finally, further potential research areas are described.

Keywords: Multi-Station analysis, uncertainty analysis, Monte Carlo simulation, sensitivity analysis, non-linear regression, condition number

Author notes

This bachelor thesis is part of BSc Applied Mathematics at Delft University of Technology - specifically the TW3050 Bachelorproject course - done in collaboration with Shell Global Solutions International B.V.

Disclaimer

All figures are made by the author unless noted otherwise.

MATLAB and Spreadsheet Link are registered trademarks of The MathWorks, Inc.

The “matrix.xla” Excel add-in is made by Leonardo Volpi.

Contents

Table of figures

Preface

Royal Dutch Shell, commonly known as Shell, is a British-Dutch multinational oil and gas company, and the most profitable company of the Netherlands. It is established in 1907 after the merger of the Dutch “Koninklijke Nederlandse Petroleum Maatschappij” and the British “Shell Transport and Trading Company Ltd”, under the resulting name “Koninklijke/Shell Groep”. Next to transportation, production and processing of gas and oil, present-day Shell is also involved in renewable energy and chemicals.

Shell Global Solutions is a division of Shell, which provides services and technologies in the above areas. Other oil field service companies related to the oil and gas industry are e.g. Halliburton Company and Baker Hughes. One of their main interests is the construction of oil wells, which is the main scope of this thesis.

Wells are constructed for winning oil and gas, and for underground CO_2 storage. To ensure that wells are correctly positioned below the Earth’s surface, well coordinates are needed. These coordinates are commonly determined by usage of a specialized measurement tool - Measurement While Drilling (MWD) tool - which is placed near the drilling bit. During drilling, the MWD sensors measures the drill bit acceleration and the Earth’s magnetic field in specified locations along the well, from which the well coordinates are derived. However, the sensor measurements contain systematic and random errors, which result in uncertainty in determining the well coordinates. This uncertainty can be expressed as an ellipsoid.

To reduce sensor measurement errors, a widely used mathematical technique called Multi-Station Analysis (MSA) is applied. With the aid of geomagnetic reference data, MSA potentially reduces sensor measurement errors and its associated uncertainty. However, experience has shown that MSA can produce unstable solutions and poorly interpretable results.

Despite extensive research on MSA, there is no standard in the oil and gas industry defining the correct use of MSA. In support of its stakeholders, e.g. Industry Steering Committee on Wellbore Survey Accuracy (ISCWSA), this thesis provides:

- a brief and self-contained introduction in well-bore engineering, MSA and its mathematical model.
- a proposed solution for the application of MSA, by assessing
    - the systematic errors uncertainty after applying MSA
    - the well coordinate uncertainty after applying MSA

  The solution is based on Monte Carlo simulation.

Additionally, the assessment of the systematic errors uncertainty is established by investigating if the condition number in the final iteration of Newton-Raphson algorithm is a reliable measure for the quality of MSA solution.

The thesis is completed with conclusions and recommendations for further areas of research.

Notes and in-chapter sources

- Throughout this thesis, notes and in-chapter sources appear in separate sections at the end of each chapter whenever needed.

- Basic information about Royal Dutch Shell and Shell Global Solutions has been acquired from https://nl.wikipedia.org/wiki/Royal_Dutch_Shell and https://www.shell.com/business-customers/global-solutions.html respectively.

Chapter 1 Introduction: basic concepts in well-bore engineering

A source of petrochemical oil - petroleum - is oil wells, which are located far beneath the Earth's surface. To extract the petroleum, a narrow three-dimensional cylindrical borehole (*well-bore*) must be drilled through the subsurface. This is done by a drilling rig, placed onshore (land operations) or offshore (sea operations) in vicinity of the oil well. The rig includes the following below surface components:

- *Drill bit*: the part that does the actual drilling work and can cut through rock. Its diameter is usually not wider than a meter.
- *Drill pipe*: steel piping. Drilling fluid is pumped through it, which cools down the drill and transports excess drilled cuttings.
- *Bottom-Hole Assembly* (BHA): a part between the drill bit and drill pipe which contains drill collars as well as Measurement While Drilling tools.
    - *Non-Magnetic Drill Collar* (NMDC): protective casing which minimizes the effect of magnetic interference in the MWD tools.
    - *Measurement While Drilling* (MWD) tools: tools like accelerometers and magnetometers which are used to determine the direction of BHA.
- *Drill string*: BHA and drill pipe. It is the part connected to the drill bit.

Figure 1-1 displays a schematic of a drilling rig, as well as its individual components, including the ones specified above.

In this thesis, the position of a drill bit is considered, which is determined using indirect measurements collected from the MWD tools in BHA. It is assumed that the position of BHA and drill bit coincide: these terms are used interchangeably in this thesis.

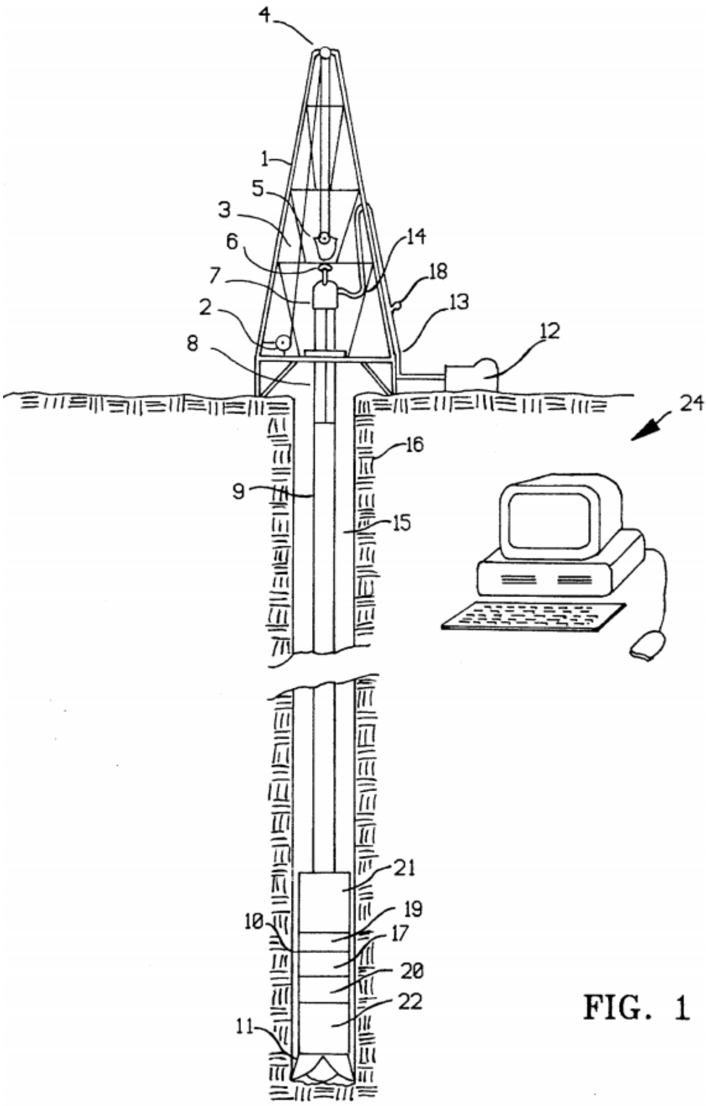

FIG. 1

Figure 1-1: Drilling rig. Drill bit (11), drill string (9), drill collars (10), NMDCs (19) and (20). MWD tools are in (17). Source: (Brooks 1997)

A short note on position coordinates and orientations

The drill bit can be modelled as a cylinder. Its front face is called *Tool Face*. The turning angle around the middle axis with respect to the direction towards the Earth's surface - *High Side* (HS) – is called *Tool Face Angle*, and the direction in which the drill bit is moving at any time is *Downhole direction*. *High Side Right* (HSR) is the remaining direction orthogonal to High Side lying across the Tool Face.

All measurements by the MWD tools are done with respect to the orientation of BHA, which is written in terms of High Side + Tool Face Angle, High Side Right + Tool Face Angle and Downhole direction coordinates. See Figure 1-2.

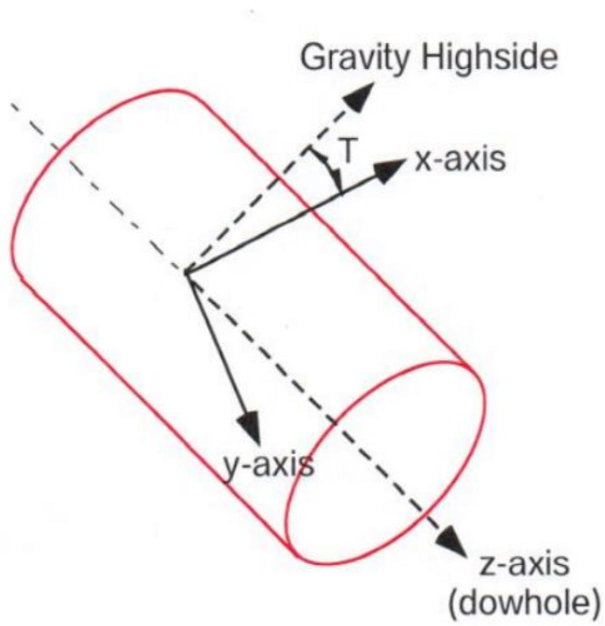

Figure 1-2: Orientation of BHA. x=High Side + T, y=High Side Right + T, z=Downhole direction, T=Tool Face Angle. Source: (Boots & Coots International, Inc. 2010)

Coordinate transformations are needed to convert the measurement data into the direction vectors. Instead of using rectangular (x, y, z) -coordinates, the direction is measured in terms of two angles:

- *Azimuth*: the clockwise angle in horizontal (x, y)-plane with respect to Magnetic North.
- *Inclination Angle*: the vertical clockwise angle (by right-hand rule) with respect to *True Vertical Distance* (TVD); the vertical component.

Both types of angles are shown in Figure 1-3.

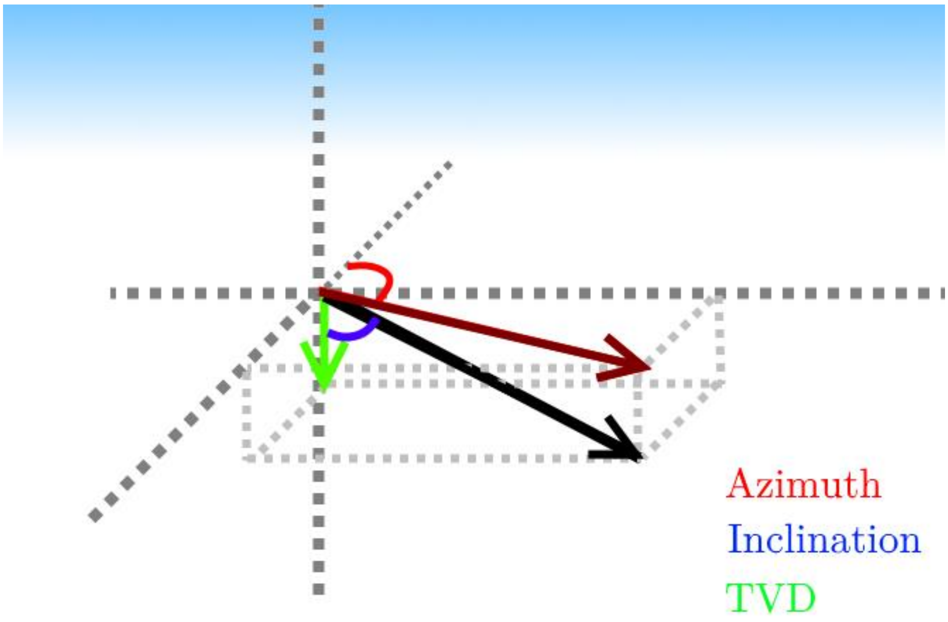

Figure 1-3: Direction of drill bit in Downhole direction. Azimuth, Inclination Angle, True Vertical Distance.

Once the size of TVD is known, then the vector representation of direction can be converted into its corresponding angular representation and vice versa.

As for the drill bit position, again instead of using rectangular coordinates, the position is expressed in North, East and Vertical coordinates. Additionally, any vector in general can also be represented with two vectors: a horizontal component along the Earth's surface and a vertical component, which is *Earth's reference frame*.

Overall methodology

To determine the desired position of BHA, the following steps are taken:

> **Step 1**: A drilling trajectory is modelled in advance. This trajectory has finite length; it has a starting position and a final position. The drill bit can move in any direction: this type of drilling is called *Directional Drilling*. On the trajectory, a discrete amount of measurement positions is taken: these are called *Stations*. For example, they can be taken each 100 meters in actual travelled distance. The actual travelled distance between starting position and position of drill bit is *Along-Hole Measured Depth* (AHD), and is always known in every Station, simply by counting the amount of drill pipe joints inserted into the borehole. See Figure 1-4.

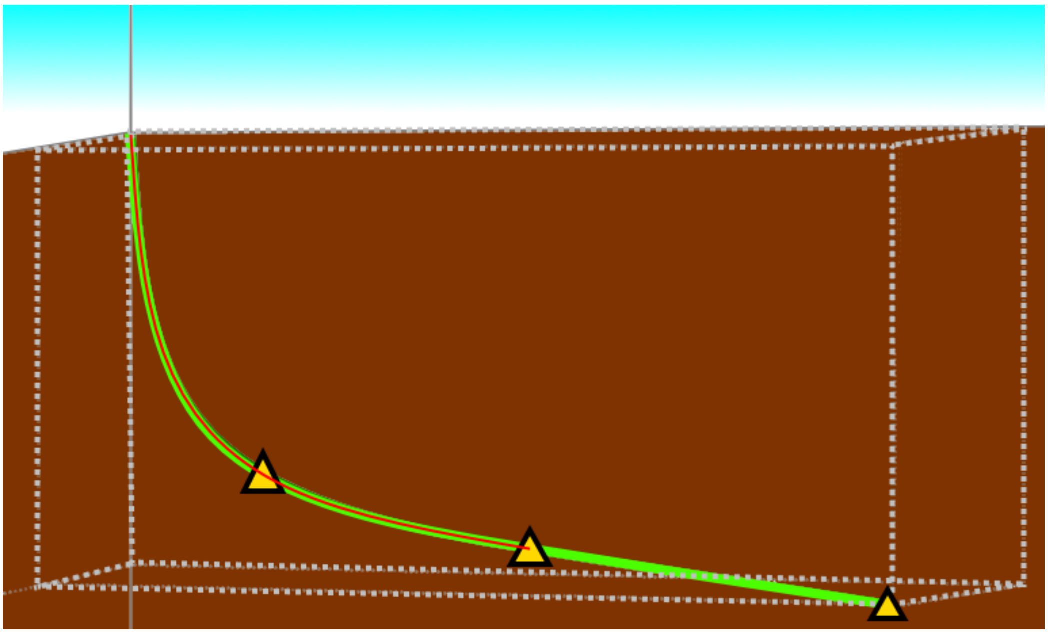

Figure 1-4: Modelled trajectory (green), including several Stations (yellow). AHD between origin and second Station is length of red curve.

Step 2: During drilling, it is assumed that the path taken by the drill bit is the modelled path. Measurements are made in each Station using the MWD tools:

- Three magnetometers are available, which measure the local Earth's magnetic field strength, from which the angle of incidence w.r.t. the Earth's horizon (*Dip Angle*) can be inferred. One magnetometer per space component, and all magnetometers work independently from each other. The data collected by these magnetometers is used to calculate Azimuth.
- Similarly, three accelerometers, which measure drill bit acceleration. The accelerometer data is used in the calculation of both Azimuth and Inclination Angle. Additionally, the TVD can be determined by this data.

Magneto- and accelerometers provide *measurement data* for six variables in each Station: three magnetic field strengths variables and three acceleration variables.

Step 3: The next step is to convert MWD measurement data into direction vectors using the earlier mentioned coordinate transforms, which involve matrix rotation operations: involving a Tool Face matrix, an Inclination matrix and an Azimuth matrix. This model is fully described in (Boots & Coots International, Inc. 2010), and only its main results to be used in this thesis will be given.

Thus, the result is a *Survey* containing the AHD, TVD, Inclination Angle and Azimuth for each Station. Examples of Surveys to be used in this thesis are given in chapter Data, on page 49.

Step 4: The final step is to convert the Survey of direction data into the overall (continuous) trajectory of the drill bit. Various methods of trajectory approximation used in the well-bore industry exist: the standard mathematical method employed in this thesis is called *Minimum Curvature Method* (Amorin and Broni-Bediako 2010), which gives a close approximation of the overall trajectory.

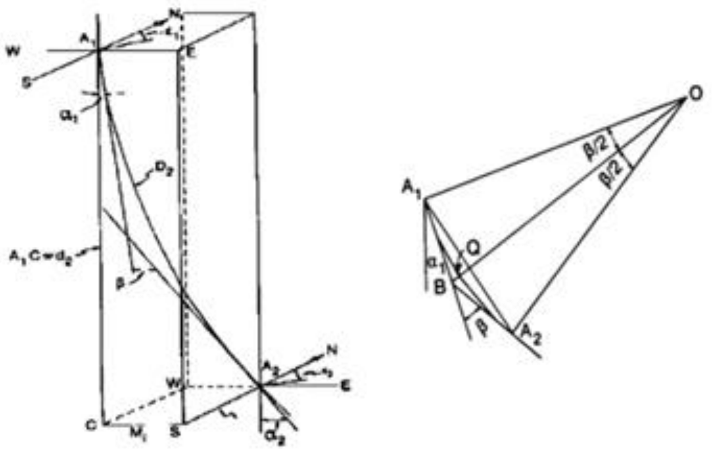

Figure 1-5: Visual representation of Minimum Curvature Method (left). Dogleg Angle helper variable (right). Source: (Amorin and Broni-Bediako 2010)

See Figure 1-5. In MCM, the trajectory taken between two consecutive Stations is assumed to be part of a circular arc, preserving the directions at each Station. This thesis assumes that MCM returns no errors in determining the trajectory, that is, the outputted trajectory associated with the Survey of direction data is the actual trajectory taken. (Amorin and Broni-Bediako 2010) provides a full mathematical description.

The overall methodology results in one of the main quantities of interest in this thesis: the final position (at the last Station) of the drill bit.

Notes and in-chapter sources

- The various definitions mentioned in the beginning can be found in several Wikipedia articles, which are only provided for clarification and are not of great importance in the overall thesis, since the focus is not on the engineering side of things.
    - https://en.wikipedia.org/wiki/Borehole
    - https://en.wikipedia.org/wiki/Measurement_while_drilling
    - https://en.wikipedia.org/wiki/Drill_bit_(well)
    - https://en.wikipedia.org/wiki/Drill_pipe
    - https://en.wikipedia.org/wiki/Drill_string
    - https://en.wikipedia.org/wiki/Drilling_fluid
    - https://en.wikipedia.org/wiki/Bottom_hole_assembly
- The two sections “A short note on position coordinates and orientations” and “Overall methodology” are cited from (Boots & Coots International, Inc. 2010) and (Elshabrawy 2018), respectively.
- When dealing with Azimuth, it is possible to use *True North* instead of Magnetic North. The difference in Azimuth then becomes *Declination Angle*. A second kind of North is *Grid North*. True and Grid North are outside the scope of this thesis.
- The curvature of Earth is disregarded.

- In this thesis, the capitalized term “Survey” refers exclusively to Survey of direction vectors. In practice, it may also be associated with measurement data.

Chapter 2 Errors, Multi-Station Analysis, problem formulation and research questions

Measurement errors in Step 2 of the overall methodology (page 14) lead to errors in determining the final position of the drill bit. Causes of measurement errors, as well as several solutions, are included in the following table:

Type	**Factors**	**Solutions**
External	Magnetic interference of objects near drill (ex.: steel drill string), self-magnetization, background noise	NMDC (physical), MIC (mathematical)
Internal	Systematic measurement errors in magnetometers and/or accelerometers (calibration), misalignment and/or displacement of MWD tools with respect to drill bit	Multi-Station Analysis (mathematical)
Other	Errors in control, manual displacement or external forces (earthquakes/shifting)	Not applicable

Table 1: Potential measurement error factors involved in uncertainty of final position. External factors and internal factors cited from (Elshabrawy 2018).

A Non-Magnetic Drill Collar minimizes magnetization effects. Its usage requires that its length needs to be of sufficient size, but this has severe drawbacks (Elshabrawy 2018), including:

- Long NMDC may make Directional Drilling control more difficult
- NMDCs are less strong than steel drill collars
- High costs of both usage and potential loss of NMDC

To keep NMDC length small, other solution techniques are employed: *Magnetic Interference Correction* (MIC) and *Multi-Station Analysis*, which are both independent methods to correct erroneous measurement data. Both methods reduce the error of the final position.

Below some brief descriptions of two MIC techniques:

- *Axial MIC* (a.k.a. Single-Station Analysis/SSA): a mathematical method in which only the Downhole direction measurements are corrected, independently for each Station.
- *Cross-Axial MIC*: method to reduce measurement errors in Tool Face plane (High Side/High Side Right) by taking multiple “rotational shots” in each Station: a minimum of four is recommended.

Both MIC methods are recommended by the drilling industry, however, the usage thereof has limitations: see (Elshabrawy 2018), chapter 2.

Multi-Station Analysis

This thesis will solely focus on *Multi-Station Analysis*, which is a mathematical method that seeks to determine the systematic errors in the magnetometer data, caused internally by the magnetometers (Elshabrawy 2018). It also relies on the assumption that no errors are present in the accelerometer data (at least for the purposes of this thesis).

The systematic errors in the magnetometer data are divided in two parts:

- A scale error, which is modelled through a *Scale Factor*.
- A bias error, which is modelled through a *Bias Factor*.

Both are due to signal gain and signal offset respectively, because of signal processing in the magnetometers. They are consistent in each Station, that is, they do not change across different Stations. The effect of Scale/Bias Factors can be seen in Figure 2-1.

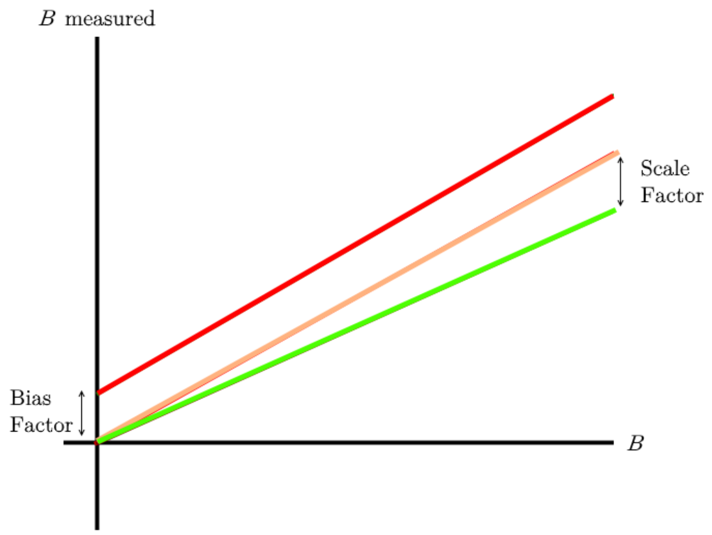

Figure 2-1: Total effect of Scale and Bias Factor in one magnetometer measurement (field strength)

Since there are three magnetometers in total, there are three Scale Factors and three Bias Errors, which may differ from each other due to their independence.

In addition to systematic errors, noise may also affect the magnetometer data. All in all, each Station produces *local errors* in the magnetometer data, composed of both systematic and random errors. The local measurement errors can accumulate as more measurements are taken and thus may produce errors in determining the final position. (This is formally called the *propagation of errors*.)

Execution steps and problem issues of Multi-Station Analysis

The mathematical process of MSA is based on the patent (Brooks 1997) and worked out in (Noy 2018). Assumed prior knowledge of mathematics is included for reference in Background information on page 46. In layman terms, MSA does the following:

Step A: Start with erroneous measurement data produced in Step 2 of the overall methodology (page 14), which can either be acquired through:

1. Direct measurement with MWD tools on location, that is, at an actual drilling site
2. Simulation by calculating measurement data based on modelled trajectory and artificial addition of Scale/Bias Factors and noise

Since the local measurement errors are not given a priori, MSA also requires local geomagnetic reference measurements - *High Definition Geomagnetic Model* (HDGM) - to be able to compare measurements. This model consists of one magnetometer measurement at the Earth's surface, represented in Earth's reference frame. The associated field strength and Dip Angle are assumed to be constant in all Stations.

Step B: Next, a minimizing function for the local errors is set up, written in terms of the six Scale and Bias Factors, which are independent variables of the function. This involves the least squares error between *corrected* measurement data and HDGM reference.

Step C: Minimizing this function yields the best Scale and Bias Factors, that is, the parameters that fit the data best, which is the *MSA solution*. Mathematically, the MSA solution is a stationary minimum of the least squares error function: each partial derivative with respect to each variable evaluated in the MSA solution is equal to zero. Thus, a system of non-linear equations needs to be solved. This can be done numerically through the method of Newton-Raphson, which is the algorithm of interest in this thesis.

Step D: The MSA solution is used to correct erroneous data. Finally, a drill operator can recalibrate the magnetometers, so that future drilling operations are improved.

However, MSA as described here is not fully without flaws:

- It does not obtain the (random) noise errors.
- HDGM reference is subject to measurement errors.
- To ensure that MSA yields improved results and to prevent misapplication, erroneous magnetometer measurement data has to satisfy certain minimum conditions before it can be applied (Nyrnes, Torkildsen, and Wilson 2009). These conditions are specified in Table 2, page 6 of the paper. Examples of parameters where such conditions apply include:
    - MSA solution: Scale/Bias parameters.
    - maximum noise.
    - maximum error in a single Survey.

  In practice, not all minimum conditions may be satisfied: the parameters of those that are not satisfied cannot be determined reliably through MSA. The paper suggests several modifications to the overall methodology (for example, clean-up), which takes these minimum conditions into account: these are specified on Figure D-1, page 12.
- The Newton-Raphson algorithm requires an approximate starting MSA solution close to the actual MSA solution to produce an output. However, in practice, the MSA solution is not known beforehand. If the starting MSA solution is not chosen well, then the Newton-Raphson algorithm may produce an unacceptable (local) MSA solution, which does not fully minimize the non-linear least-squares error function, or the algorithm may not terminate and not produce a solution at all. Therefore, MSA algorithm is an *ill-posed problem*.
- MSA is ill-conditioned. This is described in Chapter 6.
- MSA solution may also contain numerical errors caused by termination at final iteration of the Newton-Raphson algorithm: these are *iteration errors*.

- To a lesser extent: errors by utilization of a computer, like *rounding errors*. While there have been real-world instances in which rounding errors has led to catastrophic results, these have not been observed during this research and as such this thesis does not cover this aspect.

Thus, MSA will result in the presence of a *global error* in final drill bit position but it is expected that this error is reduced in comparison to not applying MSA. Unfortunately, there are instances in which position error increases after applying MSA: an example is found on page 41.

Implementation of MSA in overall methodology

Once MSA has been applied on the erroneous measurement data, step 3 and 4 in the overall methodology (page 14) are carried out on the corrected measurement data. Figure 2-2 is a conceptual visualization of the overall methodology, including the MSA process.

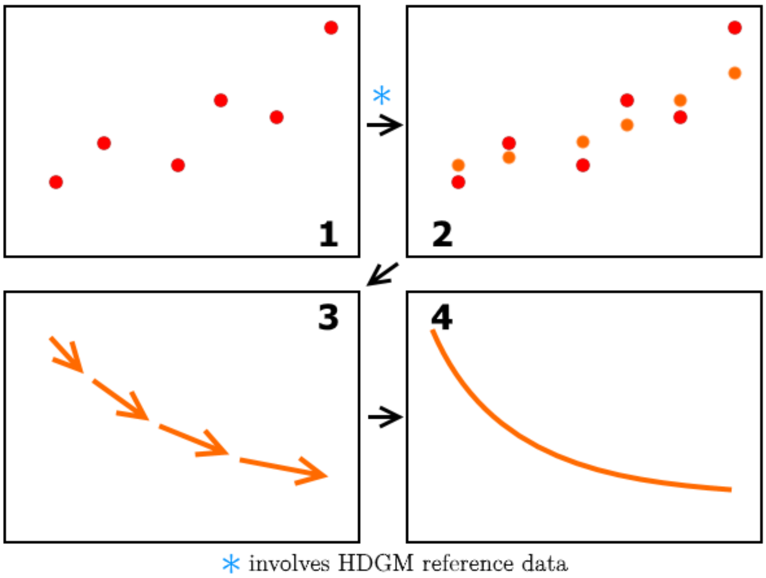

Figure 2-2: Summary of overall methodology. (1) Erroneous measurement data. (2) Partial or full correction with MSA. (3) Conversion to Survey of directions. (4) Minimum Curvature Method yields estimated trajectory of drill bit

It is noted that this process can be done in backwards order, starting with the modelled trajectory of the drill bit. Once the Stations are specified, a Survey of direction vectors is acquired, which is then converted to measurement data using modelled HDGM. This allows for simulation of *uncertainties*.

Table 2 summarizes the data that is being tracked in this process:

Measurement data	Survey of directions	Trajectory (after MCM)
AHD	AHD	AHD
Accelerometer data	Azimuth	Position vectors
Magnetometer data	Inclination Angle	(w.r.t. rectangular
(w.r.t. BHA orientation)	Tool Face	coordinates)

Table 2: Tracked quantities of overall methodology

The effect of MSA is shown in Figure 2-3, showing three different types of drill bit trajectories.

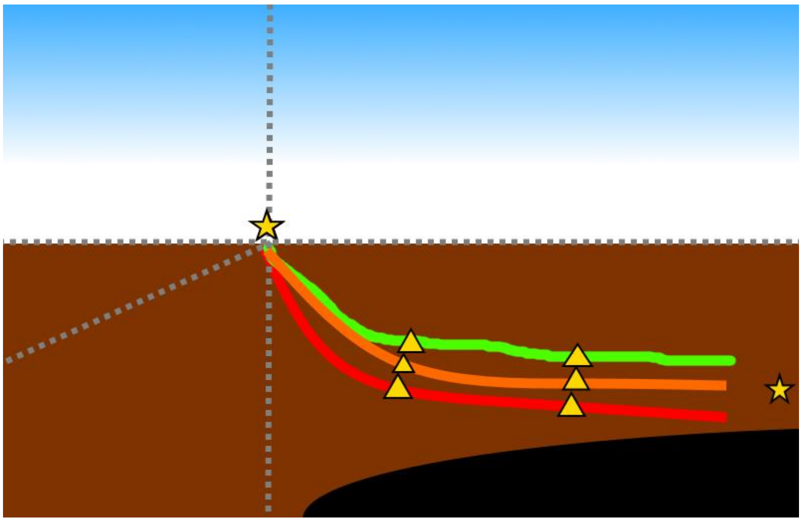

Figure 2-3: Effect of MSA. Trajectory based on erroneous data (red), correction after MSA (orange), actual trajectory taken by drill bit (green). Trajectories not on scale and greatly exaggerated.

The overall methodology results in the presence of two types of global error in the final position: one before applying MSA and one after. The latter is of interest in this thesis and will be explained in Chapter 4, on page 29.

What has been done so far

A master's thesis has been written on MSA - a Microsoft® Excel spreadsheet has been prepared, in which the effect of MSA's ability to correct errors is tested on five Surveys in five different MSA-scenarios (Elshabrawy 2018):

1. All five Surveys, all 3 Bias errors only, no HDGM error, no noise.
2. All five Surveys, all 6 Scale and Bias errors, no HDGM error, no noise.
3. All five Surveys, all 6 Scale and Bias errors, with HDGM error, no noise.
4. All five Surveys, only Bias error in Downhole direction, with HDGM error, no noise.
5. One Survey, with HDGM error, with noise:
    a. All 6 Scale and Bias errors
    b. All 3 Bias errors only
    c. Only Bias error in Downhole direction.

All noise errors have been simulated: they are assumed to be independent and identically distributed (i.i.d.) to be generated from a uniform distribution. Only Azimuth error in each Station has been determined, on which *sensitivity analysis* is performed: Azimuth error in the final Station is compared with the condition number of the Jacobian evaluated in the MSA solution. Additionally, a relationship between said condition number and quality of MSA solution is speculated (Noy 2018).

Overview of this thesis

The main research question of this thesis is: *What is the uncertainty of the MSA solution, i.e. the uncertainty of the bias solution and the scale factor solution?*

The main objective of the thesis is to derive a method that describes this uncertainty. Also, its effect on determining the final drill bit position is studied. To this end, the project mentors have provided the following background sources:

- Partial excerpts of aforementioned master's thesis on MSA (Elshabrawy 2018)
- Microsoft® PowerPoint slides on MSA (internal Shell document)
- Two additional Microsoft® Excel spreadsheets, which requires activation of the "Solver Add-in", provided by default in Excel:
  - Spreadsheet 1: basic implementation and application of only MSA + MSA sensitivity analysis, used in (Elshabrawy 2018)
  - Spreadsheet 2: implementation of overall methodology: MSA + MSA sensitivity analysis + MCM
- Additional Surveys of direction data for testing MSA in this thesis, as well as accompanying final position vectors uncertainties without MSA from a proprietary model by the drilling industry
- Various digital research papers regarding:
  - Measurement data to Survey conversion process (Boots & Coots International, Inc. 2010)
  - Minimum Curvature Method (Amorin and Broni-Bediako 2010)
  - Minimum requirements of MSA (Nyrnes, Torkildsen, and Wilson 2009)
  - Validation of MSA (Hanak, Wilson, and Gjertsen 2015)
  - HDGM error model (Maus et al. 2012)

This thesis consists of two parts, the details of which will be explained later:

1. Quantifying MSA solution uncertainty with Monte Carlo simulation as well as its effect on final drill bit position uncertainty.
2. Establishing quality control of MSA: determining whether condition number in Newton-Raphson in MSA solution is a representative measure of MSA solution quality.

All results are compared with an uncertainty model from the well-bore industry.

Stakeholders in drilling technologies hope that the techniques of MSA described in this thesis will supplement and/or replace previously existing methodologies like SSA or SUCOP (internal method developed by Shell).

Chapter 3 Model description

In this chapter, the ideas explained thus far will be formalized by giving a complete well-formulated mathematical description. First, the variables used in the model are defined. Next, the relations between these variables are cited, without proof.

Variables

This thesis utilizes the following quantities and units:

Quantity	Unit	Shorthand
Distance	meters	m
Acceleration	meters per second squared	m/s^2
G-force	g	g
Angle	radians (default) degrees	rad °
Field strength	tesla microtesla (default) nanotesla	$T = Vs/m^2$ $\mu T = 10^{-6}$ T $nT = 10^{-3}\ \mu T = 10^{-9}$ T

Table 3: Used quantities and units

Table 4, Table 5 and Table 6 denote the most important variables used throughout this thesis: one table for each relevant step in the process.

	Variable	Domain	Description
Input	N	$\mathbb{N}$	amount of Stations
	i	$\mathbb{N}$	index for Station, $1 \le i \le N$
Input HDGM reference	B_{hr}	$\mathbb{R}$	horizontal component magnetic field HDGM reference in all Stations
	B_{vr}	$\mathbb{R}$	vertical component magnetic field HDGM reference in all Stations
Input erroneous measurement data	B_{xic}	$\mathbb{R}$	measured uncorrected x-component magnetometer in Station i
	B_{yic}	$\mathbb{R}$	measured uncorrected y-component magnetometer in Station i
	B_{zic}	$\mathbb{R}$	measured uncorrected z-component magnetometer in Station i
	G_{xic}	$\mathbb{R}$	measured exact x-component accelerometer in Station i
	G_{yic}	$\mathbb{R}$	measured exact y-component accelerometer in Station i
	G_{zic}	$\mathbb{R}$	measured exact z-component accelerometer in Station i
Output corrected measurement data	B_{xi}	$\mathbb{R}$	corrected x-component magnetometer in Station i
	B_{yi}	$\mathbb{R}$	corrected y-component magnetometer in Station i
	B_{zi}	$\mathbb{R}$	corrected z-component magnetometer in Station i

	B_{vi}	$\mathbb{R}$	corrected vertical component magnetometer in Station i
	B_{hi}	$\mathbb{R}$	corrected horizontal component magnetometer in Station i
Output MSA solution	ϵ_{xS}	$\mathbb{R}$	x-Scale Factor magnetometer in all Stations
	ϵ_{yS}	$\mathbb{R}$	y-Scale Factor magnetometer in all Stations
	ϵ_{zS}	$\mathbb{R}$	z-Scale Factor magnetometer in all Stations
	ϵ_{xB}	$\mathbb{R}$	x-Bias Factor magnetometer in all Stations
	ϵ_{yB}	$\mathbb{R}$	y-Bias Factor magnetometer in all Stations
	ϵ_{zB}	$\mathbb{R}$	z-Bias Factor magnetometer in all Stations

Table 4: MSA variables, w.r.t. orientation of BHA: x=HS + Tool Face Angle, y=HSR + Tool Face Angle, z=Downhole direction

	Variable	Domain	Description
Input	(erroneous) measurement data. See also MSA variables.		
Output Survey	T	$\mathbb{R}$	Tool Face Angle
	I	$\mathbb{R}$	Inclination Angle
	A	$\mathbb{R}$	Azimuth

Table 5: Variables for conversion between data and Survey.

	Variable	Domain	Description
Input	Survey of direction vectors. See also MSA variables and conversion between data and Survey.		
	I_1	$\mathbb{R}$	Inclination Angle in a Station
	I_2	$\mathbb{R}$	Inclination Angle in next Station
	A_1	$\mathbb{R}$	Azimuth in a Station
	A_2	$\mathbb{R}$	Azimuth in next Station
	ΔMD	$\mathbb{R}$	measured distance (length) between Stations (which is taken from differences in AHD)
Output	β_{ic}	$\mathbb{R}$	Dogleg Angle (helper variable)
	RF	$\mathbb{R}$	Ratio factor (helper variable)
	ΔE	$\mathbb{R}$	displacement drill bit in East direction
	ΔN	$\mathbb{R}$	displacement drill bit in North direction
	ΔV	$\mathbb{R}$	displacement drill bit in True Vertical direction

Table 6: Variables for Minimum Curvature Method, outputting displacements in rectangular coordinates.

Formulas and equations

The equations to be described are consistent with the provided Excel spreadsheets. Modelled position vectors are assumed to be contained in one quadrant of 3D space. However, due to measurement errors, it leaves open the possibility that erroneous and corrected drill bit trajectories leave this quadrant.

MSA: magnetometer error model

MSA assumes the presence of systematic errors in the three magnetometers, which is the MSA solution, and are mathematically modelled by Scale and Bias Factors: the variables

$\epsilon_{xB}, \epsilon_{yB}, \epsilon_{zB}, \epsilon_{xS}, \epsilon_{yS}, \epsilon_{zS}$ as in Table 4. Based on Figure 2-1, the relations between uncorrected and corrected magnetometer data are:

$$
\begin{aligned}
E[B_{xic}(\epsilon_{xS}, \epsilon_{xB})] &:= \epsilon_{xS} B_{xi} + \epsilon_{xB} \\
E[B_{yic}(\epsilon_{yS}, \epsilon_{yB})] &:= \epsilon_{yS} B_{yi} + \epsilon_{yB} \\
E[B_{zic}(\epsilon_{zS}, \epsilon_{zB})] &:= \epsilon_{zS} B_{zi} + \epsilon_{zB}
\end{aligned} \tag{3.1}
$$

Uncorrected measurements $B_{xic}, B_{yic}, B_{zic}$ include additional stochastic error terms, representing random noise. The probability distribution of these error terms will have to be specified. Throughout the remainder of this thesis, they are assumed to be i.i.d. and normally distributed with zero mean, justifying the use of the expectation operators on the left-hand side of (3.1). Even though MSA does not find the outcome of the stochastic noise terms in erroneous measurement data, the above equations will still be used for correction, leading to these correction formulas:

$$
\begin{aligned}
B_{xi} &= \frac{B_{xic} - \epsilon_{xB}}{\epsilon_{xS}} \\
B_{yi} &= \frac{B_{yic} - \epsilon_{yB}}{\epsilon_{yS}} \\
B_{zi} &= \frac{B_{zic} - \epsilon_{zB}}{\epsilon_{zS}}
\end{aligned} \tag{3.2}
$$

where $\epsilon_{xB}, \epsilon_{yB}, \epsilon_{zB}, \epsilon_{xS}, \epsilon_{yS}, \epsilon_{zS}$ are found by MSA. If these coincide with actual MSA solution, then only random errors remain, which are small compared to the systematic errors.

MSA: HDGM error model

HDGM reference measurements are composed of field strength B and Dip Angle Θ. Equivalent HDGM reference measurements B_{hr}, B_{vr} - with respect to Earth's reference frame - are extracted by performing the following coordinate transformation with polar coordinates, which is easily derived using geometric arguments from Figure 3-1:

$$
\begin{aligned}
B_{hr} &= B\cos(\Theta) \\
B_{vr} &= B\sin(\Theta)
\end{aligned} \tag{3.3}
$$

Once errors are incorporated in field strength and Dip Angle, this yields erroneous HDGM measurements, from which the measurement data is compared against in MSA. Again, these errors come from stochastic error terms, which are also assumed to be normal with mean zero.

MSA: mathematical process

Defining the following helper variables, from (Noy 2018), sourced from (Brooks 1997):

$$
\begin{aligned}
B_{vic}(\epsilon_{xB}, \epsilon_{yB}, \epsilon_{zB}, \epsilon_{xS}, \epsilon_{yS}, \epsilon_{zS}) &:= \frac{B_{xic}G_{xi} + B_{yic}G_{yi} + B_{zic}G_{zi}}{(G_{xi}^2 + G_{yi}^2 + G_{zi}^2)^{0.5}} \\
B_{hic}(\epsilon_{xB}, \epsilon_{yB}, \epsilon_{zB}, \epsilon_{xS}, \epsilon_{yS}, \epsilon_{zS}) &:= (B_{xic}^2 + B_{yic}^2 + B_{zic}^2 - B_{vic}^2)^{0.5}
\end{aligned} \tag{3.4}
$$

These represent, respectively, the vertical and horizontal component of measured magnetometer data, which can be seen in Figure 3-1. Similar formulas hold for corrected magnetometer data B_{vi}, B_{hi}.

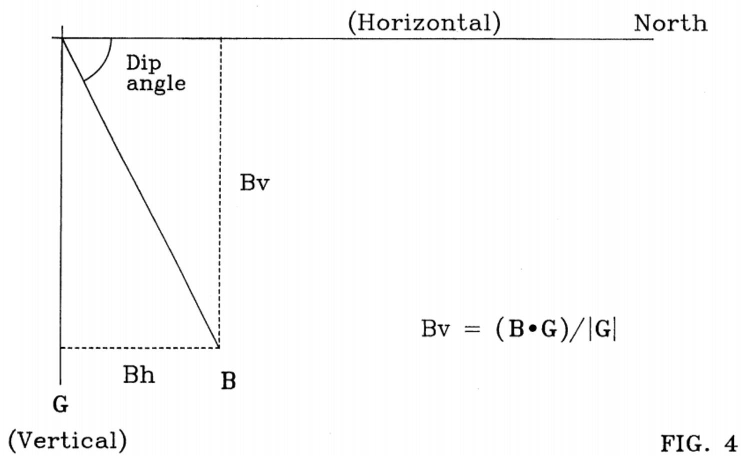

Figure 3-1: Vertical and horizontal component of magnetometer data. Source: (Brooks 1997), Figure 4.

Using these helper variables, the MSA solution associated with erroneous magnetometer measurements is found by minimizing the following non-linear least squares error function, where corrected measurement data is compared against provided HDGM reference measurements:

$$L(\epsilon_{xB}, \epsilon_{yB}, \epsilon_{zB}, \epsilon_{xS}, \epsilon_{yS}, \epsilon_{zS}) := \sum_{i=1}^{N} (B_{hi} - B_{hr})^2 + (B_{vi} - B_{vr})^2 \quad (3.5)$$

This is done by setting its partial derivatives to zero, yielding a system of non-linear equations, which is then solved with Newton-Raphson. The algorithm is specified in full on page 46. In each iteration, Newton-Raphson involves the calculation of multiple real symmetric Jacobian matrices. The condition number of the Jacobian in the final iteration is of interest, which is to be calculated using eigenvalues (see page 47). All formulas required for the calculation of the Jacobian matrix are stated in (Noy 2018).

In this thesis, uncertainty in the HDGM reference measurements is assumed. Therefore, the measurements B_{hr}, B_{vr} in (3.5) refer to erroneous measurements.

Simulation: conversion of Survey to measurement data

To be able to perform simulation, Surveys of direction data of modelled trajectories need to be converted to measurement data using HDGM, which are then used as MSA input. The equations needed are coordinate transforms (Boots & Coots International, Inc. 2010), page 28:

$$
\begin{aligned}
G_x &= -g \cdot \cos(T) \cdot \sin(I) \\
G_y &= g \cdot \sin(T) \cdot \sin(I) \\
G_z &= g \cdot \cos(I) \\
B_x &= (\cos(T)\cos(I)\cos(A) - \sin(T)\sin(A)) \cdot B_{hr} - (\cos(T)\sin(I)) \cdot B_{vr} \\
B_y &= (-\sin(T)\cos(I)\cos(A) - \sin(T)\sin(A)) \cdot B_{hr} + (\sin(T)\sin(I)) \cdot B_{vr} \\
B_z &= (\sin(I)\cos(A)) \cdot B_{hr} + (\cos(I)) \cdot B_{vr}
\end{aligned}
\tag{3.6}
$$

The variable g represents a gravitational constant, which in simulation is set to 1, since g does not affect the direction vectors of the drill bit. Also, the HDGM reference measurement data B_{hr}, B_{vr} in (3.6) refer to modelled HDGM reference measurements, not erroneous HDGM measurements.

Conversion of measurement data to Survey

Conversely, the HDGM measurements B, Θ can be extracted from known B_x, B_y, B_z using the following equations, both derived from Figure 3-1 using geometric arguments:

$$
\begin{aligned}
B &= (B_x^2 + B_y^2 + B_z^2)^{0.5} \\
\Theta &= \frac{\pi}{2} - \cos^{-1}\left[\frac{G_x B_x + G_y B_y + G_z B_z}{(G_x^2 + G_y^2 + G_z^2)^{0.5}(B_x^2 + B_y^2 + B_z^2)^{0.5}}\right]
\end{aligned}
\tag{3.7}
$$

Also, all three types of measurement data (erroneous data, corrected data after applying MSA, as well as data from a modelled trajectory acquired from the method described in the previous paragraph) can be converted to a Survey of direction vectors using the following equations: I from geometric arguments and T, A from (Boots & Coots International, Inc. 2010):

$$
\begin{aligned}
T &= \tan^{-1}\left(\frac{G_y}{-G_x}\right) \\
I &= \tan^{-1}\left[\frac{(G_x^2 + G_y^2)^{0.5}}{G_z}\right] \\
A &= \tan^{-1}\left[\frac{-B_{hsr}}{B_{hs}\cos(I) + B_z \sin(I)}\right]
\end{aligned}
\tag{3.8}
$$

with B_{hsr}, B_{hs} defined by:

$$
\begin{aligned}
B_{hsr} &= B_x \sin(T) + B_y \cos(T) \\
B_{hs} &= B_x \cos(T) - B_y \sin(T)
\end{aligned}
\tag{3.9}
$$

From (3.8), note that there are no errors in Tool Face Angle and Inclination measurements - all measurement errors in magnetometer measurements lead to Azimuth errors. However, due to the presence of arctangent in Azimuth, if arctangent is treated as an ordinary function, then its range is restricted from -90 to 90 degrees, which leads to position degeneracy when modelled Azimuth is close to these values: see Figure 3-2. In the Excel simulation to be performed in subsequent chapters of this thesis, this scenario is avoided by using the atan2 function.

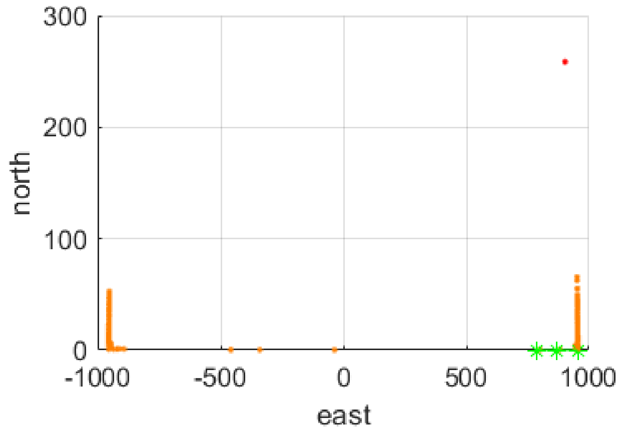

Figure 3-2: Effect of position degeneracy due to incorrect calculation of Azimuth.

Minimum Curvature Method

Given a Survey of direction vectors, define the following helper variables (Dogleg Angle and Ratio Factor respectively) for two consecutive Stations:

$$\begin{aligned} \beta_{ic} &= \cos^{-1}[\cos(I_2 - I_1) - \sin(I_1)\sin(I_2)[1-\cos(A_2 - A_1)]] \\ RF &= \frac{2}{\beta_{ic}} \cdot \tan\left(\frac{\beta_{ic}}{2}\right) \end{aligned} \tag{3.10}$$

Then, these equations for the displacement hold (Amorin and Broni-Bediako 2010):

$$\begin{aligned} \Delta E &= \frac{\Delta MD}{2} \cdot [\sin(I_1)\sin(A_1) + \sin(I_2)\sin(A_2)] \cdot RF \\ \Delta N &= \frac{\Delta MD}{2} \cdot [\sin(I_1)\cos(A_1) + \sin(I_2)\cos(A_2)] \cdot RF \\ \Delta V &= \frac{\Delta MD}{2} \cdot [\cos(I_1) + \cos(I_2)] \cdot RF \end{aligned} \tag{3.11}$$

In (Amorin and Broni-Bediako 2010) is also mentioned that whenever $\beta_{ic} < \frac{1}{4}$, then $RF = 1$ is set to avoid singularities. In this thesis, this is done when $\beta_{ic} = 0$.

The displacement equations yield an iterative algorithm which steps from the first Station right up until the second-last Station, determining approximate displacement and therefore the position vector of the drill bit in each next Station, all with respect to rectangular coordinates. The starting position is assumed to be the origin, but one may choose a different starting position if needed. If the first Station has a non-zero AHD, then the trajectory can only be partially determined. In the end, the desired final position follows.

Notes and in-chapter references

- A complete state-of-the-art reference guide regarding well-bore positioning and Multi-Station Analysis is "An Introduction to Wellbore Positioning" by Angus Jamieson et al., located at https://www.uhi.ac.uk/en/t4-media/one-web/university/research/eBook_V9_10_2017-redux.pdf.
- In (Noy 2018; Brooks 1997), Scale Factor terms $(1+\epsilon_{xS})$ etc. are used instead of ϵ_{xS} etc. as in (3.1), where the latter ϵ_{xS} etc. only represents percental change. Also, the Bias Factor errors in (3.1) are stated with a minus sign instead. These minor alterations do not lead to issues.
- The formula for North displacement is wrongly stated in (Amorin and Broni-Bediako 2010) and is corrected in this thesis.

Chapter 4 Mathematical methods of uncertainty analysis

Uncertainty analysis

The first goal is to find:

1. Uncertainty of MSA solution
2. Uncertainty of final drill bit position after MSA

Uncertainty analysis is employed, which is a branch of (pure) mathematics that studies functions of random variables: it quantifies uncertainties in the function image caused by uncertainties in its domain. A measure of uncertainty is any quantity that can be derived from the cumulative distribution function of the random variable (de Rocquigny, Devictor, and Tarantola 2008), chapter 1.2.3, page 9. Examples: standard deviation, or variance, or - in case of normality - deviation of a confidence interval. In this thesis, the latter definition has been chosen to allow for comparisons done in Chapter 5.

There are various methods to calculate uncertainty. Here, the main simulation method chosen is Monte Carlo simulation.

Uncertainty of MSA solution

As mentioned in section Implementation of MSA in overall methodology (page 20), the process to turn measurement data into drill bit trajectory can be reversed. In modelling, the actual final position of interest is known. From the conversion process, the measurement data follows. Scale/Bias Factors are modelled in advance. These are then incorporated, and background noise is generated and added. This yields artificial erroneous measurement data, which is assumed to be representative for measurement on location. The erroneous measurement data is then partially or fully corrected by MSA.

In simulation, this process can be generated repeatedly, yielding a *sample* of MSA solutions, which can be plotted in a histogram. After scaling, this histogram approximates a *probability density function* for MSA solution, which describes the MSA solution uncertainty. Approximated values for MSA solution uncertainty are calculated from the sample.

Uncertainty of final drill bit position

A similar method applies for the uncertainty of the final position. Repeating the steps above: after applying MSA, conversion from measurement data to Survey and finally MCM yields a corrected trajectory, as well as new final position. Again, simulation yields uncertainty of final position.

Since the uncertainty of the final position is bounded, it can be geometrically represented as an ellipsoid centered around the actual final position. The accompanying deviations from the actual final position along its axes of symmetry form a measure for the maximum global error uncertainty in each axis. Depending on the error model, MSA process enables shrinking of the position uncertainty ellipsoid: the result is the final position uncertainty after MSA. The MSA position uncertainty ellipsoid needs to be determined, which is specified through the *absolute global error uncertainties*. See Figure 4-1.

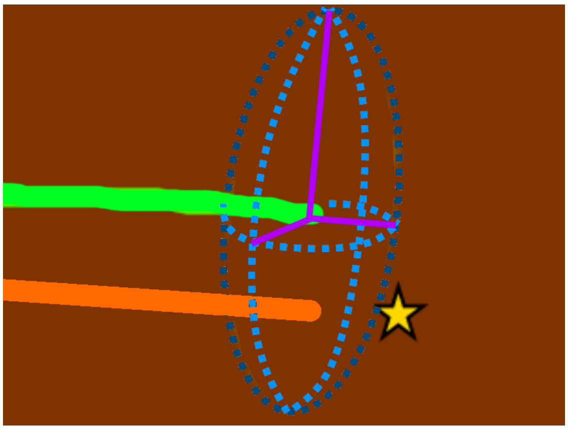

Figure 4-1: Uncertainty ellipsoid after MSA. Actual trajectory (green), trajectory after MSA (orange). Absolute global error uncertainties (purple).

Transformation to borehole coordinates

However, what may occur is that the MSA uncertainty ellipsoid is slightly tilted (not aligned in Downhole direction), whereas uncertainty is determined from position vectors that are represented in rectangular coordinates. The equations to transform position uncertainties from North, East and Vertical coordinates to borehole HS, HSR, Downhole coordinates are given in (Williamson 2000), Appendix A:

$$
\begin{aligned}
T &= \begin{pmatrix} \cos(I_N)\cos(A_N) & -\sin(A_N) & \sin(I_N)\cos(A_N) \\ \cos(I_N)\sin(I_N) & \cos(A_N) & \sin(I_N)\sin(A_N) \\ -\sin(I_N) & 0 & \cos(I_N) \end{pmatrix} \\
C_{hla} &= T^{\mathrm{T}} C_{nev} T \\
\sigma_H &= \sqrt{C_{hla}[1,1]} \\
\sigma_L &= \sqrt{C_{hla}[1,1]} \\
\sigma_A &= \sqrt{C_{hla}[1,1]}
\end{aligned} \tag{3.12}
$$

where C_{hla}, C_{nev} are covariance matrices, both related by the above orthogonal transformation. These equations are not considered in the sequel: this thesis only considers North, East and Vertical uncertainties.

Monte Carlo simulation: theory on averages

In general, the expectation of a real single-valued random variable X can be calculated directly by definition of $E(X)$. In case of a continuous random variable, $E(X)$ is an integral. To evaluate this, Monte Carlo simulation provides a probabilistic way: from M replications $X_i \simeq X$, independent and identically distributed, the average is taken:

$$a_M := \frac{1}{M}\sum_{i=1}^{M} X_i$$

a_M is an unbiased estimator for $E(X)$, which has variance $\frac{V(X_i)}{M}$.

An unbiased estimator for the variance $V(X)$ is:

$$b_M^2 := \frac{1}{M-1}\sum_{i=1}^{M}\left(X_i - a_M\right)^2$$

Based on the central limit theorem, for large values of M, the estimator a_M has approximately a normal distribution, from which a 95% confidence interval for $E(X)$ can be constructed, given by:

$$\left[a_M - \frac{1.96 b_M}{\sqrt{M}}, a_M + \frac{1.96 b_M}{\sqrt{M}}\right]$$

The choice of M affects, and therefore also controls, the quality of estimating the expectation. A trade-off between computational power and precision must be made.

This theory can be generalized for multi-valued random variables. In application, X either represents the MSA solution or the final drill bit position. Their expectations should be close to their modelled quantities, which is representative for the quality of MSA performance.

Monte Carlo simulation: uncertainty

Additionally, if X is normally distributed, then one may verify that a 95% confidence interval of X is given by:

$$\left[a_M - 1.96 b_M, a_M + 1.96 b_M\right]$$

The deviation $1.96 b_M$ represents the uncertainty in X. Simulation gives an approximation of both 95% confidence interval and uncertainty.

The number 1.96 is a *critical value*, associated with 95% confidence level. These values are assumed throughout this thesis. However, if a different percentage confidence level is needed, then all values 1.96 need to be replaced with:

Confidence level (%)	Critical value (approximates)
95	1.96
95.44	2
99	2.57 or 2.58
99.74	3

Table 7: Table of critical values

In case the normal condition does not hold, but good enough as an approximation, then the above deviation of the confidence interval can still be used as a representative measure of uncertainty. Additional analysis like transformation and probability density fitting methods can be employed to improve the uncertainties: these are not employed here in this thesis.

If none of the above is possible, then only standard deviation is used as a measure of uncertainty. However, most probability density functions in this thesis turn out to approximately follow a normal distribution, which can be seen visually in plots and/or using normality tests. In cases where this does not hold true, standard deviation is acquired by dividing 95% confidence deviation uncertainty results by critical value 1.96.

Homotopy method (optional)

As mentioned in Chapter 2, MSA is ill-posed. To acquire an MSA starting solution that is close enough to the unknown MSA solution associated with erroneous measurement data, the homotopy method for systems of non-linear equations is employed. A description of this method is found in (Kan, Segal, and Vermolen 2014), chapter 9.7.3, stated here with minor alterations. First, a starting function with a known root is required, which is taken to be:

$$f(\epsilon_{xB},\epsilon_{yB},\epsilon_{zB},\epsilon_{xS},\epsilon_{yS},\epsilon_{zS}) = (\epsilon_{xS}-1)^2\cdot(\epsilon_{yS}-1)^2\cdot(\epsilon_{zS}-1)^2\cdot{\epsilon_{xB}}^2\cdot{\epsilon_{yB}}^2\cdot{\epsilon_{zB}}^2$$

and the goal function is the MSA least-squares error function (3.5). Then, a reasonably large finite number k equations of the form

$$\lambda f(\epsilon_{xB},\epsilon_{yB},\epsilon_{zB},\epsilon_{xS},\epsilon_{yS},\epsilon_{zS}) + (1-\lambda)L(\epsilon_{xB},\epsilon_{yB},\epsilon_{zB},\epsilon_{xS},\epsilon_{yS},\epsilon_{zS}) = 0$$

is constructed, where $\lambda = 0, h, 2h, \ldots, 1$ and $0 < h < 1$ such that $kh = 1$. Solving each of these equations sequentially yields a desired starting solution. In application, since the least-squares error function may not have a root, instead of solving the above equations, the left-hand side is minimized instead.

Notes and in-chapter references

- For more general information regarding various methodologies and case studies of uncertainty and sensitivity analysis, see (de Rocquigny, Devictor, and Tarantola 2008) and (de Rocquigny 2012).
- The theory of Monte Carlo simulation is taken from (Higham 2004), chapter 15.
- The usage of Monte Carlo on a computer introduces additional sampling errors in determining the required uncertainties, due to:
    1. finite number of replications
    2. the usage of a pseudo random number generation algorithm

Usage of pseudo random generator may also lead to dependencies between random errors, violating the assumption of independency.
Ultimately, the determination of sampling errors is not considered here. To counter for these errors, a high number of replications is needed. Additionally, the uncertainty analysis can be repeated many times over again by resampling, leading to a bootstrap procedure which determines the variability and therefore the reliability of the results. This procedure has not been carried out in full by the author due to computational time.
However, based on the above criteria, by trial and error and no further knowledge of the variance to be determined, the author estimates a minimum of 900 replications for each simulation round is needed. Only 300 replications are performed for this thesis due to time constraints, where one simulation round has taken between 5 to 30 minutes, on average 10 minutes.

Chapter 5 Determining MSA solutions and final positions

Implementation in Excel

To apply Monte Carlo simulation, Spreadsheet 2 is used as basis for experimental setup, which simulates errors and performs MSA on erroneous measurement data.

For the purposes of this thesis, Spreadsheet 2 has been modified in various ways:

- Merged worksheet “Minimum Curvature Method” (Figure 8-3) in worksheet “MSA” (Figure 8-1, Figure 8-2). MCM is applied to modelled Survey, erroneous Survey and corrected Survey.
- Changed generation of background noise errors from uniform distribution to normal distribution, by applying a transform: see Background information, page 48.
- Separated columns for noise errors from erroneous measurement data.
- Implemented HDGM error model.
- Corrected erroneous copy-paste formulas.
- Increased the amount of Survey Stations that can be inserted as input.
- Implemented Monte Carlo simulation for both determining the uncertainty in MSA solution as well as final position uncertainty, using macros written in Microsoft Visual Basic for Applications 7.1 as well as MATLAB® R2018a code, communicating from and to Excel through MATLAB’s Spreadsheet Link® software.
- Implemented a small user interface (UI) for control of functionalities as well as various configuration settings. See Figure 8-4 and Figure 8-6.
- Implemented eigenvalue and condition number calculation by using matrix.xla, a third-party Excel add-in.
- Implemented robust MSA starting solution homotopy method.
- Removed redundant calculations.
- Implemented condition number heat plots using MATLAB.

The modified spreadsheet has the following major UI functionalities:

- Generate noise errors: done for magnetometer measurement data and HDGM.

- Get MSA starting solution: acquires MSA starting solution using either
    1. homotopy method (page 32)
    2. random guess close to modelled MSA starting solution

  depending on the user's configuration.
- MSA solve: performs minimization using the Solver add-in using an inputted MSA starting solution and returns MSA solution associated with measured data.
- Monte Carlo simulation: the above three functions are repeated M times, where M is configurable by the user. Its results are stored away in a separate sheet.
- Plot trajectory/Plot error distributions: generates plots of position vectors in several final Stations of modelled Survey, corrected MSA positions, MSA solutions. Histograms are also plotted.

Application of Monte Carlo simulation in MSA solution and global position uncertainty analysis

To acquire the uncertainties, Monte Carlo simulation is applied in the following way:

Input: Modelled Survey of direction data, modelled MSA solution, HDGM model, HDGM and magnetometer error model

Algorithm:

1. Insert modelled Survey of direction data in Excel spreadsheet.
2. Modelled Survey of direction data is automatically converted by Excel spreadsheet to modelled measurement data, and application of MCM gives *modelled final position vector*.
3. After pressing the "Monte Carlo simulation" button, M samples are generated in the following way:
    a. Generate normal errors in HDGM, as well as magnetometer noise
    b. Add errors to modelled measurement data, giving erroneous measurement data.
    c. Conversion is automatically applied to erroneous measurement data, giving *erroneous final position vector*.
    d. Retrieve and set MSA starting solution.
    e. Apply MSA, which returns MSA solution.
    f. The corrected measurement data is automatically calculated.
    g. Conversion is automatically applied to corrected measurement data, giving *corrected final position vector*.

    A list of M MSA solutions and corrected final position vectors has thus been acquired.
4. The required uncertainties are calculated by the methods in the previous chapter.

Output: uncertainty of MSA solution, uncertainty of final drill bit position vector. Optionally, with the modelled final position vector at hand, the uncertainty of absolute global error of final position vector can also be calculated.

Figure 5-1 summarizes the steps taken:

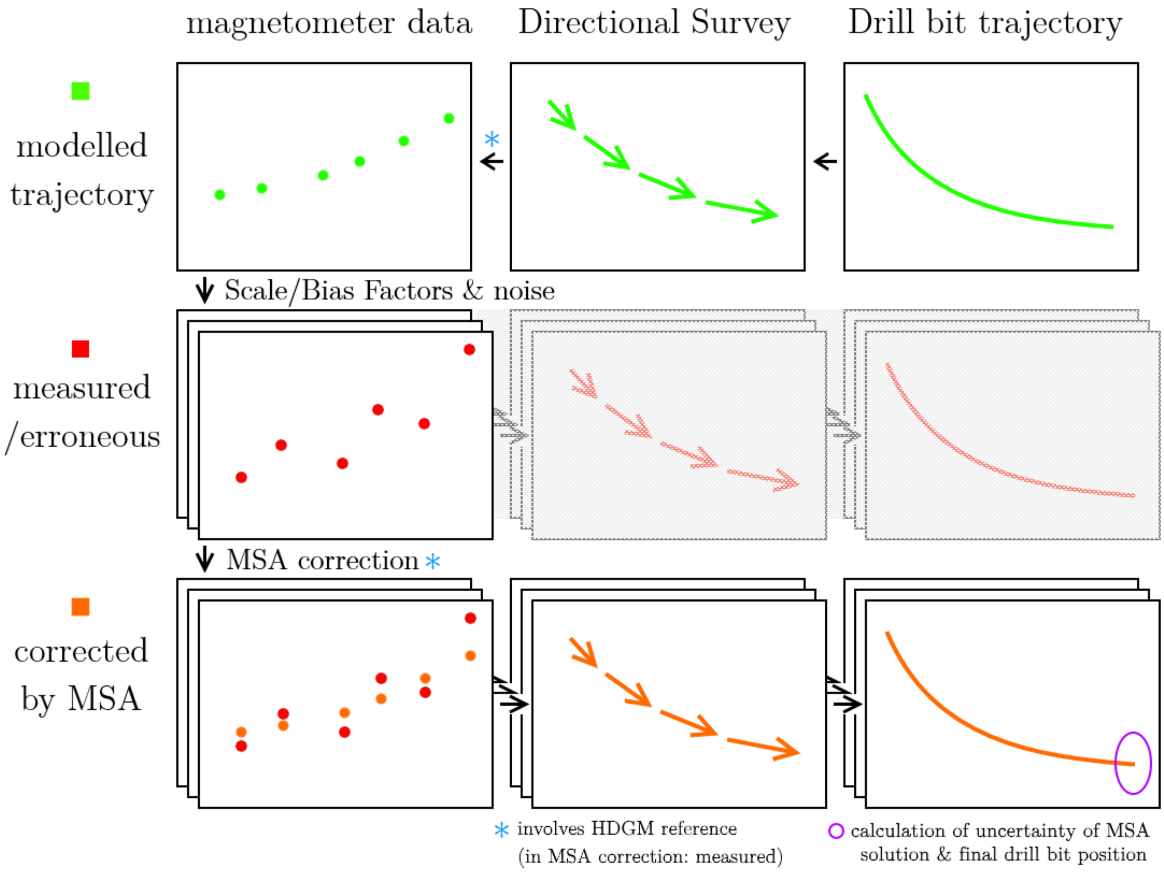

Figure 5-1: Simulation overview, starting from the modelled drill bit trajectory (top right).

In the MSA application step, a few assumptions are set:

- Given the high sensitivity of MSA, a six-decimal digit (0.000001) precision is configured in the Solver add-in. This ensures that numerical errors are minimal compared to random errors.
- Additionally, the Solver add-in utilizes relative convergence (see Background information): the default relative convergence of 0.0001 is used. A lower value is preferable - one can verify its sufficiency from the resulting MSA solution plots. The trade-off is that a lower value incurs additional iterations.
- During testing, in getting an MSA starting solution, the author did not perceive any quantitative differences using either the homotopy method (page 32) or using a random guess: for the results in this chapter, the latter is used.
- MSA solution existence and uniqueness in erroneous measurement data is assumed: only one set of systematic errors is artificially added to modelled measurement data.

Scenarios and results

Table 8 shows the parameters that have been used:

	Parameter	Expected value	Deviation
Modelled	Scale Factor X	1.1	

systematic errors (MSA solution)	Scale Factor Y	0.95	± 0.25 (starting MSA random guess)
	Scale Factor Z	1.25	
	Bias Factor X	0.25	
	Bias Factor Y	0.295	
	Bias Factor Z	-0.335	
Random errors	Noise bias	0 nT	Scenario 1, 2 and 3: 3.3 nT (standard dev.) Scenario 4: 0.3 nT
Modelled HDGM	Total field strength	51 µT	107 nT (standard dev.)
	Dip Angle	72°	0.16° (standard dev.)
Monte Carlo	# replications	300	-

Table 8: Parameters for Monte Carlo simulation.

The above modelled MSA solution are test parameters: any MSA solution with Scale Factors close to 1 and Bias Factors close to 0 can be chosen. The above HDGM error model is conform (Maus et al. 2012). The noise bias standard deviations are provided by a magnetometer expert at Baker Hughes, where scenario 4 represents expected future developments in magnetometer technology.

The following seven Surveys have been tested (also included on page 49), each of which are characterized by:

1. increasing Inclination and high Azimuth
2. increasing Inclination and low Azimuth
3. high Azimuth, different AHD starting position (missing data)
4. high amount of Surveys and bent trajectory (ISCWSA)
5. ill-behaved data
6. ill-behaved data
7. minimum Tool Face variation

Four scenarios are compared:

1. without HDGM error, with 3.3 nT sigma noise
2. with HDGM error (field strength only), with 3.3 nT sigma noise
3. with HDGM error (field strength and Dip), with 3.3 nT sigma noise
4. with HDGM error (field strength and Dip), with 0.3 nT sigma noise

The simulation results are stated in Table 9, Table 10, Table 11 and Table 12 below.

	Coordinates		**95% uncertainty: deviation (=1.96*st.dev)**		
	Position	MSA solution	Position [m]	Scale Factor	Bias Factor [µT]
1	x (North)	(HS+TFA)	0.3109277968	0.0001444448	0.0017329007
	y (East)	(HSR+TFA)	0.0271702194	0.0001121859	0.0016850436
	z (Vertical)	(Downhole)	0.0000028044	0.0004581051	0.0215095284
2	x		0.0086939433	0.0001530296	0.0022345990
	y		0.0993546099	0.0001341054	0.0018543374
	z		0.0000038756	0.0003464094	0.0165417379
3	x		5.7703611906	0.0001433809	0.0017607830

	y		0.5008533508	0.0001193468	0.0018200622
	z		0.0000047198	0.0135909274	0.1422877297
4	x		1.0762884964	0.0000305400	0.0007952551
	y		0.2883791747	0.0000295519	0.0007245822
	z		0.0000043641	0.0001320746	0.0057570424
5	x		0.0936122578	0.0000542927	0.0012910149
	y		0.1281182716	0.0000495341	0.0011491656
	z		0.0012805838	0.0000757368	0.0031003945
6	x		0.0965467684	0.0000477918	0.0012225929
	y		0.1234545406	0.0000476216	0.0012662441
	z		0.0011204412	0.0000366883	0.0016446892
7	x		61.5533830810	0.0304358845	0.2385140111
	y		61.3123001880	0.0029148284	0.1386723699
	z		0.0001296745	0.0442446047	2.3292780399

Table 9: Uncertainty of MSA solutions and final position vectors as acquired by Monte Carlo, scenario 1.

	Coordinates		**95% uncertainty: deviation (=1.96*st.dev)**		
	Position	MSA solution	Position [m]	Scale Factor	Bias Factor [μT]
1	x (North)	(HS+TFA)	0.3027900293	0.0047357332	0.0017100604
	y (East)	(HSR+TFA)	0.0264643082	0.0040715450	0.0017653756
	z (Vertical)	(Downhole)	0.0000025334	0.0053646537	0.0216185311
2	x		0.0085415525	0.0044753490	0.0020325229
	y		0.0976233712	0.0038534171	0.0017917457
	z		0.0000043571	0.0051201905	0.0165381444
3	x		22.3615675464	0.0042858312	0.0022955486
	y		1.1926539734	0.0037010757	0.0021524405
	z		0.0000502291	0.0296044653	0.3975887296
4	x		1.0315293046	0.0045099006	0.0007954642
	y		0.2763797137	0.0038927626	0.0007596106
	z		0.0000041968	0.0051301571	0.0053928946
5	x		0.0905855730	0.0044899493	0.0012856242
	y		0.1258882982	0.0038810833	0.0011884926
	z		0.0012313492	0.0051009998	0.0030069338
6	x		0.1024260586	0.0042989473	0.0012502042
	y		0.1266085712	0.0037071573	0.0012231948
	z		0.0012359169	0.0048854966	0.0016407844
7	x		58.0922786630	0.0305542020	0.2914765825
	y		56.9748850574	0.0048759336	0.1256160620
	z		0.0001215315	0.0424976054	2.2043456709

Table 10: Uncertainty of MSA solutions and final position vectors as acquired by Monte Carlo, scenario 2.

	Coordinates		**95% uncertainty: deviation (=1.96*st.dev)**		
	Position	MSA solution	Position [m]	Scale Factor	Bias Factor [μT]
1	x (North)	(HS+TFA)	57.3218846347	0.0224444802	0.0038464143
	y (East)	(HSR+TFA)	5.1828159573	0.0191109321	0.0067440619
	z (Vertical)	(Downhole)	0.0009472730	0.0717863236	3.5853179645
2	x		0.1063992451	0.0084498420	0.0078667033

	y		1.2132958111	0.0079875160	0.0219137831
	z		0.0000921307	0.0247086209	1.1829501750
3	x		247.0477227996	0.0076965664	0.0104214029
	y		28.0227316487	0.0065552702	0.0057056378
	z		0.0001692815	0.1905380299	3.7735904895
4	x		188.3934431287	0.0054709165	0.0014198121
	y		50.9278344440	0.0047243912	0.0041355067
	z		0.0005893930	0.0272680837	1.1287146363
5	x		9.6202073670	0.0054656668	0.0025110855
	y		9.8646625936	0.0047611952	0.0056288028
	z		0.0133553696	0.0125974499	0.5837494007
6	x		4.7141270573	0.0047373716	0.0114796376
	y		1.2976959702	0.0041106437	0.0030162983
	z		0.0093800964	0.0062231946	0.1410950087
7	x		84.5564948884	0.0342942677	0.7120746884
	y		114.3540286438	0.0102024099	0.5594878675
	z		0.0001765971	0.0510761751	2.7374584009

Table 11: Uncertainty of MSA solutions and final position vectors as acquired by Monte Carlo, scenario 3.

	Coordinates		**95% uncertainty: deviation (=1.96*st.dev)**		
	Position	MSA solution	Position [m]	Scale Factor	Bias Factor [µT]
1	x (North)	(HS+TFA)	54.6866816670	0.0218176635	0.0029280105
	y (East)	(HSR+TFA)	5.0297032000	0.0185894180	0.0062936052
	z (Vertical)	(Downhole)	0.0008119924	0.0691567239	3.4298256810
2	x		0.1004190033	0.0075849772	0.0074005872
	y		1.1478654955	0.0071775307	0.0207309127
	z		0.0000836039	0.0227534567	1.1259554406
3	x		262.4902477587	0.0073202671	0.0097186589
	y		28.3138221014	0.0062104873	0.0050141376
	z		0.0002636360	0.1964205923	3.9095359410
4	x		202.6169769977	0.0048392297	0.0012865961
	y		54.4887082366	0.0041819661	0.0043289785
	z		0.0007301175	0.0289007361	1.2123712608
5	x		10.0479875294	0.0057388974	0.0023276912
	y		10.3122819720	0.0049978189	0.0057753799
	z		0.0137944424	0.0133938448	0.6103900652
6	x		4.3788883724	0.0046017571	0.0106856228
	y		1.1968892406	0.0039932924	0.0025666695
	z		0.0085658774	0.0059863580	0.1310910120
7	x		70.1850525483	0.0360555059	0.3056452396
	y		70.6664886402	0.0057351010	0.3508352218
	z		0.0001786466	0.0499537412	2.6098036249

Table 12: Uncertainty of MSA solutions and final position vectors as acquired by Monte Carlo, scenario 4.

These results can be compared with results from existing industry uncertainty models that determine final position uncertainty. In this thesis, the following results were used, provided by one of the project mentors:

Coordinate	Scale	Bias
High Side	0.008	35 nT
High Side Right	0.008	35 nT
Downhole direction	0.008	35 nT

Table 13: Uncertainty standard deviations in MSA solution: input in industry model.

Survey	1	2	3	4	7
Uncertainty North [m]	10.1	0.4	42.8	107.5	15.0
Uncertainty East [m]	0.9	4.8	3.7	28.8	15.0

Table 14: 95% uncertainty deviations in MSA solution according to industry model.

An advantage of the above chosen industrial model is its non-requirement of stochastics. Its only input is a modelled Survey, the MSA solution uncertainties specified in Table 13 and a total field strength error uncertainty. The industrial model does not account for Dip Angle uncertainties, whereas the model proposed in this thesis does.

Conclusions

Various plots of the Monte Carlo simulation are included in the Appendix, starting from page 54. Errors in vertical position are negligible in all four scenarios. Additionally,

1. In the first scenario, MSA has detected the modelled MSA solution to a high degree. Except for Scale and Bias Factor Z uncertainty in scenarios 3 and 7, these results do agree with the MSA uncertainty deviations from the industry model.
   The first four Surveys shows an overly optimistic improvement in position uncertainty over the results from industry model. In Survey 7, the opposite case applies. This is consistent with the assertion that Tool Face variation is key to position determination, based on Case 1 in the master thesis (Elshabrawy 2018).
2. Despite the worse results than the first scenario with regards to MSA uncertainty deviations, the second scenario yields comparable results in position uncertainty except for Survey 3. Again, the MSA uncertainty deviations agree with the industry model.
3. In the third scenario, in the first four Surveys, significantly higher deviations in final position were observed compared to the previous scenario and returns worse MSA solution uncertainties than the industry model. Also, in all scenarios, Bias Factor Z uncertainty is significantly worse compared to Bias Factor X and Bias Factor Y uncertainty.
4. The fourth scenario yields similar conclusions as in the third scenario.

All in all, HDGM Dip Angle uncertainty is the most significant source for position uncertainty. From here onward, only scenario 4 will be considered.

Notes

- Not all digits in the above uncertainty results are significant.
- Since the above results contain sampling errors: to verify that the fourth scenario returns similar results as the third scenario, one would have to repeat the Monte Carlo simulation sufficiently many times over again to yield samples from probability distributions of the MSA solution/final position uncertainty of both scenarios, after which

a two-sample t-test should be performed. However, this procedure is computationally expensive, and therefore not done in this thesis.

Chapter 6 Quality control of MSA solution: the link between condition numbers and MSA solution error

Established in the previous chapter, Monte Carlo simulation gives an approximation of MSA solution uncertainties. The main benefit is that no major analysis of the mathematical model is required, however the exact cause for the presence of MSA solution errors remains hidden. As mentioned in Chapter 2, the condition number in the Newton-Raphson algorithm is speculated to be related to the MSA solution error. During testing of Monte Carlo simulation, large values of these condition numbers were observed, implying ill-conditioning of MSA. Continuing from the previous chapter, for scenario 4, these values are summarized in the condition number plots on page 66, where each corrected position is associated with its condition number, represented as color: colors tending towards light yellow correspond to large condition numbers, and colors tending towards dark blue correspond to small condition numbers.

From Survey 1, an ideal situation can be inferred: a large condition number when both corrected position and MSA solution are close to the modelled position and MSA solution, small otherwise, behaving in a continuous manner, and minimal near the extreme endpoints of the position/MSA solution set.

However, from Surveys 4, 5 and 6, this is not the case: the largest condition number appears at an extreme endpoint. Also, Scale Factors do not appear to follow the ideal behavior as well. Survey 4 contains a high amount of potential outlying condition numbers, but the corresponding Scale Factors do not appear at the extreme ends.

Surveys 2, 3, and 7 contain replications with large outlying condition numbers, resulting in most of the condition numbers appearing to seemingly have low condition numbers. In Survey 2 specifically, the set of Scale Factors associated with the major outlying condition number is not an outlier, and close to the modelled MSA solution, thus it cannot be removed. In Survey 7, the MSA solutions corresponding to large condition numbers are scattered close towards the modelled MSA solution and cannot be generally classed as outliers.

Based on these observations, the conclusion is that condition number - on its own without further post-processing - cannot be used to determine MSA solution quality.

Notes

- After initial acquirement of measurement data, it may be possible to acquire a second set of measurement data when the drill is transported back to the surface. From here, the condition numbers in both sets can be compared to each other to determine which set is more reliable. However, this practice is not common in the well-bore industry, as it incurs additional time and expenses.
- The condition number plots of Survey 3 contain only a few outlying condition numbers, which could be attributed to random chance. However, its Bias Factor plot contains many deviating points, relatively more in comparison to the other Surveys, which suggest that an insufficient amount of numerical algorithm iterations have been

executed. So, the Monte Carlo simulation of the previous chapter is repeated, with the only parameter change being relative convergence in Excel Solver, which is set to 0.000001. This yields the following condition number plot, in which the above anomalies disappear:

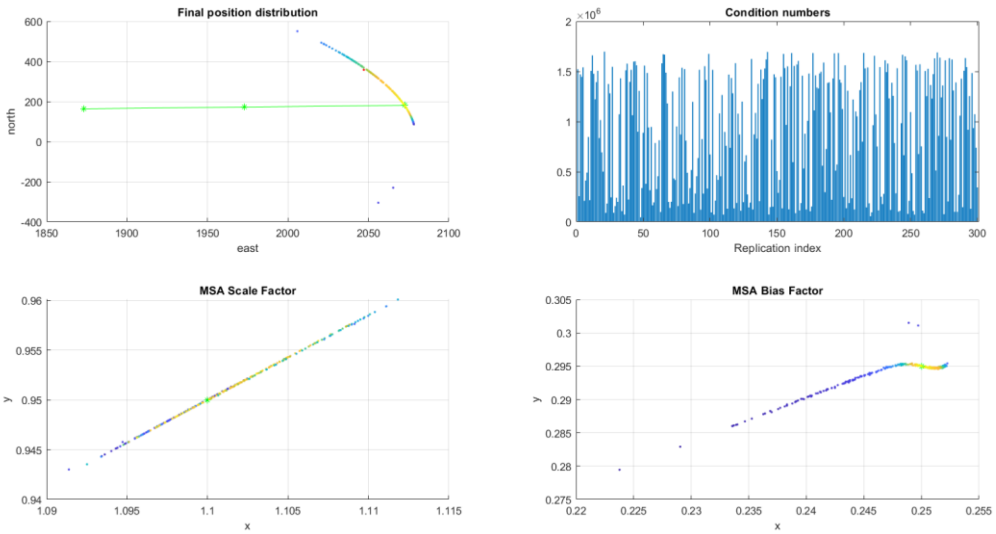

Figure 6-1: Condition plot of Survey 3, with improved relative convergence.

However, by analyzing the Scale Factors plot, the overall conclusion still holds.

- If a single drill is used for drilling one single borehole section, as for example in Survey 1, condition number may indeed be a reliable measure for determining MSA solution quality (as well as drill bit position). However, in practice, large depth boreholes are drilled in multiple sections, and potentially, multiple drills are used. In such case, one will also have to apply MSA on Surveys similarly to Survey 3, where parts of data are missing. Comparing the condition plots corresponding to those Surveys, again the overall conclusion still holds.

Chapter 7 Conclusion, recommendations and final remarks

In this thesis, the trajectory of a drill bit has been studied, which is determined by indirect measurements from accelero- and magnetometers. Erroneous measurements in the magnetometer data result in error in determining the final position of the drill bit.

Multi-Station Analysis is considered as a potential solution to improve the position uncertainty ellipsoid. With the aid of HDGM reference measurements, this method determines the systematic Scale/Bias Factors that are present in the magnetometer data, which is then used to correct the data.

The main objective of this thesis is to determine the uncertainty in the MSA solution and provide a method to do so. Here, it is based on Monte Carlo simulation. This method generates multiple replications of erroneous measurement data from modelled measurement data, each of which is representative of in-field measurements. Aside from the MSA solution uncertainty, the effect of MSA on the final position vector of the drill bit has also been considered. A prototype implementation of this method is done in Excel in conjunction with MATLAB.

This thesis has established that while on average, MSA as presented here is able to correct erroneous well-bore trajectories towards the modelled trajectory, it is however not adequate to counter for extreme erroneous cases, due to HDGM Dip Angle uncertainty. To compare and validate, a position uncertainty model from the well-bore industry produces significantly lower and therefore inaccurate uncertainties, as it does not account for HDGM Dip Angle uncertainty. Additionally, it is also established that the condition number in the final iteration of Newton-Raphson is not a reliable measure for the quality of MSA solution.

Further areas of potential research

In addition to the various problems mentioned but not covered throughout this thesis, the following areas has been identified by the author to be of potential interest regarding the overall well-bore drill position methodology:

1. A major disadvantage of the Monte Carlo simulation applied on the MSA problem is its dependence on a modelled trajectory/measurement data, which is typically not known in practice, where only one replication of erroneous measurement data is available. The worst-case scenario is when after applying MSA, a poor approximation is yielded due to improper determination of the actual Scale and Bias Factors in the erroneous measurement data.
   However, if the MSA solution uncertainty analysis does not depend on the modelled MSA solution, then the corrected measurement data with associated MSA solution can be used as modelled measurement data instead. While the MSA solution uncertainty can change due to difference between the corresponding trajectories, due to continuity, it is hypothesized that the resulting position uncertainty is close to the actual position uncertainty. Since only one set of modelling parameters has been used in this thesis, one should retest the Monte Carlo simulation with different parameters to verify the above independency.
2. In linear regression, as part of the subfield of regression diagnostics, the condition number of the design matrix is a measure for the presence of *collinearity* (near-singularities in the design matrix) in a regression problem: large condition numbers result in poor estimates of the regression coefficients (Rawlings, Pantula, and Dickey 1998), chapters 10.6, 11.3 and 13. Causes for collinearity include the presence of near-linear dependencies among the regression variables and inadequate sampling. To remedy collinearity, biased regression can be employed, which involves constructing regression coefficient estimators with smaller mean square error but include bias. An example of a biased regression method is principal component regression, which - after transformation of the regression variables into so-called principal components - eliminates the principal components that cause the collinearity problem.
   Based on the plots generated through Monte Carlo simulation performed in this thesis, there is a clear near-linear relationship among Scale Factor X and Scale Factor Y, suggesting that at least one of these variables can be reliably predicted from the

others. After performing the principal component regression, it is thus expected that MSA solution uncertainty is reduced, yielding a more representative position uncertainty ellipsoid.

3. In general, for single and multiple linear least squares regression methods, estimators for the unknown regression coefficients can be constructed analytically, from which a confidence interval is derived (Rice 2007), chapter 14. Bounds for the relative error of the least squares solution can be written in terms of the condition number of the design matrix, if the latter has full rank (Golub and Loan 2013), chapter 5.3. Can the regression uncertainty analysis be done analytically? Below are several helpful facts on regression:
   - Non-linear regression models can be linearized using transformations and/or using Taylor expansion methods. The former may lead to loss of normality in residuals. The latter leads to the Gauss-Newton method, which is the application of Newton-Raphson to least squares regression. For non-linear models, confidence intervals for the regression coefficients can also be established (Rawlings, Pantula, and Dickey 1998), chapter 15.3.
   - Residual analysis may reveal outliers.
   - Classical assumptions of regression include normality of residuals, homogeneous variance and independent errors. In case any of these are violated, robust regression techniques can be employed.

   There are several problems unique to the MSA regression model compared to the above standard regression models that complicate the regression analysis to be performed:
   - Random errors and systematic error parameters in B_x, B_y, B_z variables, multiple least squares fitting of B_h, B_v variables against *measured* HDGM reference, thus potential loss of normality and lack of goodness-of-fit.
   - Random errors in measured HDGM reference.
4. Key in finding the MSA solution associated with measured magnetometer data is the least-squares error function (3.5). Due to uncertainties covered throughout this thesis, the retrieved MSA solution may deviate significantly from the modelled MSA solution. Can a different error function be used?
   - The MSA solution found using the method described in this thesis can be used as an initial starting approximation, so the different error function needs to return an MSA solution close to it, leading to a constrained optimization problem.
   - Empirical observations during simulation testing: if the data is corrected using the modelled MSA solution, the corrected B_h, B_v values yield approximately stationary time series, whereas correcting the data using the MSA solution found from the least-squares error function (3.5) yields non-stationary time series. Therefore, if a different error function is to be used, its solution should necessarily correct B_h, B_v values towards a stationary time series, with expectation close to measured HDGM reference.
5. Based on the results of this thesis, the MSA solutions acquired from MSA can be mathematically interpreted as outcomes of an unbiased multivariate estimator

$X = [X_1, X_2, X_3, X_4, X_5, X_6]^T$ where, if possible (depending on Survey), each X_i is normally distributed. Under regularity conditions, the *Fisher information matrix* can then be used to establish the Cramér-Rao inequality, which is a lower bound on the variance of X, as well as all other unbiased MSA solution estimators, thus giving an optimality condition for minimum MSA solution uncertainty.

6. Changing statistical assumptions: in this thesis, random measurement errors were assumed to be normally distributed. In practice, inverse Gaussian and Laplacian distributions are also suggested. Also, when measurements are done electronically through solid state tools, discrete distributions apply, leading to resolution errors due to digitization. By correspondence with a survey specialist at Halliburton, magnetometer noise may unfortunately fall within resolution error, making detection harder, leading to underestimated uncertainties. Finally, this thesis has taken a frequentist approach: would a Bayesian approach yield more accurate results?
7. To get reliable MSA solution uncertainties, the Monte Carlo simulation requires many replications. Without prior knowledge on the MSA solution distribution, one will have to guess on the minimum number of replications. Richardson extrapolation is a method to yield improved estimates from numerical processes of the form $Q(h)$, if the numerical error can be expressed as a Taylor series in the variable h with finite order, see for instance (Vuik et al. 2016), chapter 3.7. Can Richardson extrapolation be used to speed up the Monte Carlo simulation, while maintaining or improving accuracy? And if so, can these results be reliable even when using a low number of replications?
8. It is desirable that the overall methodology is fully automatized by computer, without the involvement of external operators. Establishing *operator-independency* of MSA is key to improving position determination. For example, in erroneous measurement data, one may ask whether manual clean-up is necessary before applying MSA: removing outliers influences the MSA solution uncertainty. Which Survey Stations need to be removed to improve the MSA solution (and the drill bit position) and under which conditions?
9. In this thesis, modelled drill bit trajectories and MSA solution were available to determine the quality of MSA. However, these are not available at hand in practice: in this scenario, the corrected measurement data after applying MSA can be validated through covariance analysis (Hanak, Wilson, and Gjertsen 2015). Can this technique be adapted for the MSA model described in this thesis?
10. Measurement data can be retrieved from multiple MWD tools. Each set of measurement data retrieved from one MWD tool is called a stand. Multiple MSA solutions are found by performing MSA on each stand separately. After correction, what is the overall effect on the uncertainty of the final drill bit position in this scenario?
11. The MSA problem may be approached from different perspectives. In addition to the MSA mathematical model described on page 25, other formulations of MSA exist. For instance, a linear algebra approach is found in Appendix A and B of (Hanak, Wilson, and Gjertsen 2015). Further hypotheses:

- Instead of using non-linear regression to find the MSA solution, a generic stochastic optimization method may be used, e.g. simulated annealing.
- By letting the amount of Stations go to infinity, it might be possible to transform the MSA problem into a stochastic differential equation.
- A mathematical control system perspective, in which Kalman filters are used to proactively reduce the effect of noise and acquire an improved MSA solution.

Notes and in-chapter references

- For the usage of inverse Gaussian distributions, see for instance "Positioning and Position Error of Petroleum Wells", Gjerde et. al., 2011. Laplacian distributions were suggested by correspondence with a geomagnetism expert.

Final remarks

The author thanks Koen Noy and Kees Vuik for their insight and support throughout this project.

Chapter 8 Appendix

Notation

	Symbol	Description
General	$\mathbb{N}$	set of natural numbers
	$\mathbb{Z}$	set of integer numbers
	$\mathbb{R}$	set of real numbers
	$\mathbb{R}^+$	set of positive real numbers including 0
	$a := b$	a is defined by b
	$a \ll b$	a close to b, with $a < b$
	$a \gg b$	a close to b, with $a > b$
	$\sin^{-1}$	arcsine, inverse of sine function. Similar notation holds for arccosine and arctangent
Linear algebra	$\vec{v}$	column vector
	$\overrightarrow{v^{\mathrm{T}}}$	row vector
	$\lVert\vec{v}\rVert$	Euclidean norm of vector
	$\lVert A\rVert$	subordinate norm of matrix
Probability	I_S	indicator function on set S
	$X \simeq \ldots$	X having the probability distribution of
	$E(X)$	expectation of X
	$P(X \le a)$	probability of event X being smaller than a
	$V(X)$	variance of X

Background information

This thesis requires knowledge of linear algebra, numerical analysis, probability and statistics at undergraduate level. Only relevant results used in this thesis are explained.

Numerical analysis: The Newton-Raphson algorithm, systems of linear equations

A system of n non-linear equations in n variables can be written in the form

$$\vec{f}(\vec{x}) = \vec{0}, \vec{f} = (f_1 \quad f_2 \quad \cdots \quad f_n)^{\mathrm{T}}, f_i = f_i(x_1, x_2, \ldots, x_n)$$

Its solutions are roots of the system. Assume a root $\vec{p}$ exists, which needs to be found through Newton-Raphson. If $\vec{f}$ is continuous and $\vec{f}'(\vec{p}) \neq \vec{0}$, then there exists $I \subseteq \mathbb{R}^n$ containing $\vec{p}$ such that the following algorithm finds the root:

Input:

- $0 \ll \epsilon \in \mathbb{R}^+$ tolerance error
- Above system of equations
- $\vec{v_0}$ A start approximation of root

Algorithm: In each iteration i:

1. Calculate Jacobian J_{i-1} of $\vec{f}$ evaluated in $\overrightarrow{v_{i-1}}$. If this is done numerically, then the method is called Quasi-Newton.
2. Solve $J_{i-1}\vec{e} = -\vec{f}\left(\overrightarrow{v_{i-1}}\right)$.
3. Calculate new approximation $\vec{v_i} = \overrightarrow{v_{i-1}} + \vec{e}$
4. If $\left\|\vec{e}\right\| < \epsilon$, then halt, otherwise next iteration $i+1$.

Output: if the algorithm does not halt, then the start approximation has not been chosen well. Otherwise, a finite amount k of iterations has run, $\vec{v_k}$ is output, and the convergence of the sequence of approximations $\vec{v_i}$ is quadratic.

In general, solutions for systems of (non-)linear equations are solved with methods like Newton-Raphson and Picard iteration. These involve a construction of a sequence of approximations that, given a suitable start approximation, will converge to the exact solution. Thus, one may pick any approximation within suitable tolerance compared to the exact solution.

However, there is a trade-off: if the tolerance decreases, that is, if higher precision is required, then in the worst-case scenario, the algorithm that is being used requires more iterations. Therefore, it may not always be possible to set the tolerance to zero: an output approximation may thus contain an iteration error with respect to the exact solution.

These algorithms are implemented in many mathematical software packages (as solver functions). However, as of Excel 2016, it does not contain Newton-Raphson by default: Generalized Reduced Gradient (GRG) Nonlinear solver is used instead. There are two differences in using GRG over Newton-Raphson within Excel: computation speed and relative stopping condition.

Numerical analysis: sensitivity analysis of linear systems, condition number

Let $A\vec{x} = \vec{b}$ be a system of linear equations, with invertible A and unknown solution $\vec{x}$. An error in the right-hand side results in a perturbation in $\vec{x}$. From linearity, it follows:

$$A\overrightarrow{\Delta x} = \overrightarrow{\Delta b}$$

Simple analysis using norm inequalities provides an upper bound for the relative error of $\vec{x}$:

$$\frac{\left\|\overrightarrow{\Delta x}\right\|}{\left\|\vec{x}\right\|} \le \left\|A\right\| \cdot \left\|A^{-1}\right\| \frac{\left\|\overrightarrow{\Delta b}\right\|}{\left\|\vec{b}\right\|}$$

Define $\kappa(\mathrm{A}) := \left\|A\right\| \cdot \left\|A^{-1}\right\|$ as the *condition number* of the matrix A. Then for small $\overrightarrow{\Delta b}$, the following interpretations hold:

- A small condition number implies potentially but not necessarily small relative error of the solution; thus, the system of equations is said to be *ill-conditioned*.
- A small condition number implies small relative error of the solution; the system of equations is said to be *well-conditioned*.

A linear algebra theorem states that real symmetric matrices are orthogonally diagonalizable (Sadun 2001), theorem 7.8. Thus, if A is symmetric, it is orthogonally diagonalizable, and it has a largest eigenvalue $\lambda_{\max}$ of which its absolute value is equal to $\|A\|$ as well as a smallest eigenvalue $\lambda_{\min}$, of which the absolute value of its multiplicative inverse is equal to $\|A^{-1}\|$.

Therefore, the condition number is easy to calculate: $\kappa(\mathrm{A}) = \frac{|\lambda_{\max}|}{|\lambda_{\min}|}$. This thesis computes the eigenvalues numerically using the QR algorithm, which is numerically stable. Its implementation is provided by "matrix.xla" Excel add-in.

Probability and statistics

Two standard probability distributions for a continuous random variable are:

1. Uniform distribution $U(a,b)$: $[a,b] \subseteq \mathbb{R}, a < b$:

$$P(U \le x) = \int_{-\infty}^{x} \frac{1}{b-a} I_{[a,b]} dx$$

2. Normal distribution $N(\mu,\sigma)$:

$$P(N \le a) = \int_{-\infty}^{a} \frac{1}{\sigma\sqrt{2\pi}} e^{-\frac{1}{2}\left(\frac{x-\mu}{\sigma}\right)^2} dx$$

   Standard normal distribution is $N(0,1)$.

In simulation, the following is needed: to generate numbers from a random variable X from some uniform random variable from 0 to 1, it only needs to be transformed by applying the inverse cumulative distribution function of X. See (Rice 2007), Proposition D, page 63.

Notes and in-chapter references

- Linear algebra: (Sadun 2001)
- Numerical analysis: (Vuik et al. 2016). Newton-Raphson is found in chapter 4. Condition numbers of linear systems are found in chapter 7, paragraph 3.
  - Bounds for the eigenvalues are provided by Gershgorin's theorem.
  - A description of Excel GRG solver settings are found at https://www.solver.com/excel-solver-change-options-grg-nonlinear-solving-method, and information about relative stopping condition at https://www.solver.com/excel-solver-grg-nonlinear-solving-method-stopping-conditions.
- Probability and statistics: (Rice 2007)

Data

Survey 1				Survey 2			
Along Hole Depth	Toolface	Inclination	Azimuth	Along Hole Depth	Toolface	Inclination	Azimuth
0.00	25.00	0.00	85.00	0.00	25.00	0.00	5.00
1000.00	115.00	0.00	85.00	1000.00	115.00	0.00	5.00
1100.00	205.00	3.00	85.00	1100.00	205.00	3.00	5.00
1200.00	295.00	6.00	85.00	1200.00	295.00	6.00	5.00
1300.00	25.00	9.00	85.00	1300.00	25.00	9.00	5.00
1400.00	115.00	12.00	85.00	1400.00	115.00	12.00	5.00
1500.00	205.00	15.00	85.00	1500.00	205.00	15.00	5.00
1600.00	295.00	18.00	85.00	1600.00	295.00	18.00	5.00
1700.00	25.00	21.00	85.00	1700.00	25.00	21.00	5.00
1800.00	115.00	24.00	85.00	1800.00	115.00	24.00	5.00
1900.00	205.00	27.00	85.00	1900.00	205.00	27.00	5.00
2000.00	295.00	30.00	85.00	2000.00	295.00	30.00	5.00
2100.00	25.00	33.00	85.00	2100.00	25.00	33.00	5.00
2200.00	115.00	36.00	85.00	2200.00	115.00	36.00	5.00
2300.00	205.00	39.00	85.00	2300.00	205.00	39.00	5.00
2400.00	295.00	42.00	85.00	2400.00	295.00	42.00	5.00
2500.00	25.00	45.00	85.00	2500.00	25.00	45.00	5.00
2600.00	115.00	48.00	85.00	2600.00	115.00	48.00	5.00
2700.00	205.00	51.00	85.00	2700.00	205.00	51.00	5.00
2800.00	295.00	54.00	85.00	2800.00	295.00	54.00	5.00
2900.00	25.00	57.00	85.00	2900.00	25.00	57.00	5.00
3000.00	115.00	60.00	85.00	3000.00	115.00	60.00	5.00

Survey 3				Survey 4			
Along Hole Depth	Toolface	Inclination	Azimuth	Along Hole Depth	Toolface	Inclination	Azimuth
900.00	25.00	77.50	85.00	0.00	25.00	0.00	0.00
1000.00	115.00	78.00	85.00	100.00	115.00	0.00	0.00
1100.00	205.00	78.50	85.00	200.00	205.00	0.00	0.00
1200.00	295.00	79.00	85.00	300.00	295.00	0.00	0.00
1300.00	25.00	79.50	85.00	400.00	25.00	0.00	0.00
1400.00	115.00	80.00	85.00	500.00	115.00	0.00	0.00
1500.00	205.00	80.50	85.00	600.00	205.00	0.00	0.00
1600.00	295.00	81.00	85.00	700.00	295.00	0.00	0.00
1700.00	25.00	81.50	85.00	800.00	25.00	0.00	0.00
1800.00	115.00	82.00	85.00	900.00	115.00	0.00	0.00
1900.00	205.00	82.50	85.00	1000.00	205.00	0.00	0.00
2000.00	295.00	83.00	85.00	1100.00	295.00	0.00	0.00
2100.00	25.00	83.50	85.00	1200.00	25.00	0.00	75.00
2200.00	115.00	84.00	85.00	1300.00	115.00	6.67	75.00
2300.00	205.00	84.50	85.00	1400.00	205.00	13.33	75.00
2400.00	295.00	85.00	85.00	1500.00	295.00	20.00	75.00
2500.00	25.00	85.50	85.00	1600.00	25.00	26.67	75.00
2600.00	115.00	86.00	85.00	1700.00	115.00	33.33	75.00
2700.00	205.00	86.50	85.00	1800.00	205.00	40.00	75.00
2800.00	295.00	87.00	85.00	1900.00	295.00	46.67	75.00
2900.00	25.00	87.50	85.00	2000.00	25.00	53.33	75.00
3000.00	115.00	88.00	85.00	2100.00	115.00	60.00	75.00

Survey 4			
Along Hole Depth	Toolface	Inclination	Azimuth
2200.00	205.00	60.00	75.00
2300.00	295.00	60.00	75.00
2400.00	25.00	60.00	75.00
2500.00	115.00	60.00	75.00
2600.00	205.00	60.00	75.00
2700.00	295.00	60.00	75.00
2800.00	25.00	60.00	75.00
2900.00	115.00	60.00	75.00
3000.00	205.00	60.00	75.00
3100.00	295.00	60.00	75.00
3200.00	25.00	60.00	75.00
3300.00	115.00	60.00	75.00
3400.00	205.00	60.00	75.00
3500.00	295.00	60.00	75.00
3600.00	25.00	60.00	75.00
3700.00	115.00	60.00	75.00
3800.00	205.00	60.00	75.00
3900.00	295.00	60.00	75.00
4000.00	25.00	60.00	75.00
4100.00	115.00	60.00	75.00
4200.00	205.00	60.00	75.00
4300.00	295.00	60.00	75.00
4400.00	25.00	60.00	75.00
4500.00	115.00	60.00	75.00
4600.00	205.00	60.00	75.00
4700.00	295.00	60.00	75.00
4800.00	25.00	60.00	75.00
4900.00	115.00	60.00	75.00
5000.00	205.00	60.00	75.00
5100.00	295.00	60.00	75.00
5200.00	25.00	70.00	75.00
5300.00	115.00	80.00	75.00
5400.00	205.00	90.00	75.00
5500.00	295.00	90.00	75.00
5600.00	25.00	90.00	75.00
5700.00	115.00	90.00	75.00
5800.00	205.00	90.00	75.00
5900.00	295.00	90.00	75.00
6000.00	25.00	90.00	75.00
6100.00	115.00	90.00	75.00
6200.00	205.00	90.00	75.00
6300.00	295.00	90.00	75.00
6400.00	25.00	90.00	75.00
6500.00	115.00	90.00	75.00
6600.00	205.00	90.00	75.00
6700.00	295.00	90.00	75.00
6800.00	25.00	90.00	75.00
6900.00	115.00	90.00	75.00
7000.00	205.00	90.00	75.00
7100.00	295.00	90.00	75.00
7200.00	25.00	90.00	75.00
7300.00	115.00	90.00	75.00
7400.00	205.00	90.00	75.00
7500.00	295.00	90.00	75.00
7600.00	25.00	90.00	75.00
7700.00	115.00	90.00	75.00
7800.00	205.00	90.00	75.00
7900.00	295.00	90.00	75.00
8000.00	25.00	90.00	75.00

Survey 5			
Along Hole Depth	Toolface	Inclination	Azimuth
0.00	25.00	0.00	0.00
100.00	115.00	0.00	0.00
200.00	205.00	0.00	0.00
300.00	295.00	0.00	0.00
400.00	25.00	0.00	0.00
500.00	115.00	0.00	0.00
600.00	205.00	0.00	0.00
609.60	295.00	0.00	0.00
700.00	25.00	5.93	2.00
800.00	115.00	12.49	2.00
900.00	205.00	19.06	2.00
1000.00	295.00	25.62	2.00
1097.28	25.00	32.00	2.00
1100.00	115.00	32.00	2.00
1200.00	205.00	32.00	2.00
1300.00	295.00	32.00	2.00
1400.00	25.00	32.00	2.00
1500.00	115.00	32.00	2.00
1524.00	205.00	32.00	2.00
1600.00	295.00	31.12	16.22
1684.18	25.00	32.00	32.00
1700.00	115.00	31.69	34.89
1800.00	205.00	31.29	53.78
1844.37	295.00	32.00	62.00
1900.00	25.00	31.20	72.35

Survey 5			
Along Hole Depth	Toolface	Inclination	Azimuth
2000.00	115.00	31.90	91.17
2004.55	205.00	32.00	92.00
2100.00	295.00	31.15	109.92
2164.74	25.00	32.00	122.00
2200.00	115.00	30.78	128.24
2300.00	205.00	29.16	147.75
2400.00	295.00	30.49	167.44
2500.00	25.00	34.43	184.32
2600.00	115.00	40.21	197.50
2700.00	205.00	47.16	207.64
2800.00	295.00	54.81	215.62
2864.66	25.00	60.00	220.00
2900.00	115.00	60.00	220.00
3000.00	205.00	60.00	220.00
3100.00	295.00	60.00	220.00
3200.00	25.00	60.00	220.00
3300.00	115.00	60.00	220.00
3400.00	205.00	60.00	220.00
3500.00	295.00	60.00	220.00
3600.00	25.00	60.00	220.00
3700.00	115.00	60.00	220.00
3800.00	205.00	60.00	220.00
3810.00	295.00	60.00	220.00

Survey 6			
Along Hole Depth	Toolface	Inclination	Azimuth
0.00	25.00	0.00	0.00
100.00	115.00	0.00	0.00
200.00	205.00	0.00	0.00
300.00	295.00	0.00	0.00
400.00	25.00	0.00	0.00
500.00	115.00	0.00	0.00
600.00	205.00	8.33	0.00
700.00	295.00	16.67	0.00
800.00	25.00	25.00	0.00
900.00	115.00	33.33	0.00
1000.00	205.00	41.67	0.00
1100.00	295.00	50.00	0.00
1200.00	25.00	50.00	0.00
1300.00	115.00	50.00	0.00
1400.00	205.00	50.00	0.00
1500.00	295.00	50.00	0.00
1600.00	25.00	50.00	0.00
1700.00	115.00	50.00	0.00
1800.00	205.00	43.33	0.00
1900.00	295.00	36.67	0.00
2000.00	25.00	30.00	0.00
2100.00	115.00	23.33	0.00
2200.00	205.00	16.67	0.00
2300.00	295.00	10.00	0.00

Survey 6			
Along Hole Depth	Toolface	Inclination	Azimuth
2400.00	25.00	3.33	0.00
2450.00	115.00	0.00	0.00
2500.00	205.00	0.00	0.00
2600.00	295.00	0.00	0.00
2700.00	25.00	0.00	0.00
2800.00	115.00	0.00	0.00
2850.00	205.00	0.00	0.00
2900.00	295.00	25.00	283.00
3000.00	25.00	75.00	283.00
3030.00	115.00	90.00	283.00
3100.00	205.00	90.00	283.00
3200.00	295.00	90.00	283.00
3300.00	25.00	90.00	283.00
3400.00	115.00	90.00	283.00
3430.00	205.00	90.00	283.00
3500.00	295.00	97.04	263.16
3600.00	25.00	105.41	233.75
3700.00	115.00	109.74	202.57
3730.00	205.00	110.00	193.00
3800.00	295.00	110.00	193.00
3900.00	25.00	110.00	193.00
4000.00	115.00	110.00	193.00
4030.00	205.00	110.00	193.00

Survey 7			
Along Hole Depth	Toolface	Inclination	Azimuth
0.00	25.00	25.00	45.00
100.00	26.00	26.00	45.00
200.00	27.00	27.00	45.00
300.00	28.00	28.00	45.00
400.00	29.00	29.00	45.00
500.00	30.00	30.00	45.00
600.00	31.00	31.00	45.00
700.00	32.00	32.00	45.00
800.00	33.00	33.00	45.00
900.00	34.00	34.00	45.00
1000.00	35.00	35.00	45.00
1100.00	36.00	36.00	45.00
1200.00	37.00	37.00	45.00
1300.00	38.00	38.00	45.00
1400.00	39.00	39.00	45.00
1500.00	40.00	40.00	45.00
1600.00	41.00	41.00	45.00
1700.00	42.00	42.00	45.00
1800.00	43.00	43.00	45.00
1900.00	44.00	44.00	45.00
2000.00	45.00	45.00	45.00
2100.00	46.00	46.00	45.00
2200.00	47.00	47.00	45.00
2300.00	48.00	48.00	45.00
2400.00	49.00	49.00	45.00
2450.00	50.00	50.00	45.00
2500.00	51.00	51.00	45.00
2600.00	52.00	52.00	45.00
2700.00	53.00	53.00	45.00
2800.00	50.00	54.00	45.00
2850.00	51.00	55.00	45.00
2900.00	52.00	56.00	45.00
3000.00	53.00	57.00	45.00

Figures

Spreadsheets

Modelling		Modelling				Geomagnetic data		
SFx	1.1000	exm	0.2500			B	50.000	uT
SFy	0.9500	eym	0.2950			Dip	10.000	deg
SFz	1.2500	ezm	-0.3350	Bias noise	0 nT	Bh	49.240	uT
						Bv	8.682	uT
						G	1	g

Bo	50.000	uT
Dipo	10.000	deg
Bho	49.240	uT
Bvo	8.682	uT
G	1	g

Survey				Modelled raw survey data						
AHD	Tf	Inc	Azi	AHD	Ax	Ay	Az	Bx	By	Bz
0	25	5	45	0	-0.08	0.04	1.00	16.04	-45.90	11.68
1000	115	7	47	1000	0.05	0.11	0.99	-46.28	-14.03	12.71
1100	205	9	49	1100	0.14	-0.07	0.99	-11.98	46.59	13.63
1200	295	11	51	1200	-0.08	-0.17	0.98	46.84	9.89	14.44
1300	25	13	53	1300	-0.20	0.10	0.97	7.78	-47.02	15.13
1400	115	15	55	1400	0.11	0.23	0.97	-47.14	-5.64	15.70
1500	205	17	57	1500	0.26	-0.12	0.96	-3.49	47.19	16.14
1600	295	19	59	1600	-0.14	-0.30	0.95	47.19	1.33	16.47
1700	25	21	61	1700	-0.32	0.15	0.93	-0.82	-47.14	16.66
1800	115	23	63	1800	0.17	0.35	0.92	-47.03	2.97	16.73
1900	205	25	65	1900	0.38	-0.18	0.91	5.09	46.87	16.66
2000	295	27	67	2000	-0.19	-0.41	0.89	46.66	-7.19	16.47
2100	25	29	69	2100	-0.44	0.20	0.87	-9.25	-46.41	16.15
2200	115	31	71	2200	0.22	0.47	0.86	-46.11	11.28	15.70
2300	205	33	73	2300	0.49	-0.23	0.84	13.24	45.78	15.12
2400	295	35	75	2400	-0.24	-0.52	0.82	45.41	-15.15	14.42
2500	25	37	77	2500	-0.55	0.25	0.80	-16.99	-45.01	13.60
2600	115	39	79	2600	0.27	0.57	0.78	-44.58	18.76	12.66
2700	205	41	81	2700	0.59	-0.28	0.75	20.45	44.13	11.61
2800	295	43	83	2800	-0.29	-0.62	0.73	43.65	-22.04	10.44
2900	25	45	85	2900	-0.64	0.30	0.71	-23.54	-43.14	9.17
3000	115	47	87	3000	0.31	0.66	0.68	-42.62	24.94	7.81

Measured raw survey data (includes scale factor and bias errors)							Computed survey without MSA applied					
AHD	Ax	Ay	Az	Bxmi	Bymi	Bzmi	AHD	TfM	IncM	AziM	Dipm	Bm
0	-0.08	0.04	1.00	17.89	-43.31	14.27	0	25.0	5.0	41.7	13.2	49.0
1000	0.05	0.11	0.99	-50.66	-13.03	15.55	1000	115.0	7.0	49.2	12.0	54.6
1100	0.14	-0.07	0.99	-12.93	44.56	16.70	1100	205.0	9.0	46.8	13.7	49.3
1200	-0.08	-0.17	0.98	51.77	9.70	17.71	1200	295.0	11.0	52.0	12.0	55.6
1300	-0.20	0.10	0.97	8.81	-44.37	18.57	1300	25.0	13.0	50.4	14.3	48.9
1400	0.11	0.23	0.97	-51.60	-5.06	19.29	1400	115.0	15.0	55.7	12.3	55.3
1500	0.26	-0.12	0.96	-3.59	45.13	19.84	1500	205.0	17.0	55.4	14.6	49.4
1600	-0.14	-0.30	0.95	52.16	1.56	20.25	1600	295.0	19.0	58.3	11.9	56.0
1700	-0.32	0.15	0.93	-0.65	-44.48	20.49	1700	25.0	21.0	59.1	14.9	49.0
1800	0.17	0.35	0.92	-51.48	3.11	20.57	1800	115.0	23.0	62.0	12.0	55.5
1900	0.38	-0.18	0.91	5.85	44.82	20.49	1900	205.0	25.0	64.0	15.0	49.6
2000	-0.19	-0.41	0.89	51.57	-6.54	20.25	2000	295.0	27.0	64.8	11.2	55.8
2100	-0.44	0.20	0.87	-9.93	-43.79	19.85	2100	25.0	29.0	67.8	15.1	49.1
2200	0.22	0.47	0.86	-50.47	11.01	19.29	2200	115.0	31.0	68.7	11.2	55.1
2300	0.49	-0.23	0.84	14.82	43.79	18.57	2300	205.0	33.0	72.6	14.9	49.8
2400	-0.24	-0.52	0.82	50.20	-14.10	17.69	2400	295.0	35.0	71.7	10.1	55.1
2500	-0.55	0.25	0.80	-18.44	-42.47	16.67	2500	25.0	37.0	76.6	14.8	49.2
2600	0.27	0.57	0.78	-48.79	18.12	15.49	2600	115.0	39.0	75.9	10.0	54.3
2700	0.59	-0.28	0.75	22.74	42.22	14.17	2700	205.0	41.0	81.4	14.5	50.0
2800	-0.29	-0.62	0.73	48.26	-20.65	12.72	2800	295.0	43.0	79.3	8.7	54.0
2900	-0.64	0.30	0.71	-25.65	-40.69	11.13	2900	25.0	45.0	85.7	14.2	49.4
3000	0.31	0.66	0.68	-46.64	23.99	9.42	3000	115.0	47.0	84.0	8.5	53.3

General Surveying Data | MSA | Sheet1 | + | Sum: 0

Figure 8-1: Spreadsheet 2, MSA

Solver results

Results		Difference between Actual error value and the solution		we want this to be close to zero
SFx	1.1000	dSFx	0.0000	
SFy	0.9500	dSFy	0.0000	
SFz	1.2500	dSFz	0.0000	
ex	0.2500109	dBx	0.00001	
ey	0.2949499	dBy	-0.00005	
ez	-0.3344272	dBz	0.00057	

sum of L^2: 0.00 | Set to Zero: 0.00

MSA applied		Computed Azimuth with MSA applied	Azimuth error	Regression													
Dipm	Bm	AziM		Bxci	Byci	Bzci	Dipm	Bm	Bhc	Bvc	dBx	dBy	dBz	E^2	L^2	a11	a12=a2
13.2	49.0	45.0	0.00	16.04	-45.90	11.68	10.00	50.00	49.24	8.68	0.00001	-0.00002	0.00008	0.00	0.00		
12.0	54.6	47.0	0.00	-46.28	-14.03	12.71	10.00	50.00	49.24	8.68	0.00000	-0.00004	0.00005	0.00	0.00	0.90308	0.29454
13.7	49.3	49.0	0.00	-11.98	46.59	13.63	10.00	50.00	49.24	8.68	0.00001	-0.00008	0.00002	0.00	0.00	0.092096	-0.26637
12.0	55.6	51.0	0.00	46.84	9.89	14.44	10.00	50.00	49.24	8.68	0.00002	-0.00006	-0.00001	0.00	0.00	0.938517	0.23738
14.3	48.9	53.0	0.00	7.78	-47.02	15.13	10.00	50.00	49.24	8.68	0.00001	-0.00002	-0.00003	0.00	0.00	0.079174	-0.20781
12.3	55.3	55.0	0.00	-47.14	-5.64	15.70	10.00	50.00	49.24	8.68	0.00000	-0.00005	-0.00005	0.00	0.00	0.965611	0.177935
14.6	49.4	57.0	0.00	-3.49	47.19	16.14	10.00	50.00	49.24	8.68	0.00001	-0.00008	-0.00006	0.00	0.00	0.084046	-0.148018
11.9	56.0	59.0	0.00	47.19	1.33	16.47	10.00	50.00	49.24	8.68	0.00002	-0.00005	-0.00007	0.00	0.00	0.984558	0.118325
14.9	49.0	61.0	0.00	-0.82	-47.14	16.66	10.00	50.00	49.24	8.68	0.00001	-0.00002	-0.00008	0.00	0.00	0.107136	-0.089112
12.0	55.5	63.0	0.00	-47.03	2.97	16.73	10.00	50.00	49.24	8.68	0.00000	-0.00005	-0.00008	0.00	0.00	0.995797	0.060631
15.0	49.6	65.0	0.00	5.09	46.87	16.66	10.00	50.00	49.24	8.68	0.00001	-0.00008	-0.00008	0.00	0.00	0.147995	-0.033125
11.2	55.8	67.0	0.00	46.66	-7.19	16.47	10.00	50.00	49.24	8.68	0.00002	-0.00005	-0.00007	0.00	0.00	0.999944	0.006816
15.1	49.1	69.0	0.00	-9.25	-46.41	16.15	10.00	50.00	49.24	8.68	0.00001	-0.00002	-0.00006	0.00	0.00	0.205266	0.018085
11.2	55.1	71.0	0.00	-46.11	11.28	15.70	10.00	50.00	49.24	8.68	0.00000	-0.00006	-0.00005	0.00	0.00	0.997748	-0.041385
14.9	49.8	73.0	0.00	13.24	45.78	15.12	10.00	50.00	49.24	8.68	0.00001	-0.00008	-0.00003	0.00	0.00	0.276748	0.062907
10.1	55.1	75.0	0.00	45.41	-15.15	14.42	10.00	50.00	49.24	8.68	0.00001	-0.00004	-0.00001	0.00	0.00	0.990036	-0.082501
14.8	49.2	77.0	0.00	-16.99	-45.01	13.60	10.00	50.00	49.24	8.68	0.00001	-0.00002	0.00002	0.00	0.00	0.359477	0.100035
10.0	54.3	79.0	0.00	-44.58	18.76	12.66	10.00	50.00	49.24	8.68	0.00000	-0.00007	0.00005	0.00	0.00	0.977658	-0.115396
14.5	50.0	81.0	0.00	20.45	44.13	11.61	10.00	50.00	49.24	8.68	0.00001	-0.00008	0.00008	0.00	0.00	0.449897	0.128497
8.7	54.0	83.0	0.00	43.65	-22.04	10.44	10.00	50.00	49.24	8.68	0.00001	-0.00004	0.00012	0.00	0.00	0.961455	-0.139275
14.2	49.4	85.0	0.00	-23.54	-43.14	9.17	10.00	50.00	49.24	8.68	0.00001	-0.00002	0.00016	0.00	0.00	0.544037	0.147685
8.5	53.3	87.0	0.00	-42.62	24.94	7.81	10.00	50.00	49.24	8.68	0.00001	-0.00007	0.00021	0.00	0.00	0.942207	-0.15370

a11	a12=a2
13.00248	0.076135

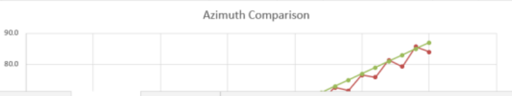

General Surveying Data | MSA | Sheet1 | + | Sum: 0

Figure 8-2: Spreadsheet 2, MSA

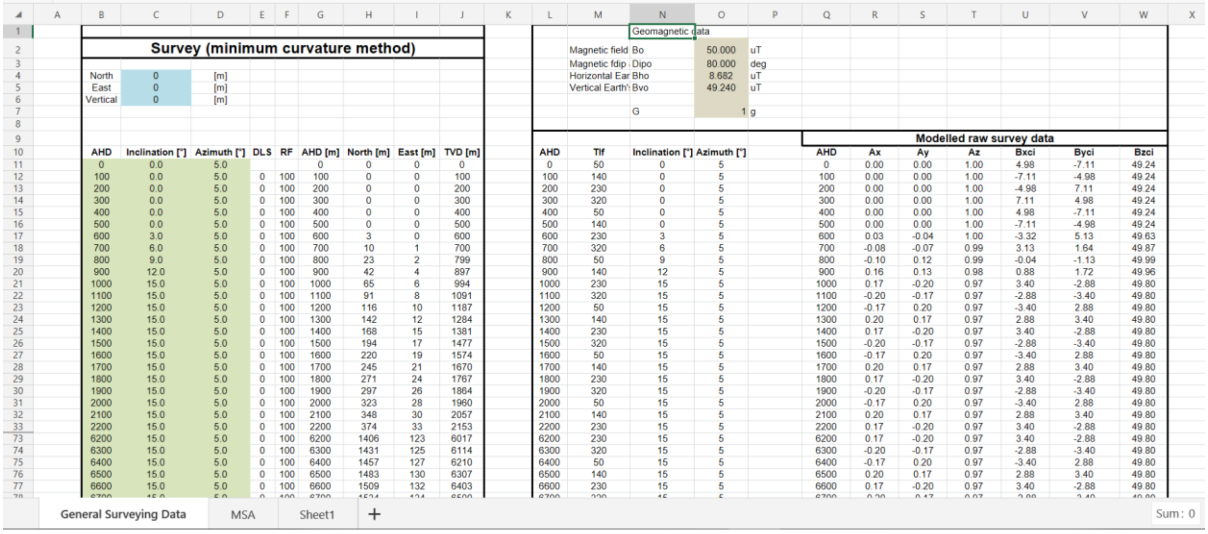

Figure 8-3: Spreadsheet 2, Minimum Curvature Method

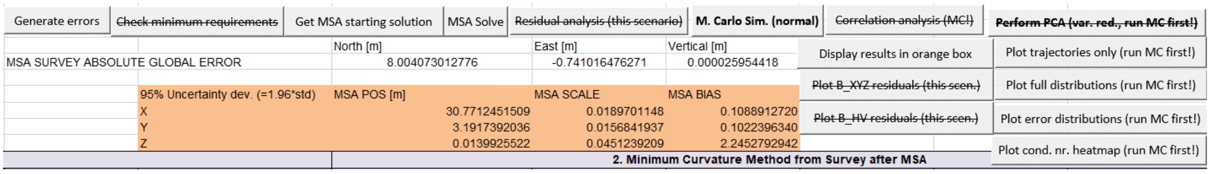

Figure 8-4: UI of modified Spreadsheet

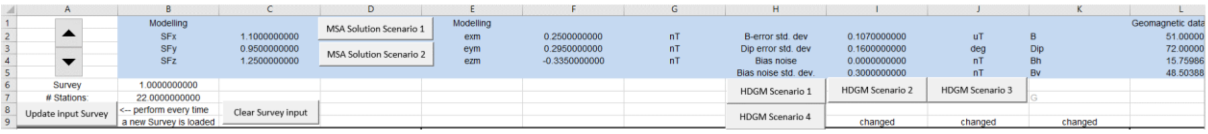

Figure 8-5: Modelling settings of modified Spreadsheet.

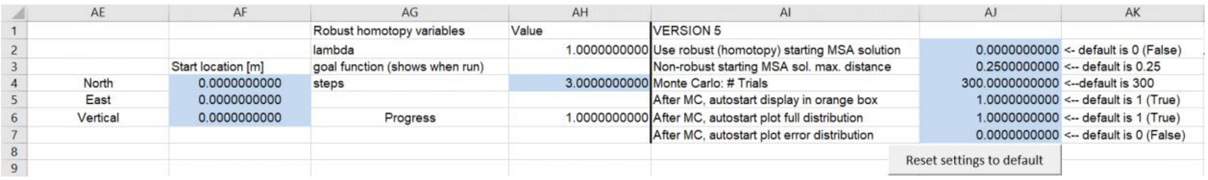

Figure 8-6: Additional configuration settings of modified Spreadsheet.

MSA Monte Carlo simulation plots

The figures below are generated by the modified Excel spreadsheet using the “Plot full distributions” function. Each figure represents a Survey, given in increasing order - Survey 1 to 7.

Scenario 1

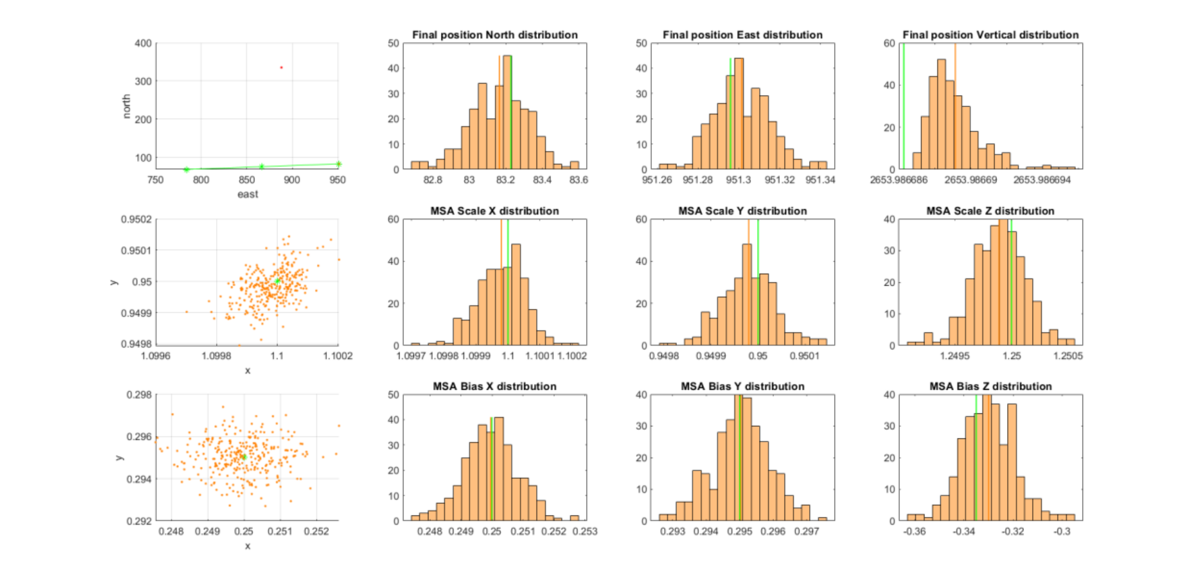

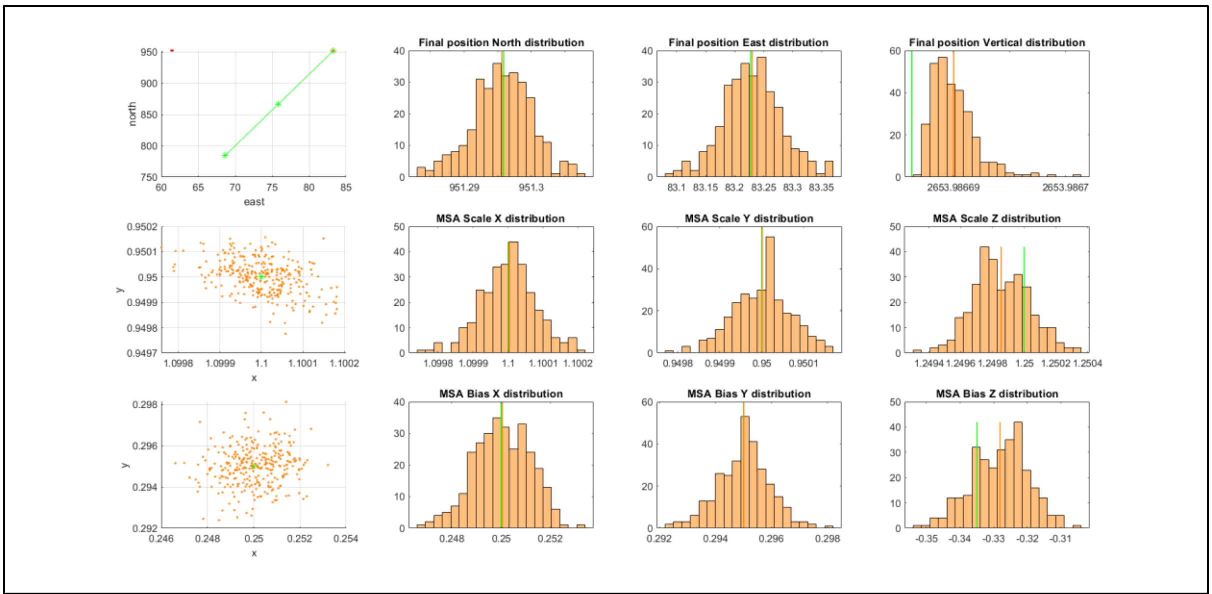

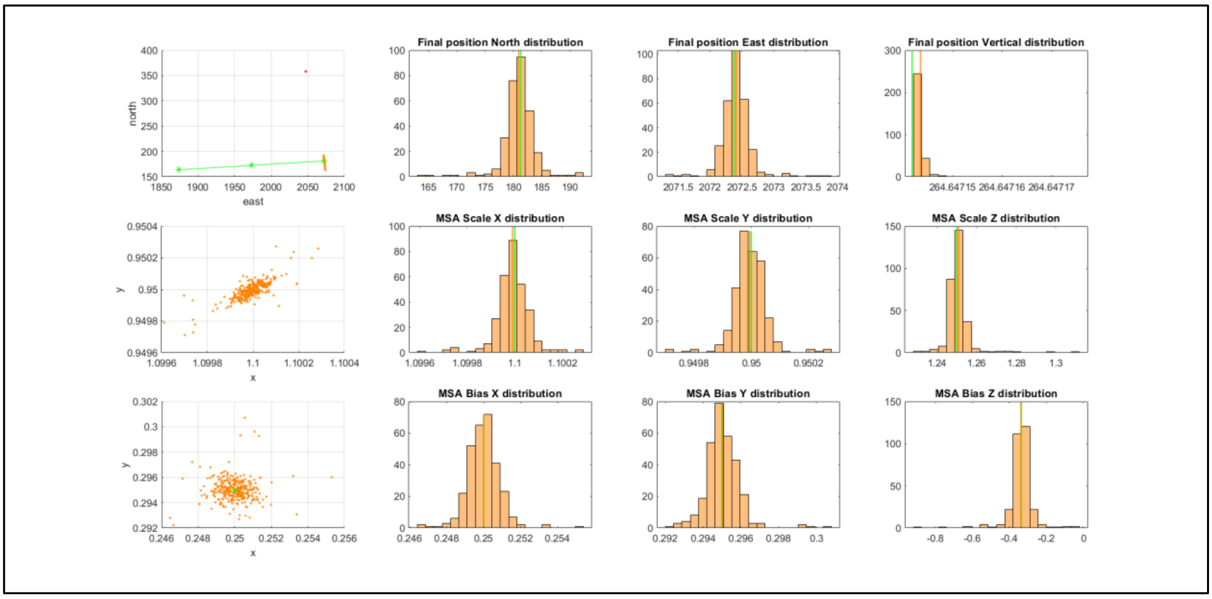
north
east
y
x
Final position North distribution
Final position East distribution
Final position Vertical distribution
MSA Scale X distribution
MSA Scale Y distribution
MSA Scale Z distribution
MSA Bias X distribution
MSA Bias Y distribution
MSA Bias Z distribution

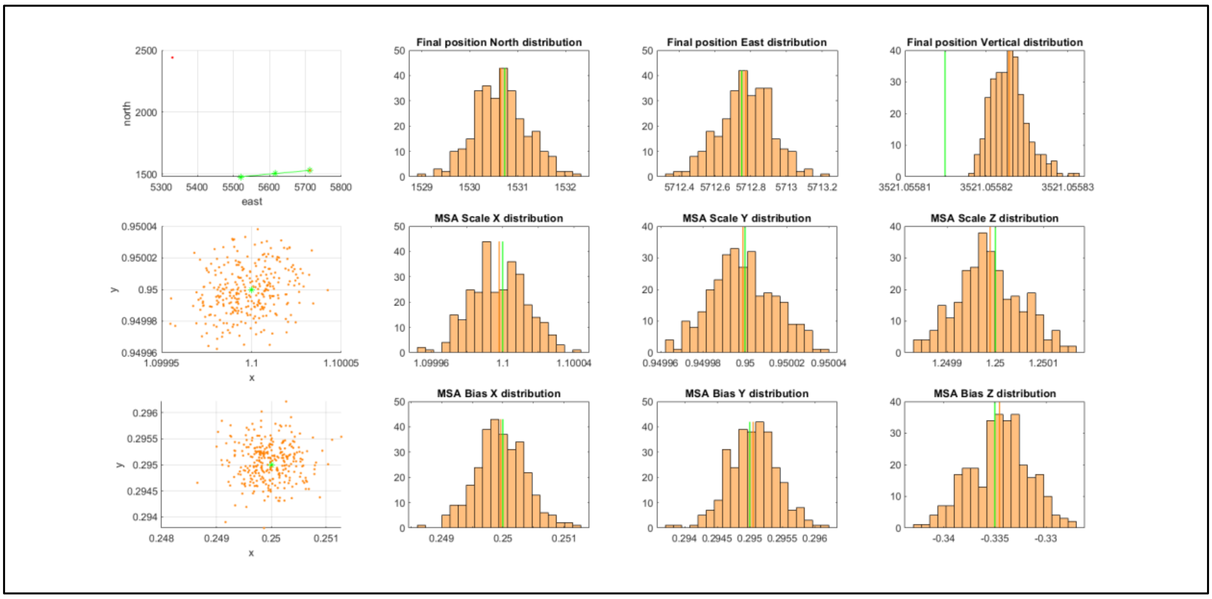
north
east
y
x
Final position North distribution
Final position East distribution
Final position Vertical distribution
MSA Scale X distribution
MSA Scale Y distribution
MSA Scale Z distribution
MSA Bias X distribution
MSA Bias Y distribution
MSA Bias Z distribution

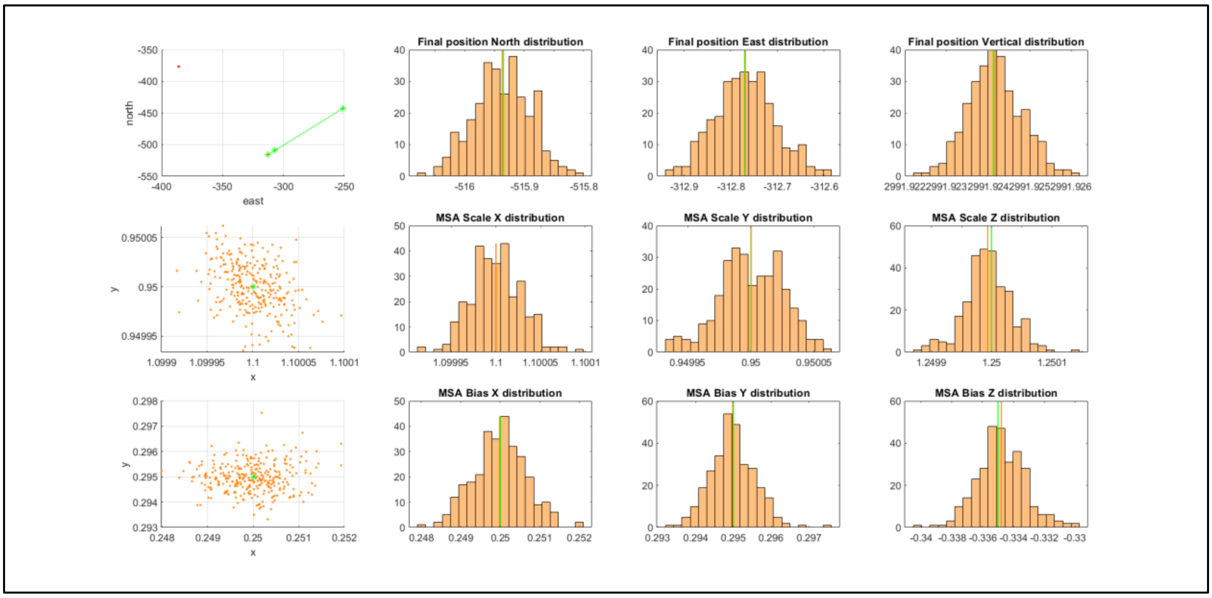
north
east
y
x
Final position North distribution
Final position East distribution
Final position Vertical distribution
MSA Scale X distribution
MSA Scale Y distribution
MSA Scale Z distribution
MSA Bias X distribution
MSA Bias Y distribution
MSA Bias Z distribution

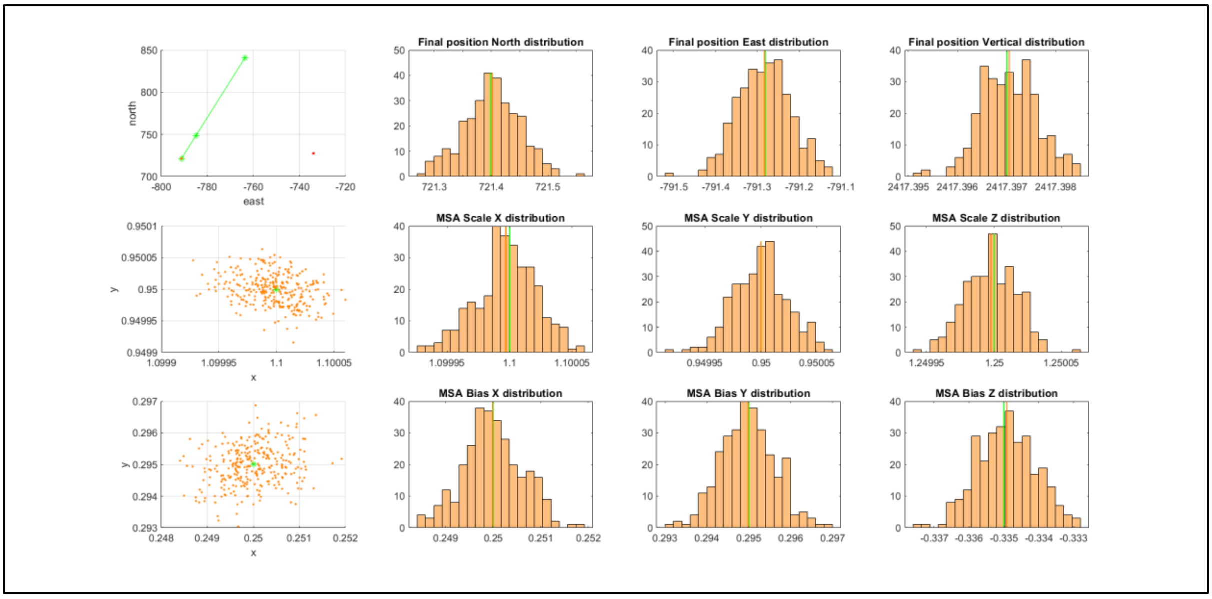
north
east
y
x
y
x
Final position North distribution
Final position East distribution
Final position Vertical distribution
MSA Scale X distribution
MSA Scale Y distribution
MSA Scale Z distribution
MSA Bias X distribution
MSA Bias Y distribution
MSA Bias Z distribution

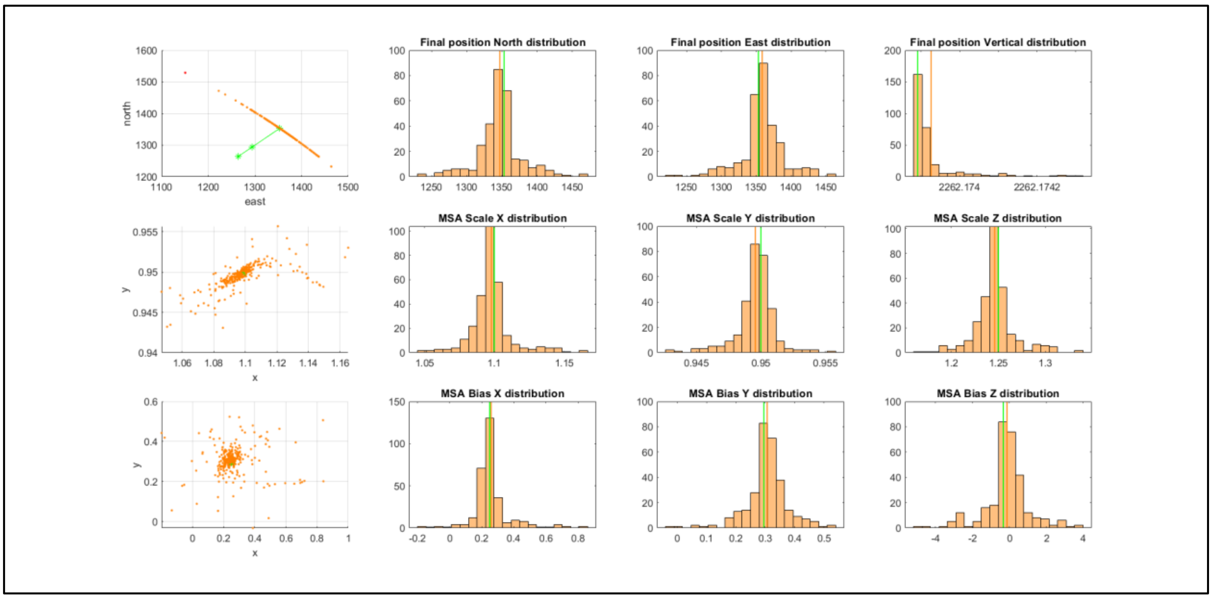
north
east
y
x
y
x
Final position North distribution
Final position East distribution
Final position Vertical distribution
MSA Scale X distribution
MSA Scale Y distribution
MSA Scale Z distribution
MSA Bias X distribution
MSA Bias Y distribution
MSA Bias Z distribution

Scenario 2

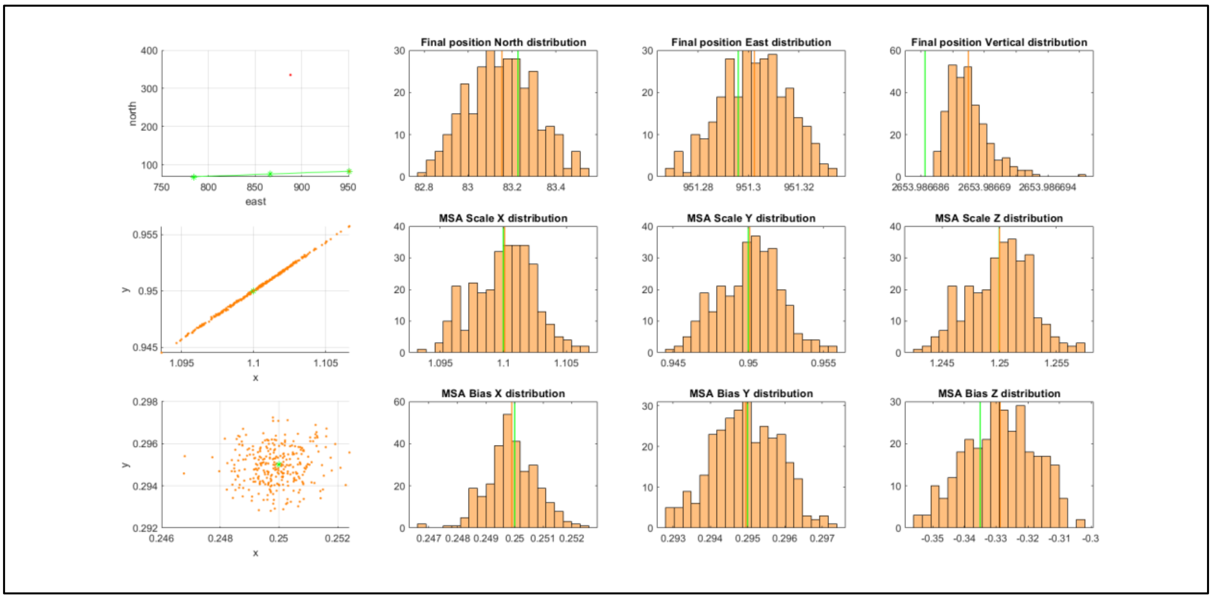

north
east
y
x
Final position North distribution
Final position East distribution
Final position Vertical distribution
MSA Scale X distribution
MSA Scale Y distribution
MSA Scale Z distribution
MSA Bias X distribution
MSA Bias Y distribution
MSA Bias Z distribution

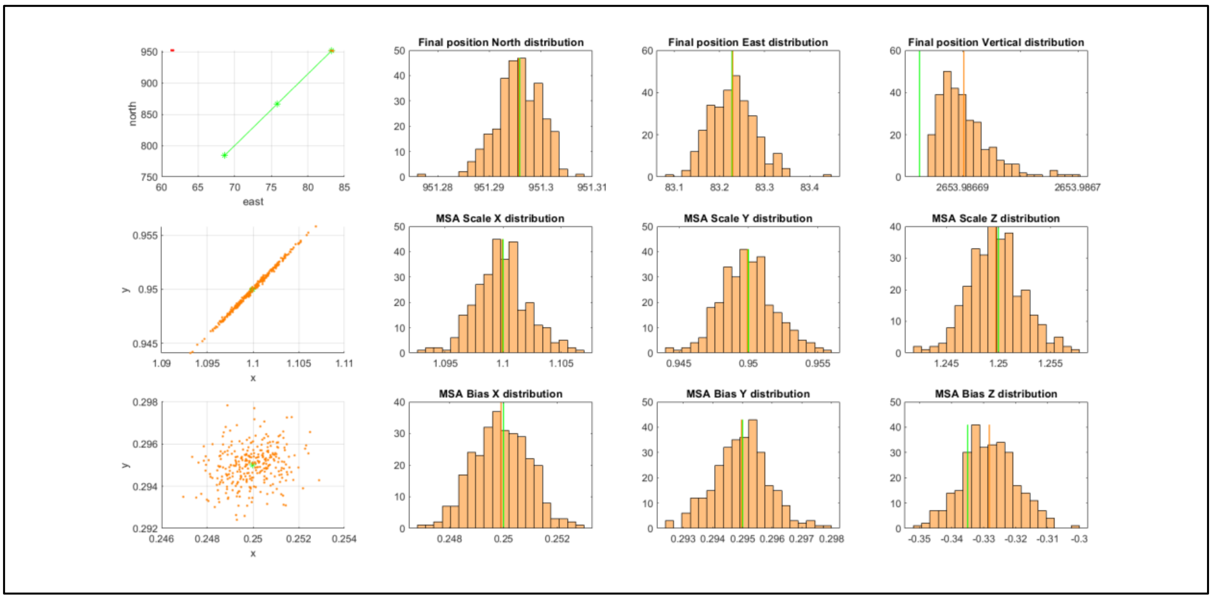

north
east
y
x
Final position North distribution
Final position East distribution
Final position Vertical distribution
MSA Scale X distribution
MSA Scale Y distribution
MSA Scale Z distribution
MSA Bias X distribution
MSA Bias Y distribution
MSA Bias Z distribution

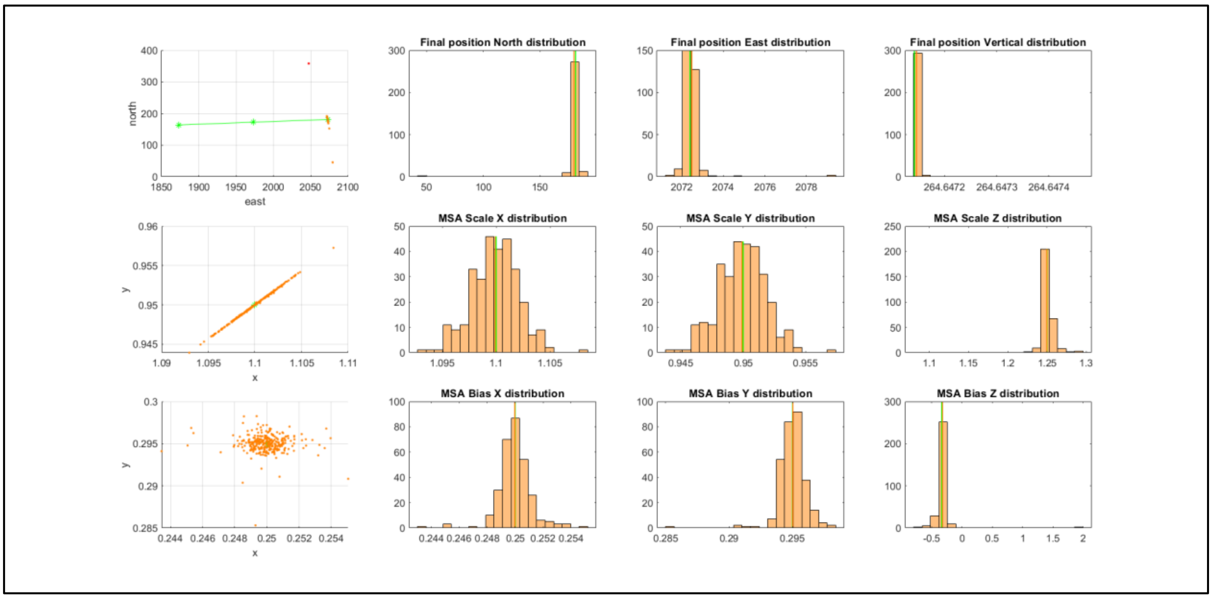

north
east
y
x
Final position North distribution
Final position East distribution
Final position Vertical distribution
MSA Scale X distribution
MSA Scale Y distribution
MSA Scale Z distribution
MSA Bias X distribution
MSA Bias Y distribution
MSA Bias Z distribution

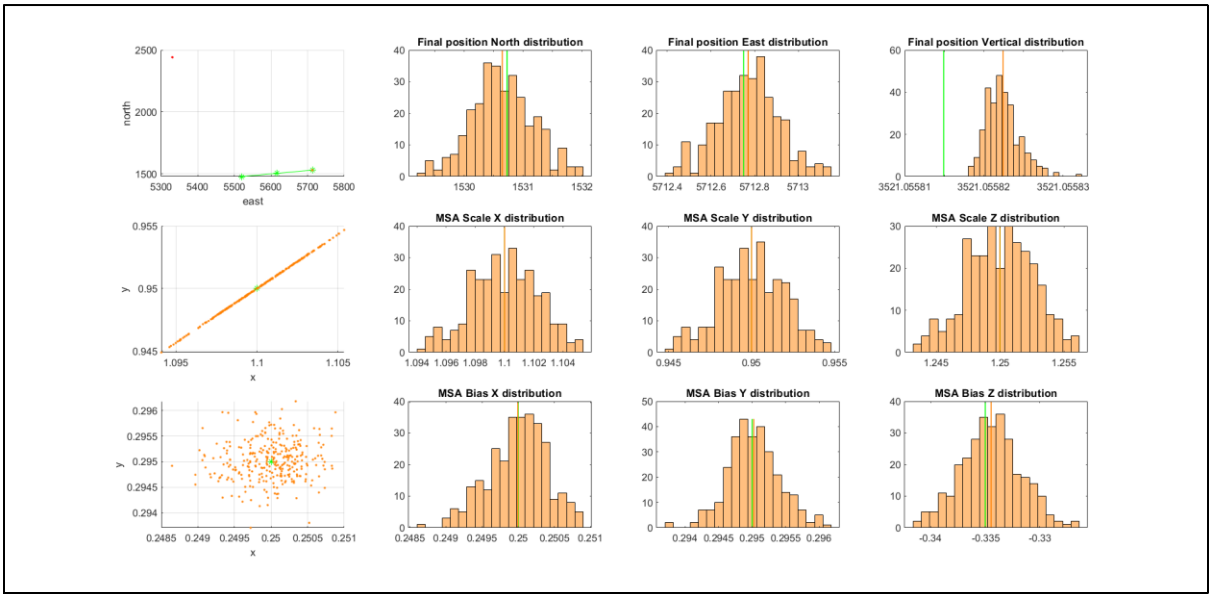
north
east
Final position North distribution
Final position East distribution
Final position Vertical distribution
y
x
MSA Scale X distribution
MSA Scale Y distribution
MSA Scale Z distribution
y
x
MSA Bias X distribution
MSA Bias Y distribution
MSA Bias Z distribution

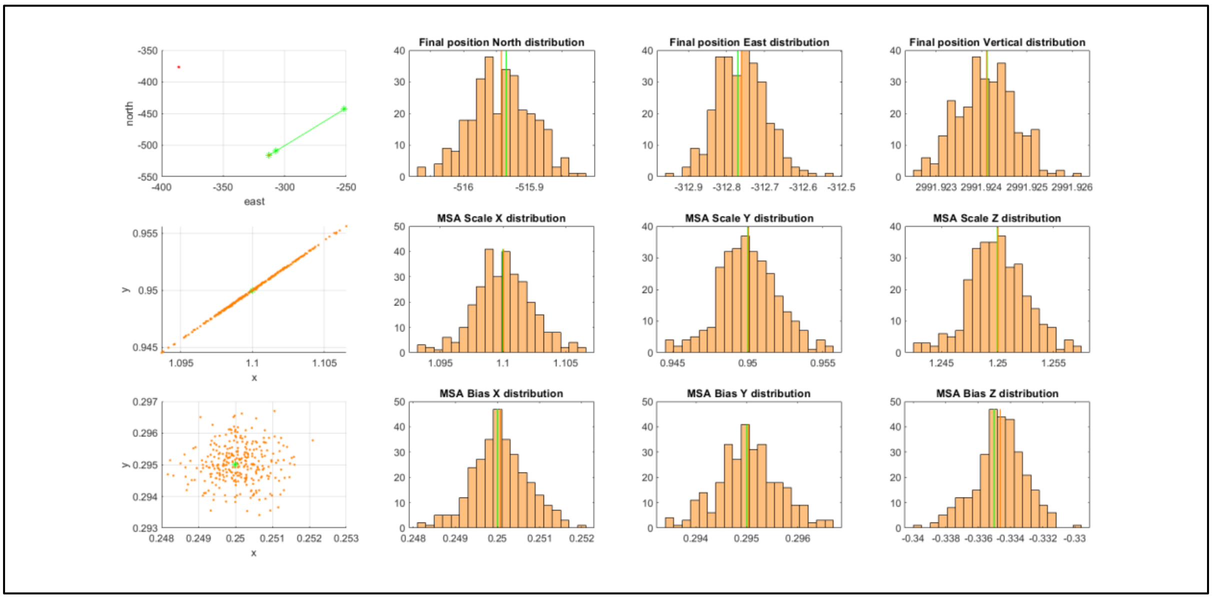
north
east
Final position North distribution
Final position East distribution
Final position Vertical distribution
y
x
MSA Scale X distribution
MSA Scale Y distribution
MSA Scale Z distribution
y
x
MSA Bias X distribution
MSA Bias Y distribution
MSA Bias Z distribution

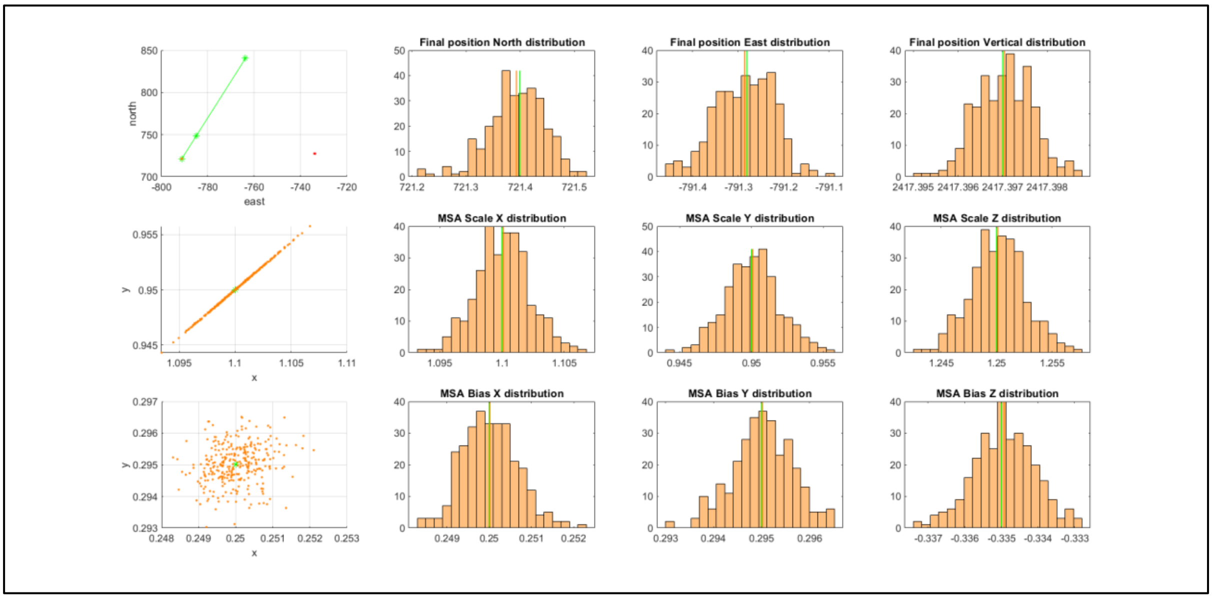
Final position North distribution
Final position East distribution
Final position Vertical distribution
MSA Scale X distribution
MSA Scale Y distribution
MSA Scale Z distribution
MSA Bias X distribution
MSA Bias Y distribution
MSA Bias Z distribution
north
east
y
x

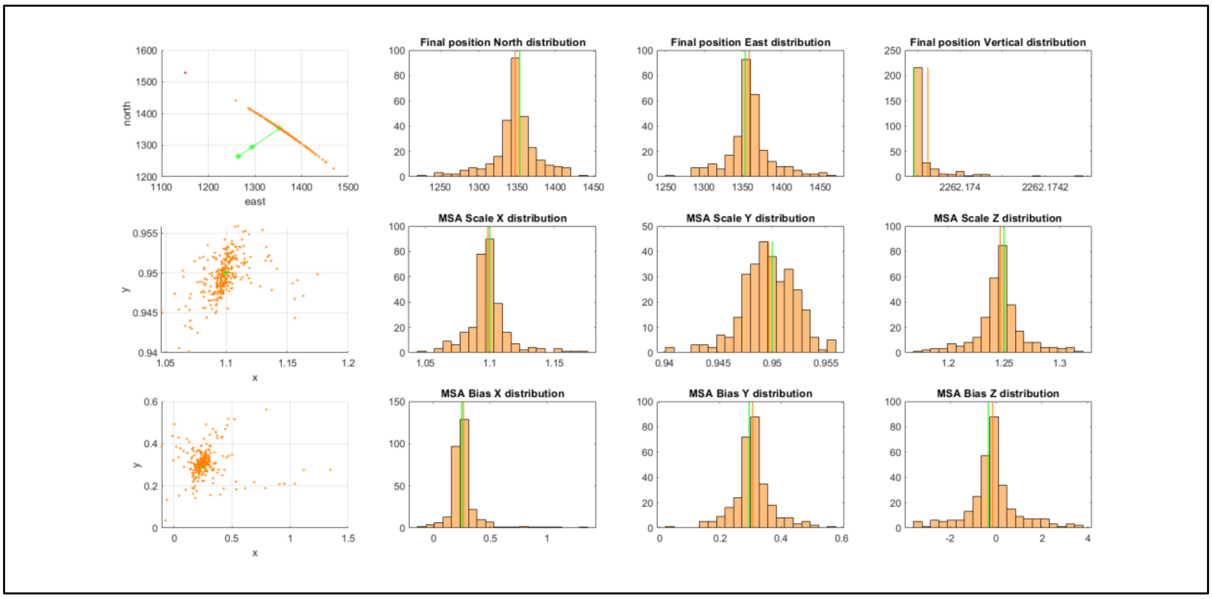
Final position North distribution
Final position East distribution
Final position Vertical distribution
MSA Scale X distribution
MSA Scale Y distribution
MSA Scale Z distribution
MSA Bias X distribution
MSA Bias Y distribution
MSA Bias Z distribution
north
east
y
x

Scenario 3

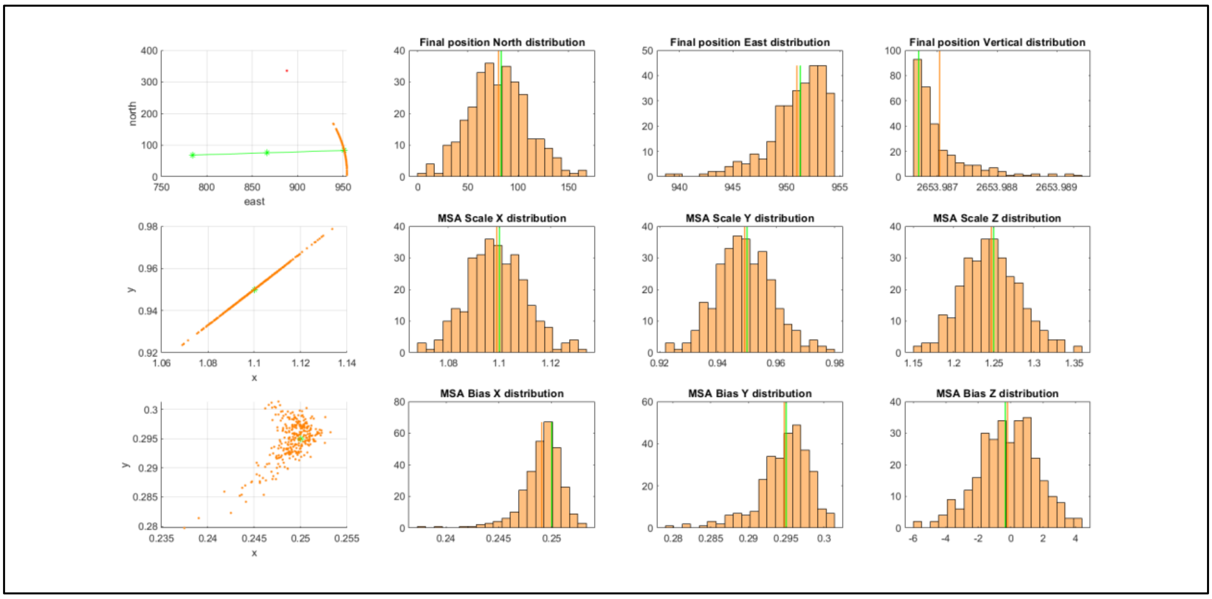
north
east
y
x
Final position North distribution
Final position East distribution
Final position Vertical distribution
MSA Scale X distribution
MSA Scale Y distribution
MSA Scale Z distribution
MSA Bias X distribution
MSA Bias Y distribution
MSA Bias Z distribution

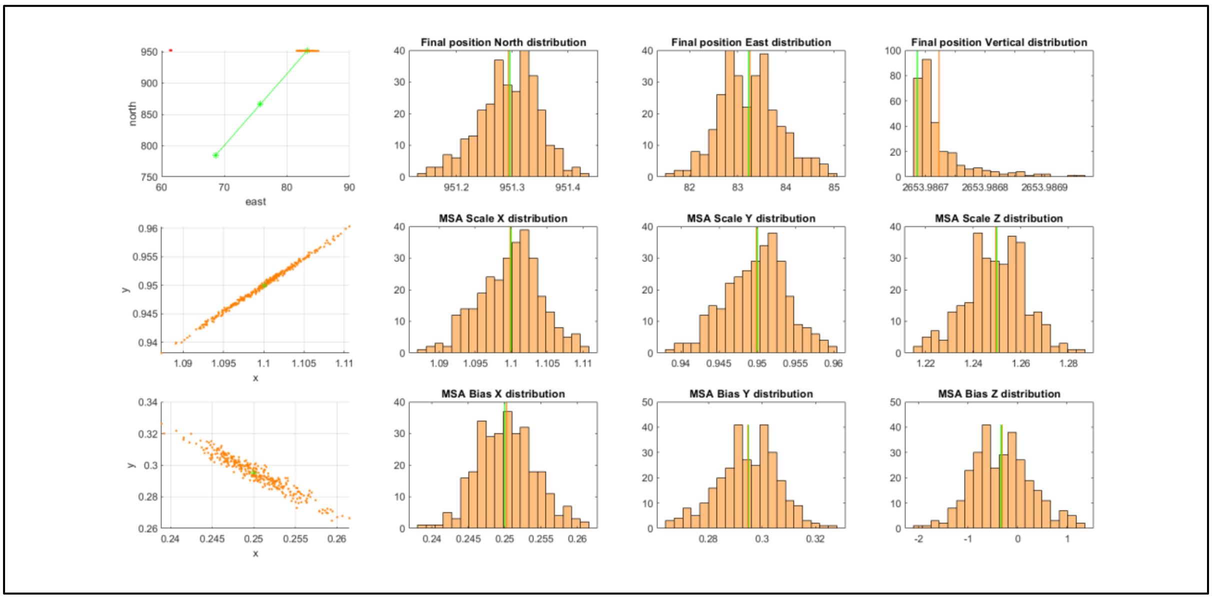
north
east
y
x
Final position North distribution
Final position East distribution
Final position Vertical distribution
MSA Scale X distribution
MSA Scale Y distribution
MSA Scale Z distribution
MSA Bias X distribution
MSA Bias Y distribution
MSA Bias Z distribution

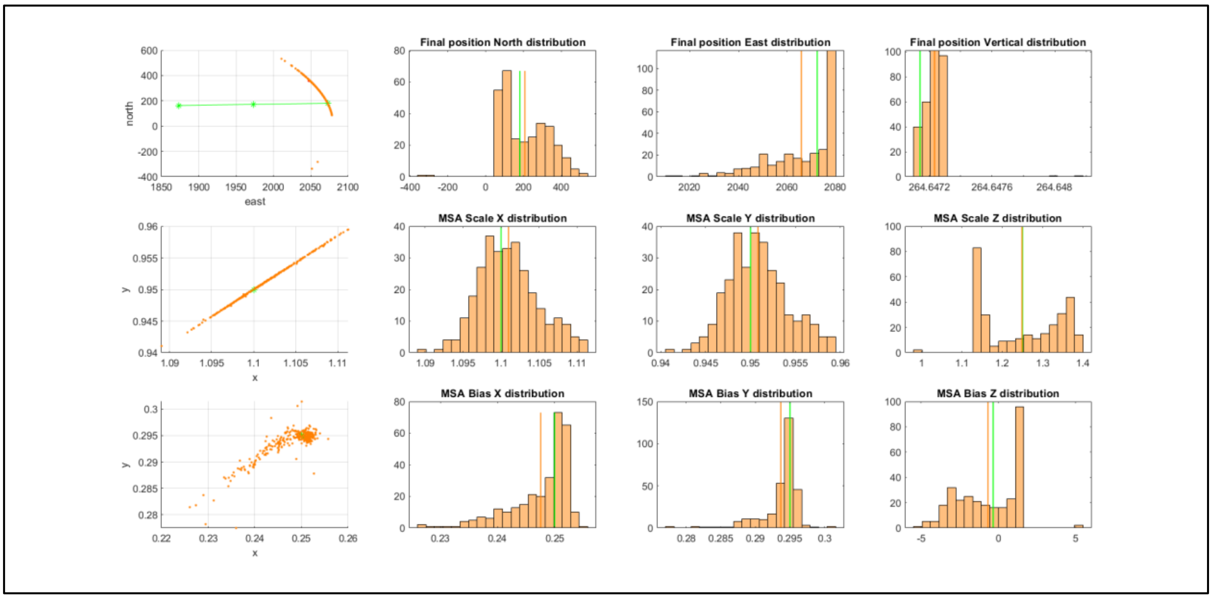
north
east
y
x
Final position North distribution
Final position East distribution
Final position Vertical distribution
MSA Scale X distribution
MSA Scale Y distribution
MSA Scale Z distribution
MSA Bias X distribution
MSA Bias Y distribution
MSA Bias Z distribution

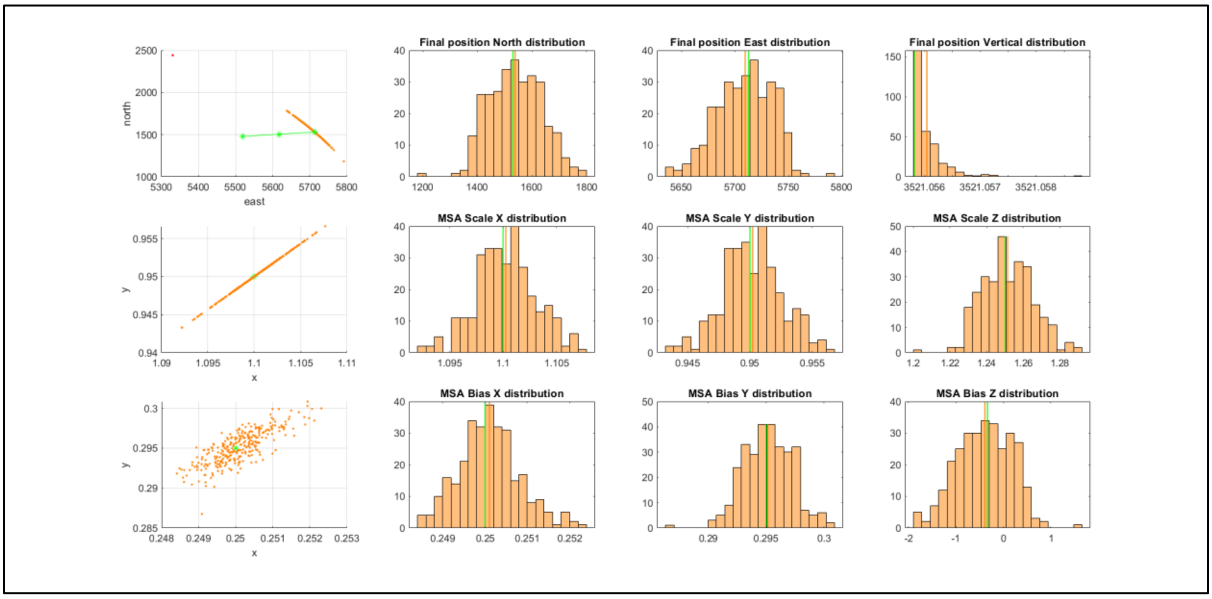
north
east
y
x
y
x
Final position North distribution
Final position East distribution
Final position Vertical distribution
MSA Scale X distribution
MSA Scale Y distribution
MSA Scale Z distribution
MSA Bias X distribution
MSA Bias Y distribution
MSA Bias Z distribution

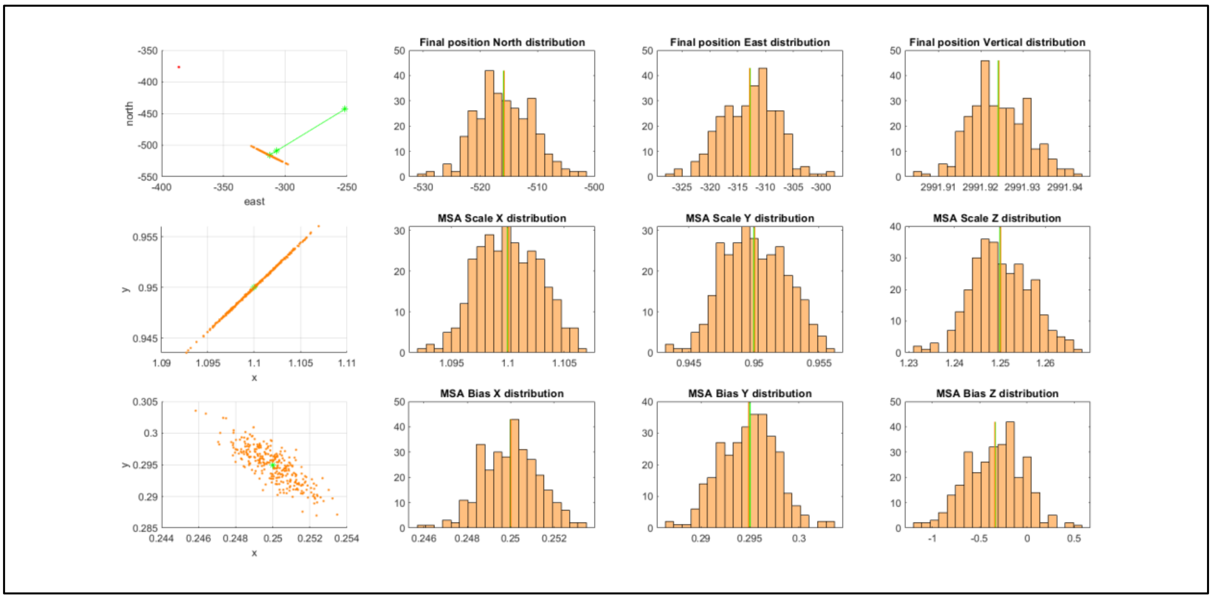
north
east
y
x
y
x
Final position North distribution
Final position East distribution
Final position Vertical distribution
MSA Scale X distribution
MSA Scale Y distribution
MSA Scale Z distribution
MSA Bias X distribution
MSA Bias Y distribution
MSA Bias Z distribution

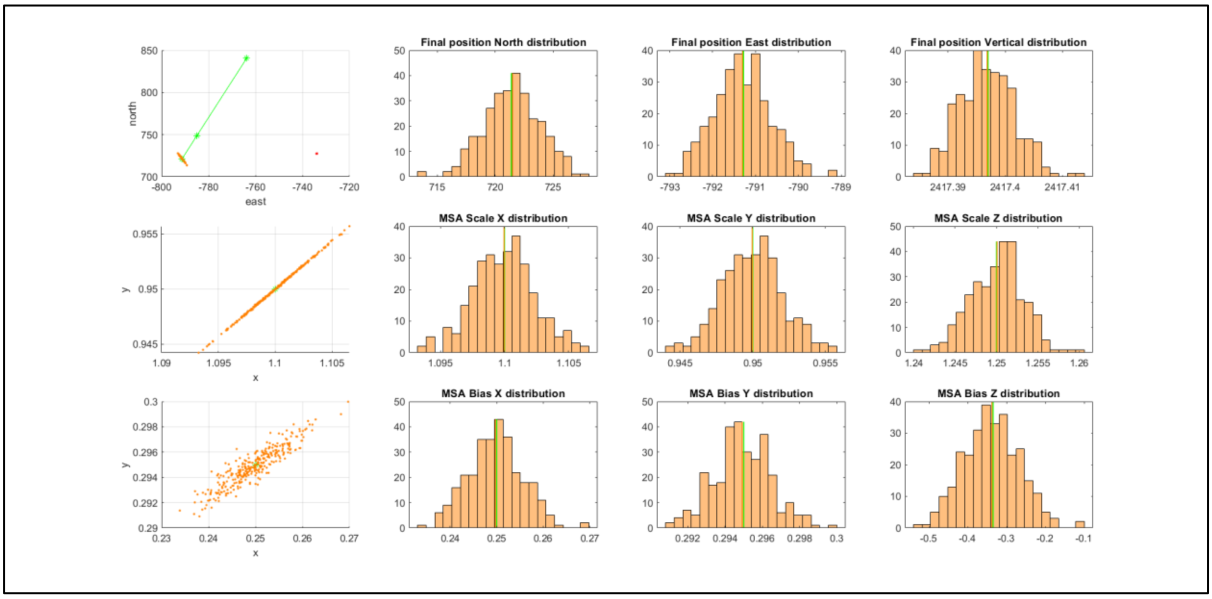
north
east
Final position North distribution
Final position East distribution
Final position Vertical distribution
y
x
MSA Scale X distribution
MSA Scale Y distribution
MSA Scale Z distribution
y
x
MSA Bias X distribution
MSA Bias Y distribution
MSA Bias Z distribution

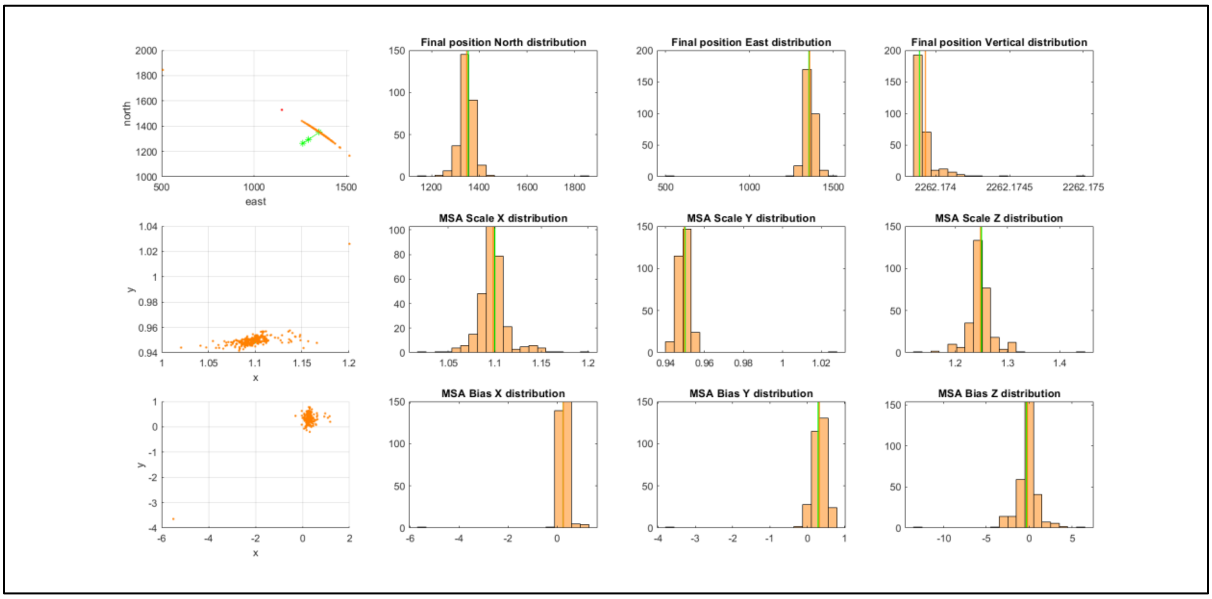
north
east
Final position North distribution
Final position East distribution
Final position Vertical distribution
y
x
MSA Scale X distribution
MSA Scale Y distribution
MSA Scale Z distribution
y
x
MSA Bias X distribution
MSA Bias Y distribution
MSA Bias Z distribution

Scenario 4

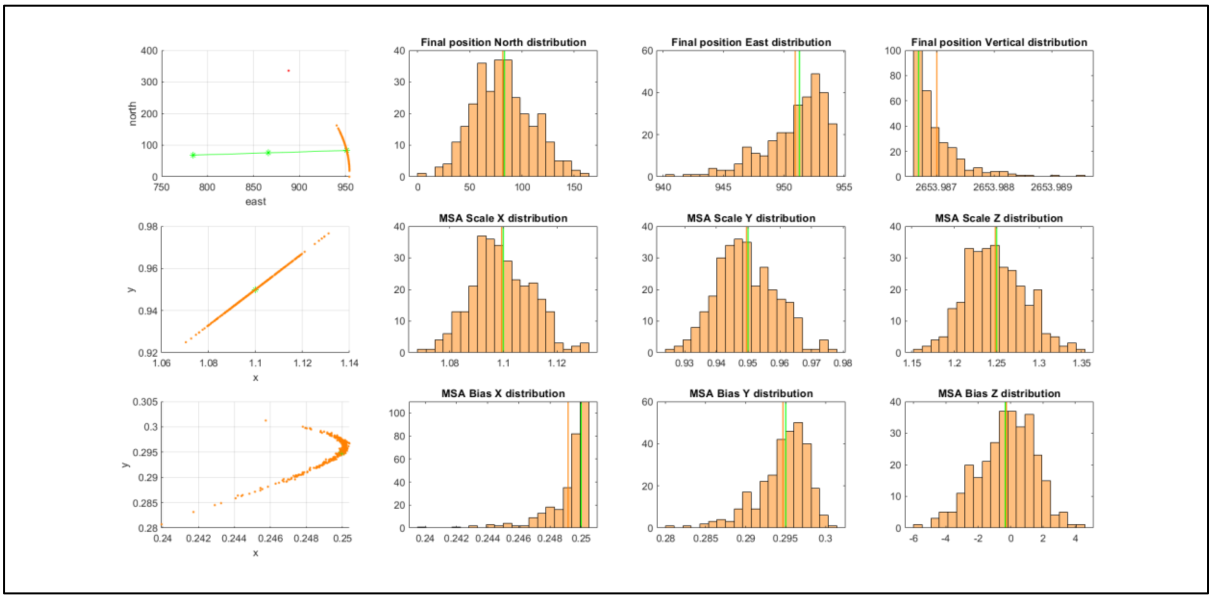
north
east
Final position North distribution
Final position East distribution
Final position Vertical distribution
y
x
MSA Scale X distribution
MSA Scale Y distribution
MSA Scale Z distribution
MSA Bias X distribution
MSA Bias Y distribution
MSA Bias Z distribution

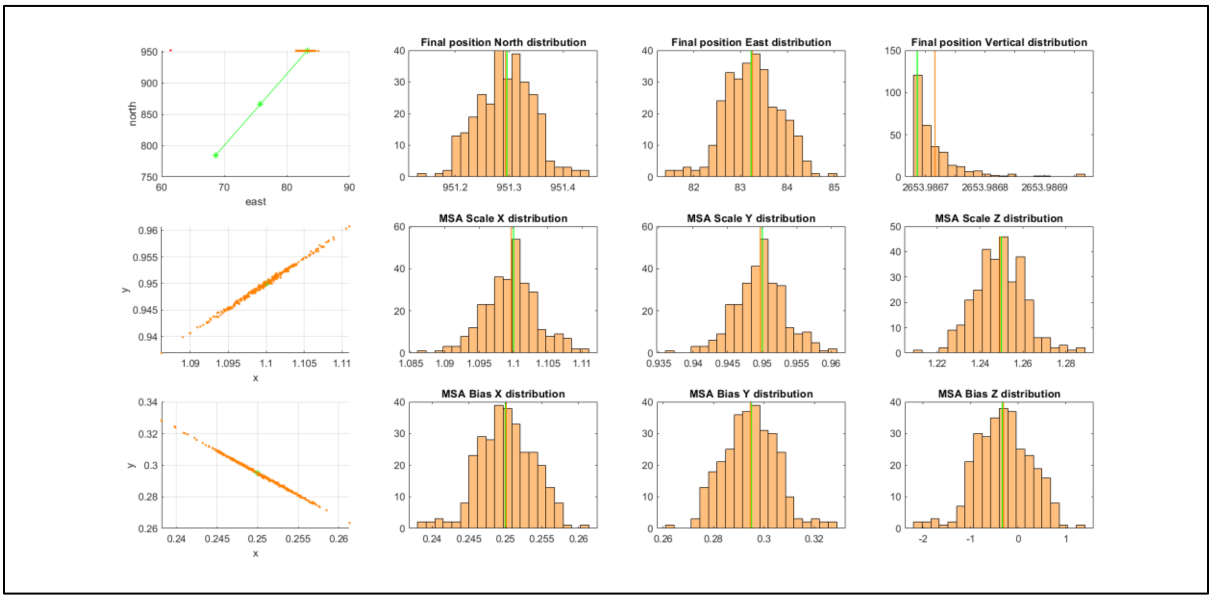
north
east
Final position North distribution
Final position East distribution
Final position Vertical distribution
y
x
MSA Scale X distribution
MSA Scale Y distribution
MSA Scale Z distribution
MSA Bias X distribution
MSA Bias Y distribution
MSA Bias Z distribution

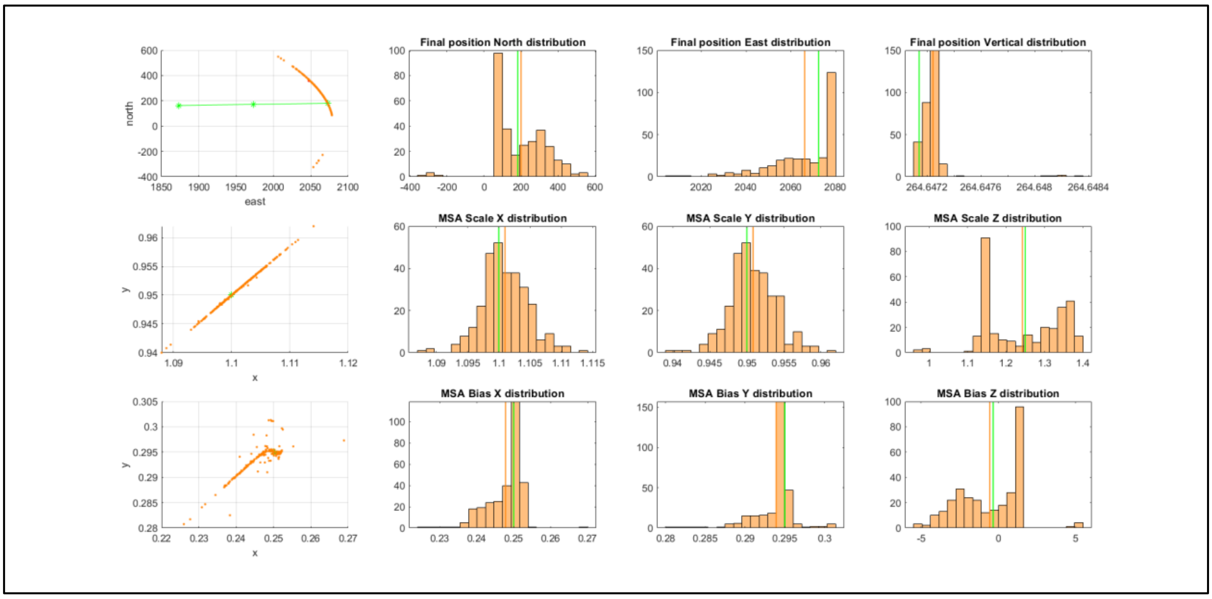
north
east
Final position North distribution
Final position East distribution
Final position Vertical distribution
y
x
MSA Scale X distribution
MSA Scale Y distribution
MSA Scale Z distribution
MSA Bias X distribution
MSA Bias Y distribution
MSA Bias Z distribution

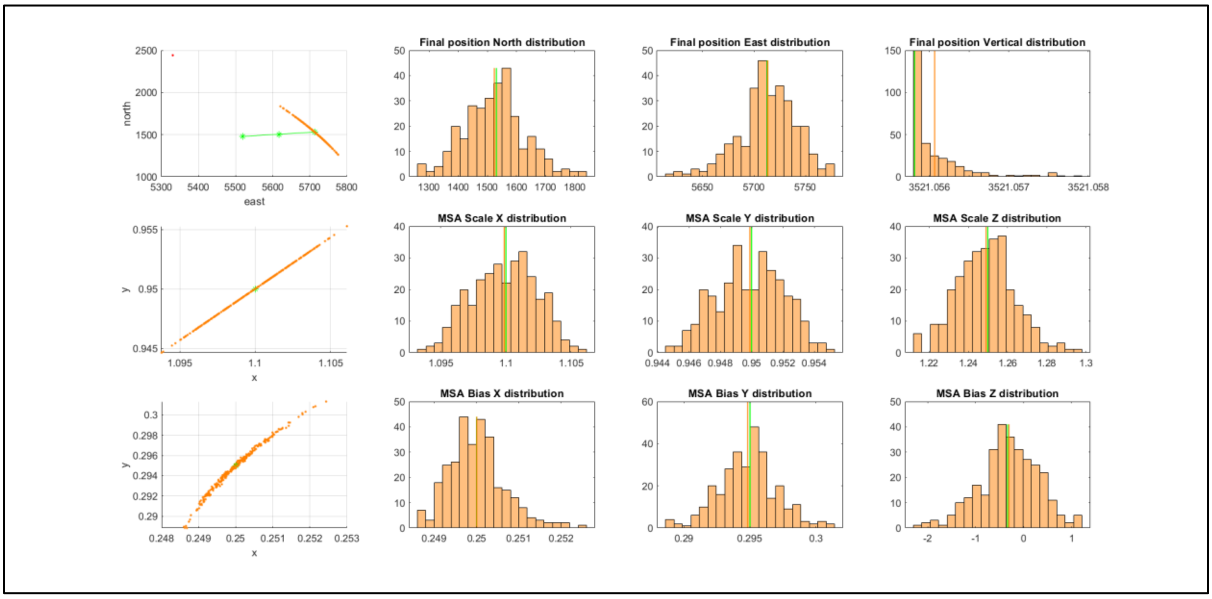
north
east
Final position North distribution
Final position East distribution
Final position Vertical distribution
y
x
MSA Scale X distribution
MSA Scale Y distribution
MSA Scale Z distribution
y
x
MSA Bias X distribution
MSA Bias Y distribution
MSA Bias Z distribution

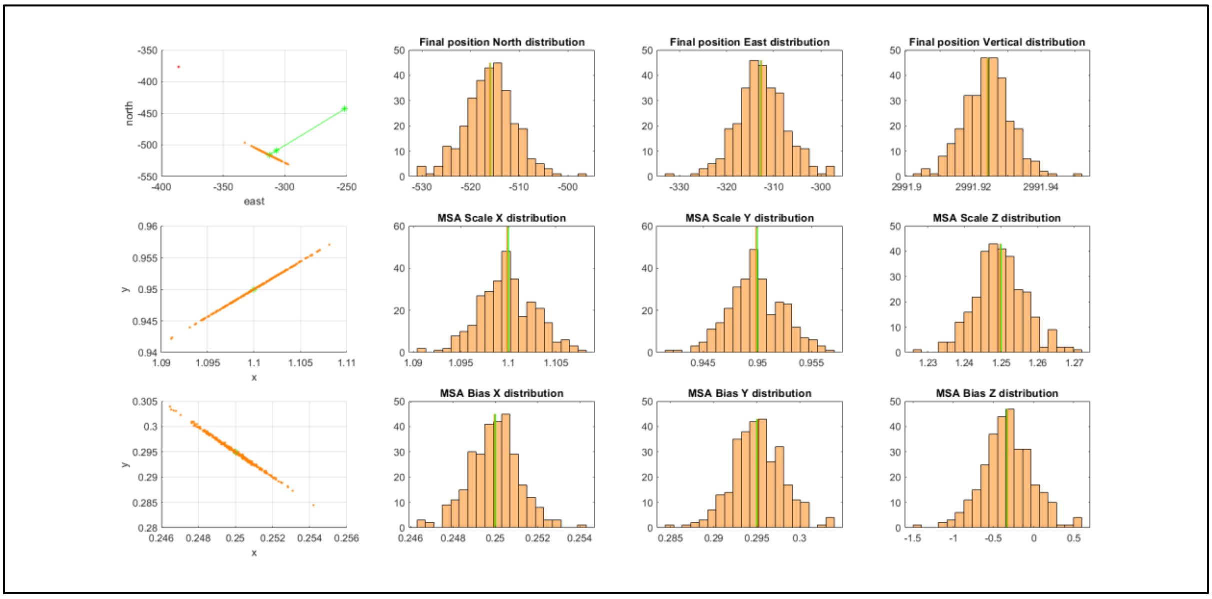
north
east
Final position North distribution
Final position East distribution
Final position Vertical distribution
y
x
MSA Scale X distribution
MSA Scale Y distribution
MSA Scale Z distribution
y
x
MSA Bias X distribution
MSA Bias Y distribution
MSA Bias Z distribution

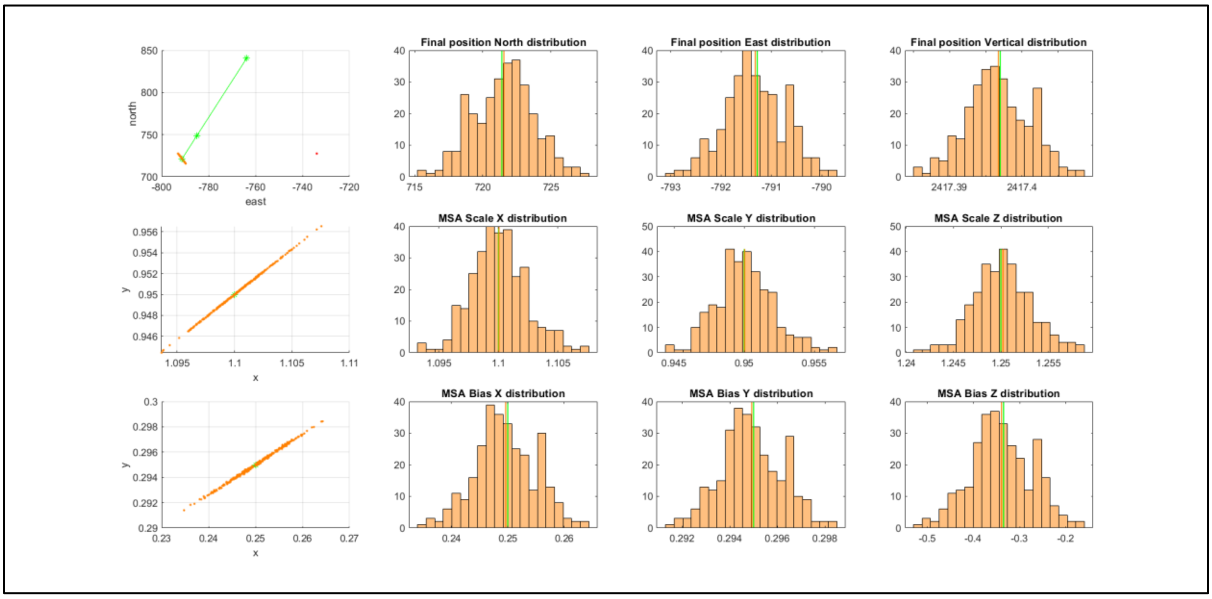
Final position North distribution
Final position East distribution
Final position Vertical distribution
MSA Scale X distribution
MSA Scale Y distribution
MSA Scale Z distribution
MSA Bias X distribution
MSA Bias Y distribution
MSA Bias Z distribution
north
east
y
x

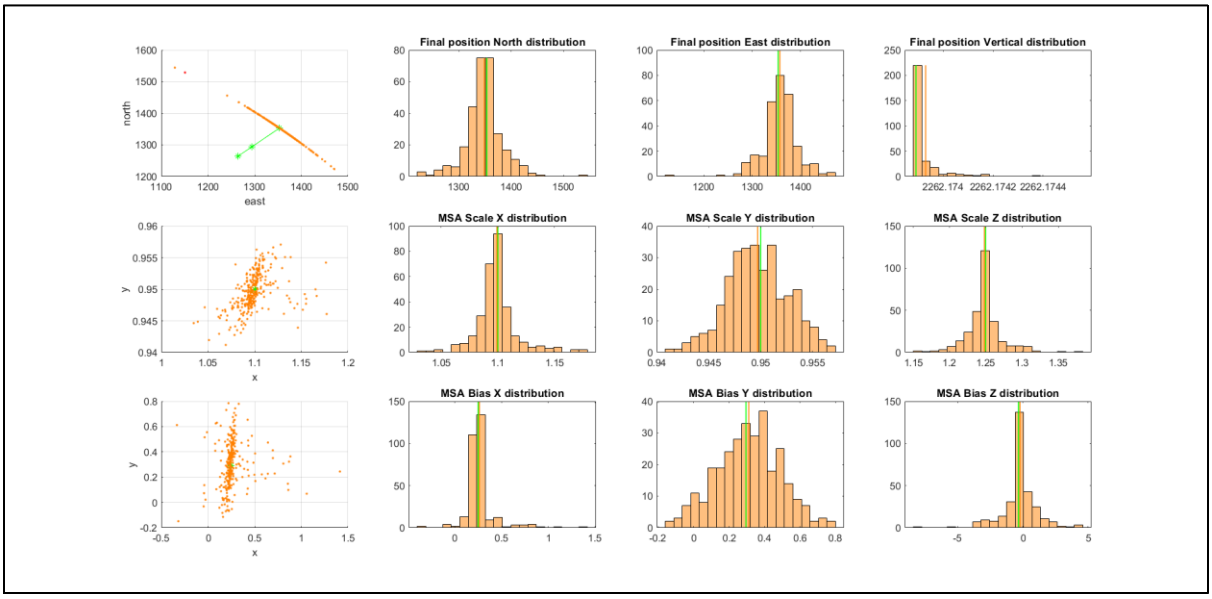
Final position North distribution
Final position East distribution
Final position Vertical distribution
MSA Scale X distribution
MSA Scale Y distribution
MSA Scale Z distribution
MSA Bias X distribution
MSA Bias Y distribution
MSA Bias Z distribution
north
east
y
x

MSA condition number plots (scenario 4)

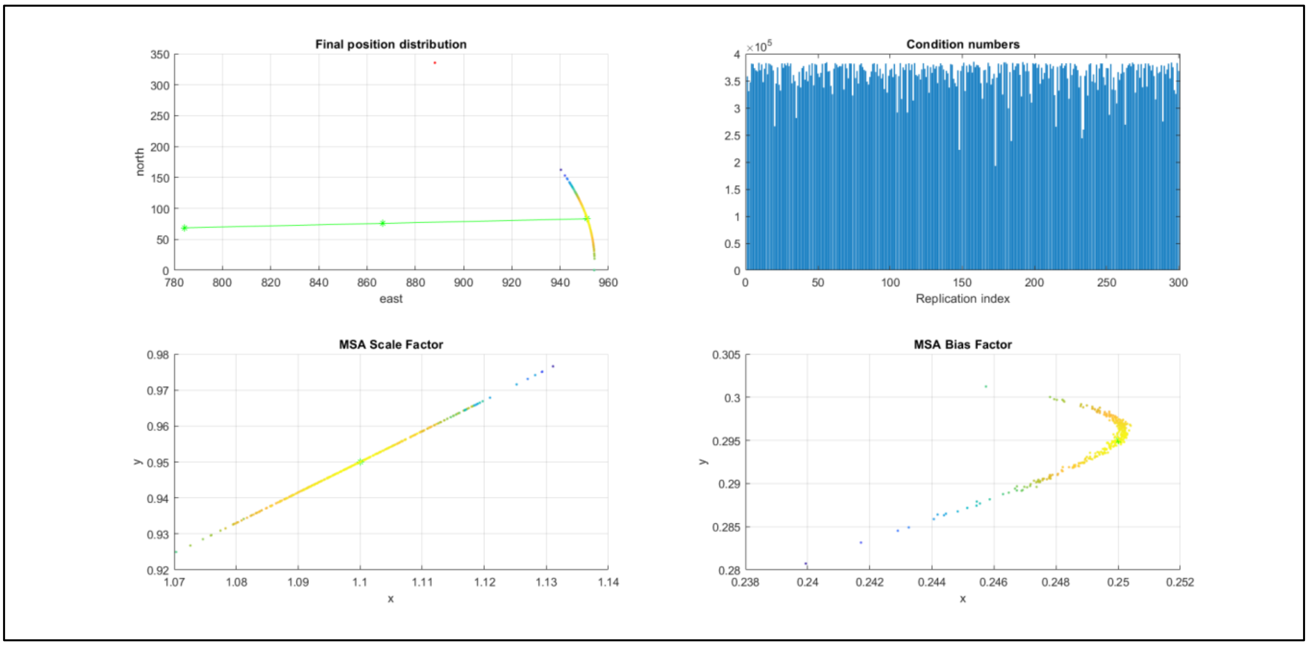

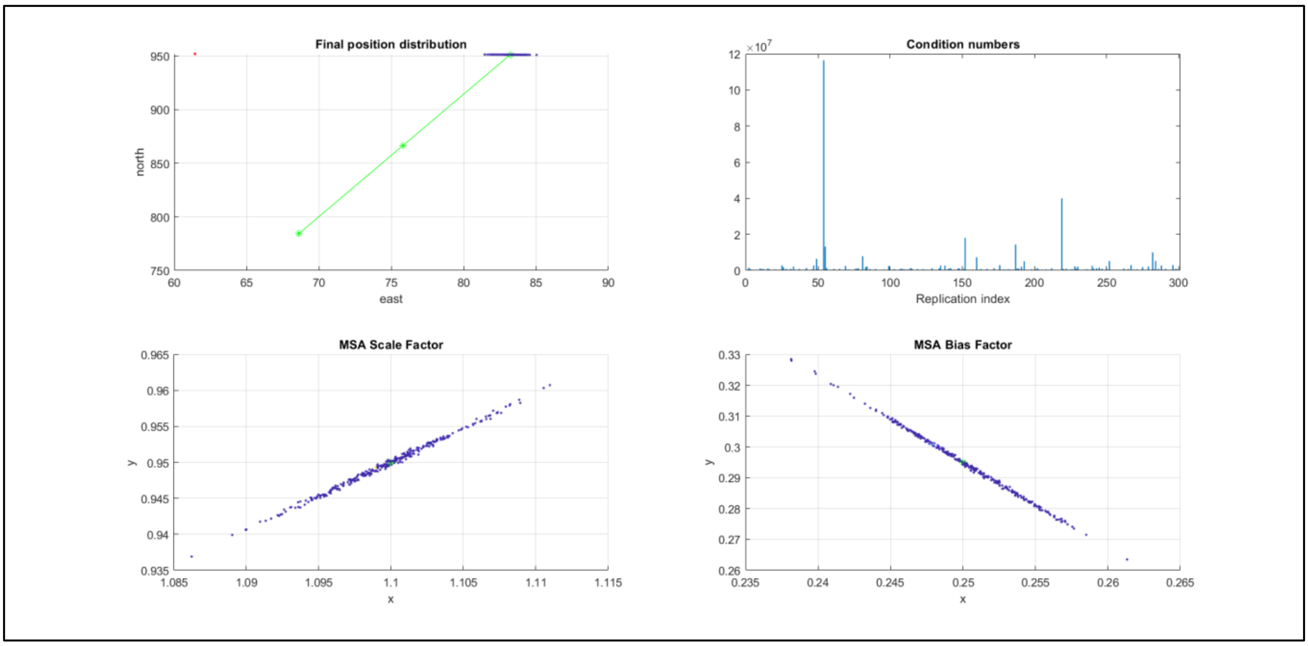

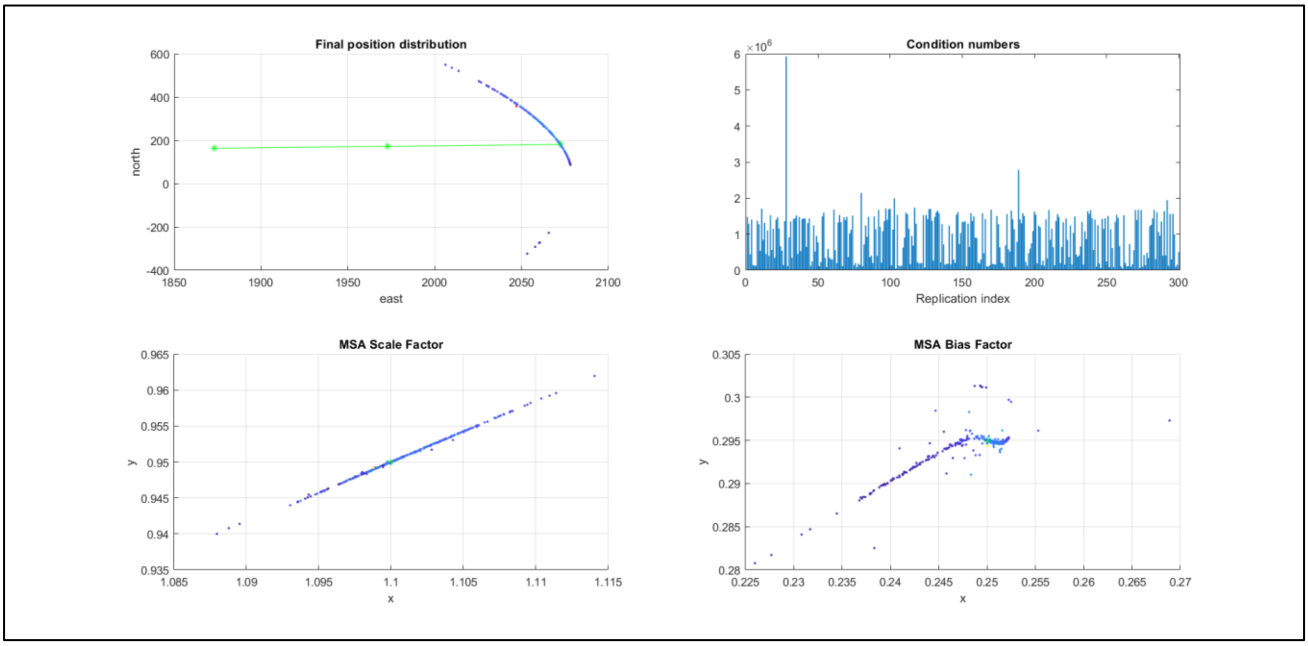
Final position distribution
north
east
Condition numbers
×10^6
Replication index
MSA Scale Factor
y
x
MSA Bias Factor
y
x

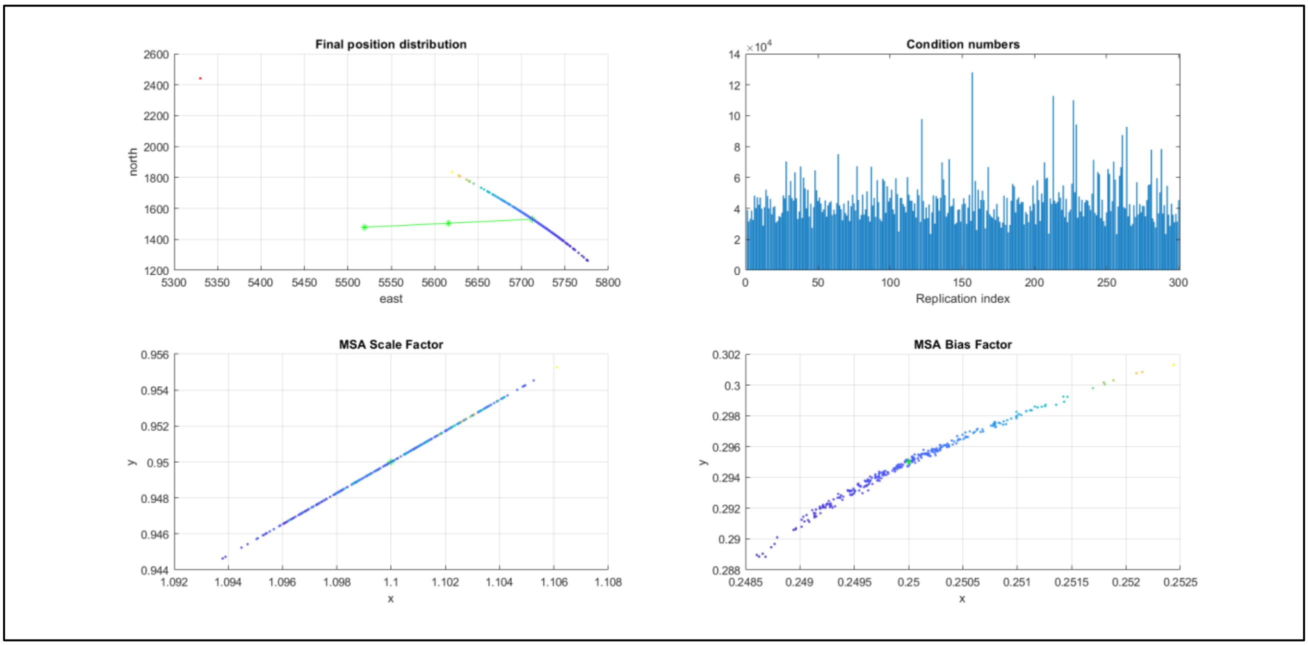
Final position distribution
north
east
Condition numbers
×10^4
Replication index
MSA Scale Factor
y
x
MSA Bias Factor
y
x

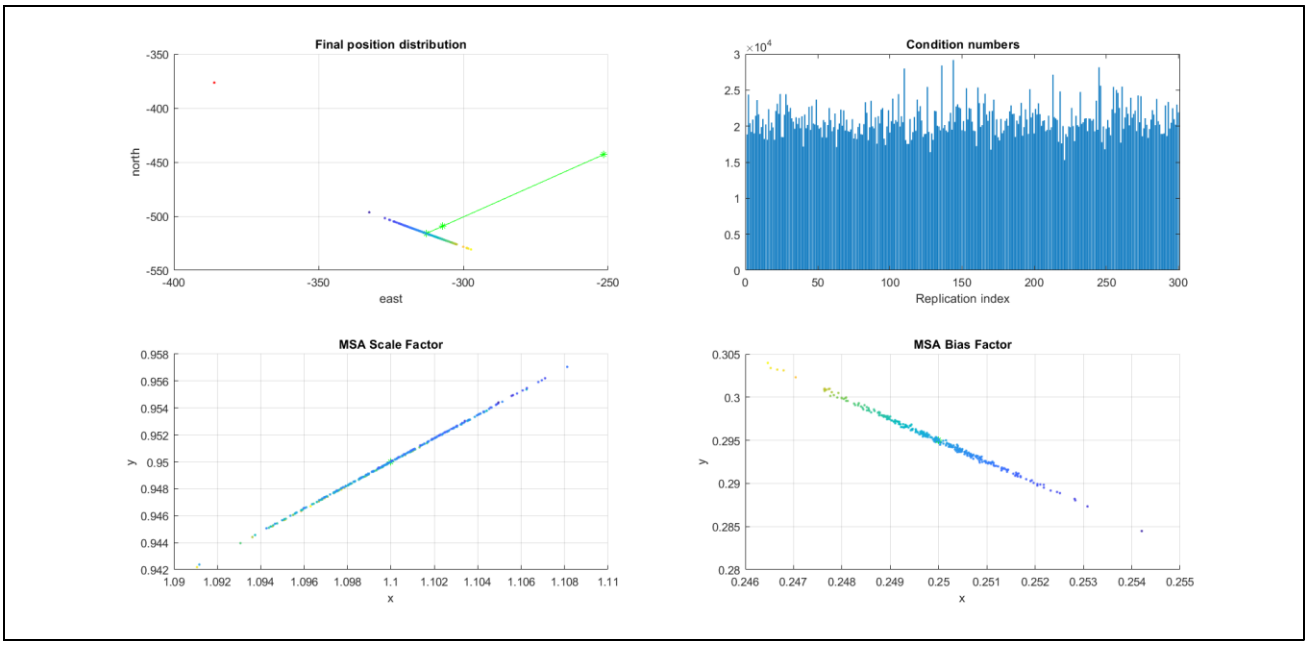
Final position distribution
north
east
Condition numbers
×10^4
Replication index
MSA Scale Factor
y
x
MSA Bias Factor
y
x

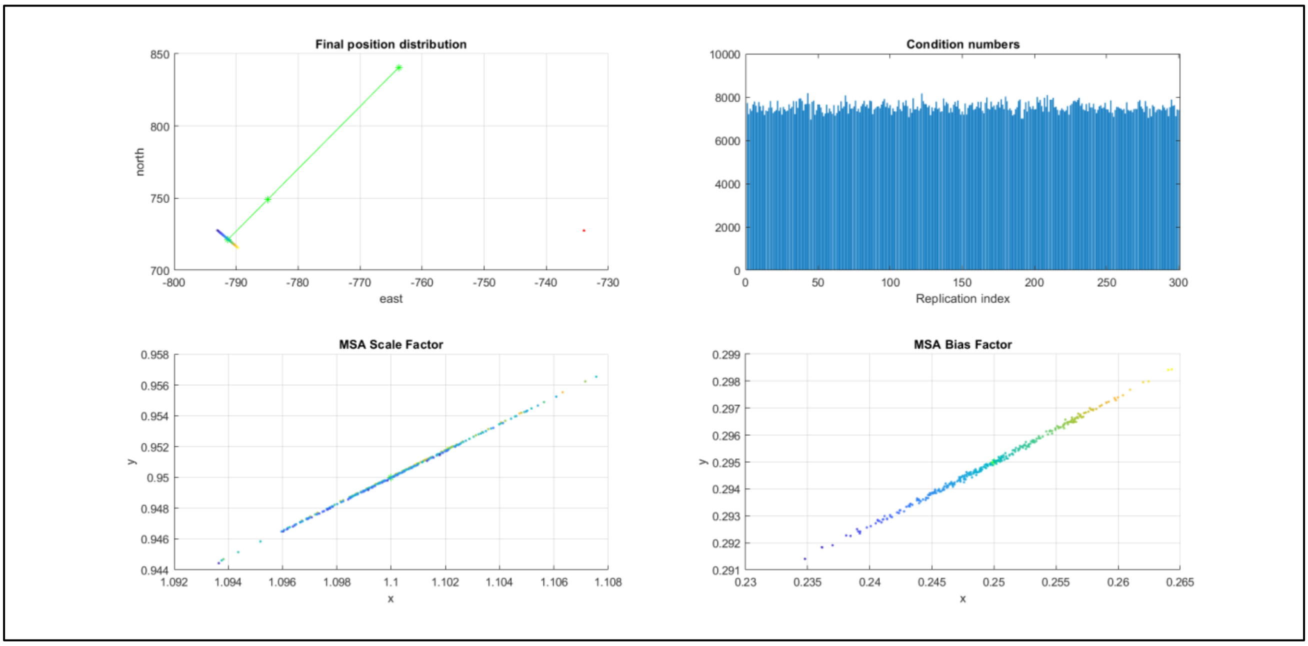
Final position distribution
north
east
Condition numbers
Replication index
MSA Scale Factor
y
x
MSA Bias Factor
y
x

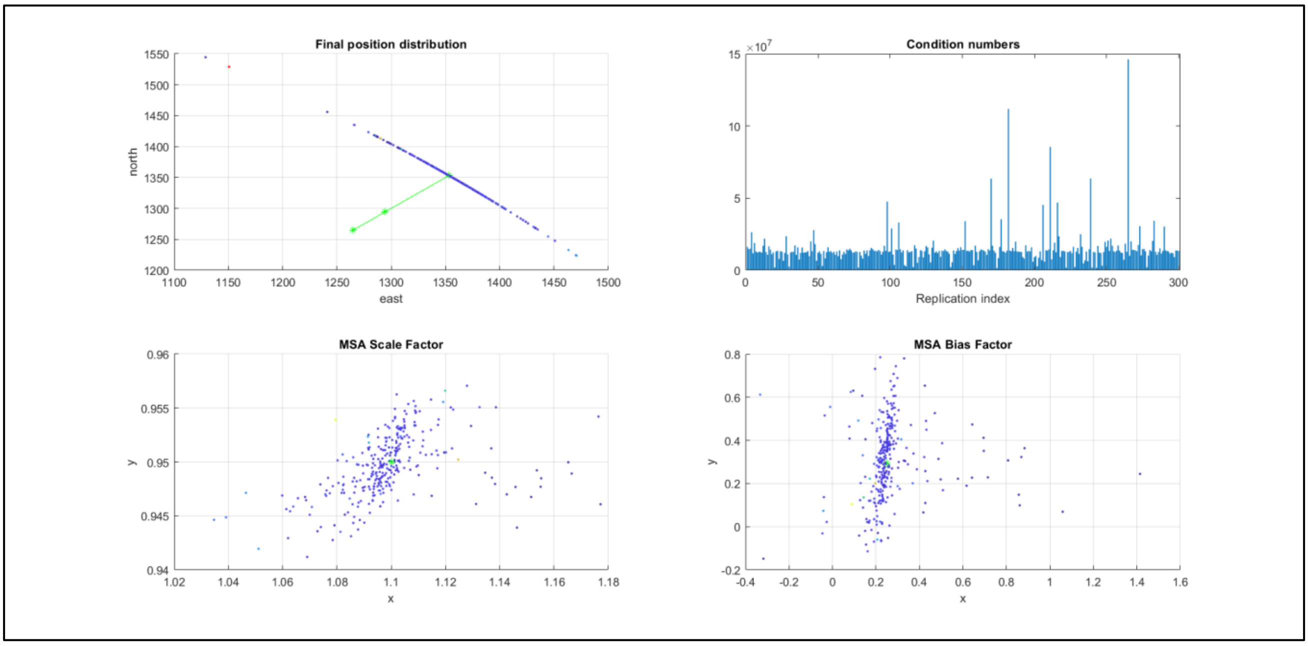

Project log

- 27-2-2018: initial project assignment
- 15-3-2018: official start of project
- 15-3-2018 to 15-4-2018: literature study, initial drafts of report
- 15-4-2018 to 15-5-2018: assembly and implementation of Excel simulation
- 15-5-2018 to 12-6-2018: refinement of simulation
- 12-6-2018 to 15-7-2018: writing report, researching further exploration topics, near-final changes
- 15-7-2018: end of research
- 14-8-2018: hardcopy report prior to presentation
- 27-8-2018: presentation
- 28-8-2018 to 31-8-2018: final changes to report

In addition to e-mail, communication between author and project mentors was mostly done in physical presence approximately every 1 to 2 weeks after start of project, up to 10-7-2018.

References

Amorin, R., and E. Broni-Bediako. 2010. “Application of Minimum Curvature Method to Wellpath Calculations.” *Research Journal of Applied Sciences, Engineering and Technology* 2 (7): 679–86.

Boots & Coots International, Inc. 2010. “Passive Magnetic Ranging Documentation,” February.

Brooks, Andrew G. 1997. Method of Correcting Axial and Transverse Error Components in Magnetometer Readings During Wellbore Survey Operations. US5623407, issued April 1997.

Elshabrawy, Mohamed Soliman Abdelrazik Abdelhamid. 2018. “Relief Well Plan for a Complex Well Including Multiphase Hydraulic Model and Multi-Station Analysis Applicability Study.” Master’s thesis, Robert Gordon University.

Golub, Gene H., and Charles F. Van Loan. 2013. *Matrix Computations, 4th Edition*. Johns Hopkins Studies in the Mathematical Sciences. The John Hopkins University Press.

Hanak, F. Chad, Harry Wilson, and Morten Gjertsen. 2015. “Assessment of the Validity of MWD Survey Accuracy Following Multistation Analysis.” In . London, United Kingdom.

Higham, Desmond J. 2004. *An Introduction to Financial Option Valuation*. Cambridge University Press.

Kan, J.J.I.M. van, A Segal, and F.J Vermolen. 2014. *Numerical Methods in Scientific Computing*. Delft: Delft Academic Press.

Maus, Stefan, Manoj C. Nair, Benny Poedjono, Shola Okewunmi, Derek Fairhead, Udo Barckhausen, Peter R. Milligan, and Jürgen Matzka. 2012. “High Definition Geomagnetic Models: A New Perspective for Improved Wellbore Positioning.” In . San Diego, California, USA.

Noy, Koen. 2018. *Derivation of MSA Quality Assurance and Control for Borehole Surveying for Only Magnetometer Bias Errors*.

Nyrnes, Erik, Torgeir Torkildsen, and Harry Wilson. 2009. “Minimum Requirements for Multi-Station Analysis of MWD Magnetic Directional Survey.” In . Manama, Bahrain.

Rawlings, John O., Sastry G. Pantula, and David A. Dickey. 1998. *Applied Regression Analysis: A Research Tool*. 2nd ed. Springer Texts in Statistics. New York: Springer.

Rice, John A. 2007. *Mathematical Statistics and Data Analysis, Third Edition*. Duxbury.

Rocquigny, Etienne de, ed. 2012. *Modelling Under Risk and Uncertainty: An Introduction to Statistical, Phenomenological and Computational Methods*. John Wiley & Sons.

Rocquigny, Etienne de, Nicolas Devictor, and Stefano Tarantola, eds. 2008. *Uncertainty in Industrial Practice: A Guide to Quantitative Uncertainty Management*. John Wiley & Sons.

Sadun, Lorenzo A. 2001. *Applied Linear Algebra: The Decoupling Principle*. Prentice Hall, Inc.

Vuik, C., F. J. Vermolen, M. B. van Gijzen, and M. J. Vuik. 2016. *Numerical Methods of Ordinary Differential Equations, Second Edition*. Delft Academic Press.

Williamson, Hugh S. 2000. “Accuracy Prediction for Directional MWD.” In . Houston, Texas, USA.

Index